Title
Enzymatic Degradation of Cellulose by the Filamentous Fungus Neurospora crassa

Author
Phillips, Christopher Michael

Publication Date
2011

Peer reviewed|Thesis/dissertation

Enzymatic Degradation of Cellulose by the Filamentous Fungus *Neurospora crassa*

By

Christopher Michael Phillips

A dissertation submitted in partial satisfaction of the

requirements for the degree of

Doctor of Philosophy

in

Molecular and Cell Biology

in the

Graduate Division

of the

University of California, Berkeley

Committee in charge:

Professor Michael A. Marletta, Chair
Professor Susan Marqusee
Professor Michelle Chang
Professor Chris Somerville

Fall 2011

Enzymatic Degradation of Cellulose by the Filamentous Fungus *Neurospora crassa*

by Christopher Michael Phillips

ABSTRACT

Enzymatic Degradation of Cellulose by the Filamentous Fungus *Neurospora crassa*

by

Christopher Michael Phillips

Doctor of Philosophy of Molecular and Cell Biology

University of California, Berkeley

Professor Michael A. Marletta, Chair

Lignocellulosic biomass is an abundant renewable resource that can be used as a feedstock for production of second-generation biofuels. Currently, the bottleneck to generation of such fuels lies in the expensive and technically challenging process for converting biomass to fermentable sugars. Filamentous fungi are efficient at depolymerizing plant biomass. These fungi are also used for the production of industrial enzymes due to their ability to secrete large quantities of enzymes. The filamentous fungus *Neurospora crassa* is a genetically tractable model organism and a proficient degrader of plant biomass. In this dissertation, the enzymatic depolymerization of cellulose by *Neurospora crassa* was investigated using a combination of quantitative proteomics, genetics, and biochemistry.

Chapter 1 is an introduction to lignocellulosic biomass and the organisms and enzymes that degrade it. In Chapter 2, a quantitative proteomic approach was taken to characterize the secretome of *Neurospora crassa* during growth on microcrystalline cellulose. Depolymerization of cellulose occurs by endoglucanases that hydrolyze internal glycosidic bonds and cellobiohydrolases that hydrolyze cellobiose from the reducing or non-reducing chain ends of cellulose. In addition to these canonical cellulases, a number of other proteins were quantified including a β-glucosidase, a cellobiose dehydrogenase (CDH), and glycosyl hydrolase family 61 (GH61) enzymes. The beta-glucosidase and 3 cellulases were purified and biochemically characterized. While these 4 enzymes represent more than 85% of the cellulase in the secretome, they were significantly impaired in their rate of cellulose degradation relative to the complete set of enzymes in the secretome. This result suggested that proteins other than canonical cellulases may be important in cellulose depolymerization by fungi.

The deletion of a gene encoding cellobiose dehydrogenase in *N. crassa* is described in Chapter 3. Cellobiose dehydrogenase (CDH) catalyzes the oxidation of cellobiose to cellobionolactone, but the biological function of this protein was previously unknown. Deletion of *cdh-1* reduced cellulase activity 37-49% and addition of purified CDHs to the Δ*cdh-1* strain resulted in a 1.6 to 2.0-fold stimulation in cellulase activity. The stimulatory effect of CDH required the presence of molecular oxygen and other secreted metalloproteins. The discovery that cellobiose dehydrogenase plays an integral role in degradation of cellulose marked a significant shift from previous models centered on the degradation of cellulose by mixtures of glycosyl hydrolases.

To determine the molecular mechanisms by which CDH can enhance cellulase activity, a fractionation strategy was employed as described in Chapter 4 to identify synergistic metalloproteins in the *N. crassa* secretome. CDH was shown to enhance cellulose degradation

by coupling the oxidation of cellobiose to the reductive activation of copper-dependent polysaccharide monooxygenases (PMOs), previously called GH61 enzymes. These enzymes catalyze the insertion of oxygen into C-H bonds adjacent to the glycosidic linkage and facilitate elimination of the adjacent carbohydrate moiety. A further discussion of the mechanism of copper-dependent PMOs is discussed in Chapter 5. Here, the action of different PMOs was shown to be regiospecific resulting in oxidized products modified at C1 on the reducing end or C4 on the non-reducing end. CDHs and proteins related to the PMOs are found in cellulolytic species throughout the fungal kingdom. When added to mixtures of cellulases, these proteins enhance cellulose depolymerization and could significantly reduce the cost of biofuel production.

In chapter 6, the development of *N. crassa* as a host for recombinant expression of secreted enzymes is described. Expression of the endocellulase GH5-1 is used to complement the phenotype of a Δ*gh5-1* deletion strain. Experiments with GH5-1 fused to GFP (green fluorescent protein) were used to visualize the binding of this endocellulase to plant biomass. Additional applications for *N. crassa* as an expression host for fundamental studies of biomass depolymerizing enzymes are described.

DEDICATION

For my wife, Paola, and daughter, Luciana

TABLE OF CONTENTS

LIST OF FIGURES

LIST OF TABLES

PREFACE: Motivation for lignocellulosic biofuels

The use of science and technology to improve the world's energy security and limit the human influence on climate change is one of the grand challenges of the 21st century. The importance of these issues is highlighted by multiple national and international agencies including the United Nations as a part of the Millennium Development Goals (*1*). More recently, other documents including the National Academy of Engineering's "Grand Challenges for the 21st century" and President Obama's "Strategy for Innovation" call on the use of innovation in science and engineering to design novel routes for the production of renewable energy that is both affordable and sustainable (*2, 3*).

While many opportunities exist for the development of renewable energy in general, one area that is particularly challenging is the production of alternative transportation fuels. Transportation fuels such as those used in aviation, shipping, and ground transportation require a high energy density to be effective. This high energy density has traditionally been supplied through the use of petroleum refining to generate jet fuel, gasoline, and diesel. Poltical instability in the Middle East, and an increasing demand for petroleum resources, has caused significant volatility in oil prices over the past decade. The price of a barrel of West Texas Intermediate (WTI) crude has fluctuated from its low of $18/barrel in 2001 to a high of $145/barrel in 2008. These volatile oil prices have had a significant impact on economies worldwide and were noted as a major contributing factor in the recent financial crisis. Furthermore, in 2010 nearly half (49%) of oil used in the US was imported and much of this came from regions that are hostile to the US or politically unstable (*4*). Hence, the desire to use a domestically produced and sustainable feedstock for generation of transportation fuels represents an important challenge, and opportunity, for securing a future of both energy security and economic prosperity.

In addition to meeting the worlds growing demand for liquid fuels, there is also a significant incentive to produce, and use, energy in a more sustainable way. The use of fossil fuels as an energy source is unsustainable and a significant body of scientific evidence supports the fact that the burning of fossil fuels is responsible for an increase in the global mean surface temperature. According to the international governmental panel on climate change (IPCC), the global mean temperature has increased by 0.8 °C since the pre-industrial era and the concentration of CO_2 has increased from 280 ppm to more than 380 ppm during the same time period (*5*). The last IPCC report,stated that eleven of the last 12 years (1995-2006) ranked among the 12 warmest years on record. Replacing petroleum-derived fuels with low carbon substitutes represents an opportunity to decrease our carbon emissions and limit negative consequences from climate change.

Alternative feedstocks for production of liquid transportation fuels, such as plant biomass, have the potential to substantially improve the current situation in both energy security and environmental sustainability. Through the use of photosynthesis, plants capture energy from sunlight and can utilize atmospheric CO_2 to synthesize organic molecules. Hence, the energy captured from sunlight is stored in the chemical bonds of plant biomass. Taking this biomass and converting it to useful chemicals and fuels represents a significant technical challenge for science and engineering. If successful, these processes would be carbon neutral, or near neutral. Similar processes exist, particularly in reference to the fermentation of sugars to ethanol.

Technology for the production of ethanol from sugar cane has been widely used in Brazil since 1974 as a result of Pro-alcool, a government sponsored program to reduce the country's dependence on oil imports by increasing sugar cane alcohol production. In this process, the sugar cane is squeezed to remove the sugar that is later fermented to ethanol by yeast. Many

sugar/ethanol refineries have been operating unsubsidized for nearly two decades (*6*). As a result of this program, and the high productivity of sugar cane in Brazil, the sugar cane ethanol industry produced nearly 7 billion gallons of ethanol in 2010 and accounts for nearly one half of Brazilian transportation fuel (*7*).

In the past decade, corn ethanol has also been widely adopted in the United States with fuel ethanol production increasing from 1.6 billion gallons in 2000 to 13.2 billion gallons in 2010 (*7*). The corn ethanol industry uses a process to convert cornstarch to fuel. Cornstarch is a polymer of glucose and as a result it must be treated with hydrolytic enzymes before fermentation to ethanol. While both sugar cane and corn are renewable resources, both of these feedstocks have been criticized for competing with the global food supply. One alternative lies in the use of non-edible plant biomass for the production of ethanol or other second-generation fuels that can be produced through advances in genetic engineering.

Lignocellulosic biomass is the most abundant renewable resource on Earth and its production does not directly compete with food production. In 2005, a study was released by the US Department of Energy stating that more than 1 billion tons of plant biomass could be sustainably produced for biofuel production (*8*). A recent update of that study confirmed earlier predictions (*9*). This biomass would be supplied through a combination of agriculture and forest residues, as well as dedicated energy crops to be planted on marginal lands. The major advantage associated with the use of lignocellulosic biomass is that these processes could use waste from agriculture or forestry and have very low greenhouse gas emissions. In addition, many dedicated energy crops have higher yields and use less water and fertilizer when compared to traditional crops such as corn or soy (*10*).

The primary bottleneck associated with development of both economically and environmentally sustainable lignocellulosic biofuels lies in the development of an inexpensive process for the conversion of plant biomass to simple sugars (*11*). Unlike the sucrose or starch processes, a conversion process for lignocellulosic biomass requires extensive thermochemical pretreatment. Generally, dilute sulfuric acid, ammonia, or steam is used to disrupt the ultrastructure of the plant cell wall and increase accessibility. Then, a combination of enzymes is used to break down the polysaccharides to soluble, fermentable sugars (Figure I). Capital costs associated with thermochemical pretreatment and long incubation times for the enzymatic hydrolysis are significant contributors to the cost of the process. In addition, the cost of enzyme production remains a very significant part of the operating costs because enzymes cannot be recycled with current technology (Table I). The 2011 techno-economic assessment published at the National Renewable Energy Lab (NREL), estimates that the cost of enzyme production contributes $0.35-0.50/gallon ethanol (*12*). When combined, the cost of converting biomass to fuel likely accounts for ~65% of the minimal selling price for cellulosic ethanol. Historically, most cost reductions in this process have been due to improved enzyme cocktails (*13*). Improved enzymes can result in 1) the use of milder pretreatments that are less capital intensive and reduce the inhibition of fermenting organisms, 2) reduced cost of enzyme production by decreasing the amount of enzyme that needs to be used, 3) shorter incubation times for enzymatic degradation, and 4) higher solid loadings that increase ethanol titers for more inexpensive distillations and generation of less wastewater.

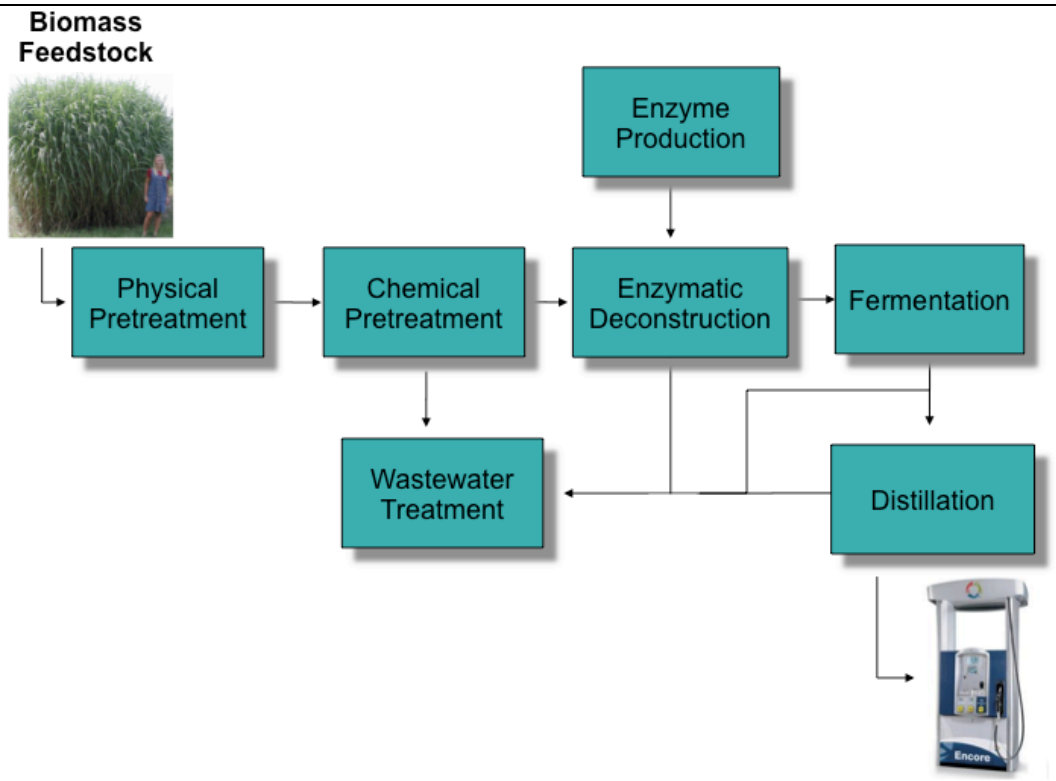

Figure I. Schematic of a Lignocellulosic Biofuel Process. The process for conversion of lignocellulosic biomass to fuel requires a number of steps to 1) depolymerize the polysaccharides in the plant cell wall to soluble sugars, and 2) ferment those sugars for production of a fuel. Depolymerization of polysaccharides in the plant cell wall requires physical pretreatment, or grinding, and chemical pretreatments that typically include the addition of dilute sulfuric acid at elevated temperatures. Following pretreatment, cellulolytic and hemicellulolytic enzymes are added to the biomass to degrade the polysaccharides to soluble, fermentable sugars. These enzymes must be purchased or produced on site. Finally, fermentation of sugars to ethanol, or another advanced biofuel, is performed and the resulting fuel is distilled or phase separated. Most of the above processes generate waste water that must be treated before reuse in the process.

Itemized Costs per Gallon of Cellulosic Ethanol	
Biomass Feedstock	$0.74
Pretreatment	$0.29
Enzyme Production[1]	$0.34 to $0.50
Enzymatic Deconstruction/Fermentation	$0.20
Wastewater Treatment	$0.34
Distillation	$0.12
Other	$0.10
Total	**$2.15 to $2.31**

1 – Range for cost of enzyme production depends on whether production is on or off-site

Table I. 2011 NREL technoeconomic analysis for biochemical conversion of lignocellulosic biomass to ethanol(*12*).

Given these analyses, I began to investigate technical barriers and potential solutions to the enzymatic conversion of biomass to sugars. Over the past 5 years I have made an attempt to extensively investigate the field of biomass degradation using an interdisciplinary approach. The Energy Bioscience Institute's harbors expertise in areas as diverse as plant and fungal biology, chemistry, chemical engineering, and economics that have contributed significantly to this research. The interdisciplinary approach taken by my advisor, Michael Marletta, in working at the interface between biology and chemistry has also led to a series of important scientific findings in our research program. Many of these findings are outlined in this dissertation.

In the following introduction, the molecular basis for biomass recalcitrance and the approaches microorganisms have evolved to degrade this biomass will be described. Then, I will outline our approach to use *Neurospora crassa* as a model organism to enhance our understanding of biomass degradation by fungi and give an overview of the general research strategy. This disseration begins with the use of quantitative proteomics to identify candidate enzymes for novel mechanisms of cellulose degradation. It concludes with the discovery, characterization, and a proposed mechanism for a wide-spread and industrially relevant family of oxidative enzymes involved in degradation of crystalline cellulose.

ACKNOWLEDGEMENTS

Filing a Ph.D. dissertation marks the culmination of a significant amount of effort both by the student, and all those involved in helping him/her develop as an academic throughout 20+ years of schooling. Perhaps the most important decision for a successful Ph.D. is the choice of a graduate advisor. My decision to work with Michael Marletta was deliberate and had a profound effect on my growth as a scientist. In addition to being an extraordinary and rigorous scientist, Michael is an excellent leader and manager. His guidance, sound judgement, and rigorous nature ensure excellent scientific advice and mentorship. The freedom he allows to his students enables scientific independence and future success beyond graduate school. The qualities that Michael possesses are the things I will look for in future mentors, and I truly appreciate his support and guidance.

Many other professors have also had an effect on my development as a scientist at UC-Berkeley. My thesis committee members include Michelle Chang, Chris Somerville, and Susan Marqusee. Each has been instrumental in monitoring my progress and making suggestions as my graduate research has advanced. In particular, interactions with Michelle and Chris have been helpful. Michelle helped teach me the value of hard work and laboratory humor during my rotation in her lab. I have enjoyed getting her scientific feedback and perspective. Chris has encouraged multiple instrumental collaborations and has enabled many projects through his optimism and desire to provide any resources necessary to facilitate progress. Louise Glass has also served as an important mentor in both fungal biology and science in general. Jamie Cate and his lab have also been important collaborators.

I have been fortunate to have many excellent colleagues and collaborators the last several years, but none as productive as that which I maintained with Will Beeson. Will's extremely intense approach to science helped elevate my own scientific work. His friendship made lab a more enjoyable place to work. I also want to thank all the past and present members of the Marletta Lab, especially Josh Woodward. Many members of the EBI in Calvin Hall have also been helpful for feedback and discussions. Stefan Bauer in particular has been an excellent resource for helping enable my research and working with me to develop solutions to analytical problems.

In addition to those at UC-Berkeley I would also like to thank the people that helped initiate my interest in science. My Dad, Michael Phillips, had a significant influence on my decision to select a career that is both challenging and enjoyable. His advice to study something that you love was the predominant reason for why I chose to immerse myself so fully in science during my undergraduate and graduate studies. I would also like to thank Mark Nielsen, my undergraduate research advisor that gave me the opportunity to work in his lab and encouraged me to apply to UC-Berkeley.

Finally, I need to thank my wife for her love and support, and my daughter for helping distract me from even the most frustrating days in lab. Without you two, my life would not be nearly as enjoyable or meaningful as it now is.

CHAPTER 1: INTRODUCTION

Biomass Recalcitrance

Lignocellulosic biomass is a complex material comprised primarily of polysaccharides including cellulose, hemicellulose, and pectins. Other components in plant biomass include proteins and lignin. These materials are organized into a complex ultrastructure in the plant cell wall to provide structural support and impart resistance to biotic and abiotic stresses (*1, 2, 14*).

Cellulose, a homopolymer of β-1,4-glucose, is the most abundant polysaccharide in plant biomass and is highly organized into micro and macrofibrils. Microfibrils are comprised of 30 to 36 glucan chains that are held together by tight inter and intra-chain hydrogen bonds. Macrofibrils are bundles of the smaller microfibrils and are generally 50 to 250 nm in diameter (*15*). This strong hydrogen bonding network between glucan chains, coupled with the long degree of polymerization, limits accessibility of enzymes to the semi-crystalline cellulose surface. Connecting the cellulose microfibrils is a network of hemicellulose comprised of both pentose and hexose sugars (*2*). The organization and abundance of different types of hemicellulose is highly varied by species and tissue (*6*). Efficient degradation of hemicellulose and utilization of the resulting sugars is imperative for the efficient use of plant biomass. However, most hemicellulose is highly substituted and is significantly more susceptible to hydrolysis by acids or enzymes than cellulose.

The third major component of plant biomass is lignin, a poorly defined and heterogenous material comprised of phenylpropanoid units. The synthesis of lignin is mediated through a process involving radical chemistry and as a result this polymer is highly heterogeneous. Lignin is the second most abundant organic substance on earth and its presence is thought to inhibit the action of degrading enzymes (*16*). This is due to its ability to reduce the accessibility to polysaccharide substrates and because its hydrophobic surface can adsorb, and potentially inactivate, degrading enzymes.

Microbial Utilization of Cellulose

Due to the abundance of plant biomass in nature, many microorganisms have evolved strategies devised to utilize this abundant material as a source of energy for growth. Cellulolytic organisms are found throughout both the bacterial and fungal kingdoms, and recently, some animals were found to secrete cellulases as well (*17, 18*). All of these organisms secrete complex mixtures of cellulolytic enzymes with many producing 10-30 different cellulases at one time. Cellulolytic organisms can be split into two broad classes; those using free enzymes, and those using a multi-enzyme complex termed the cellulosome. Cellulosomes are generally found in anaerobic microorganisms such as *Clostridia* species or the Chytridomycetes, a primitive division of fungi. These cellulosomes can be 0.6-2 MDa in size and are often attached to the cell wall of the host, a mechanism that is thought to help organisms better compete for sugar uptake in a complex microbial community. Free cellulase systems are found in aerobic bacteria and all known cellulolytic filamentous fungi (*17*).

In nature, filamentous fungi are the predominant degrader of plant biomass. In addition, filamentous fungi are excellent hosts for production of large amounts of protein. Species of *Aspergillus* and *Trichoderma* are used for enzyme production on an industrial scale (*19*). Some batch fed fermentations of *Trichoderma* have been shown to reach more than 75-200 grams protein per liter of culture depending on the methods used for protein quantitation (*13*). All commercial cellulase cocktails are derived from filamentous fungi further substantiating the importance of these organisms for production of an efficient process for cellulosic biofuels.

Background on fungal cellulases

Degradation of cellulose by fungal enzymes occurs by a combination of exoglucanases, endoglucanases, and β-glucosidases. These enzymes contain an active site cleft or tunnel lined with aromatic residues that facilitate the separation of a glucan chain for a hydrolytic reaction catalyzed by Glu or Asp residues. Exoglucanases (or cellobiohydrolases) hydrolyze cellobiose units from the chain ends of cellulose and their tunnel-like active site enables tight substrate binding and varying degrees of processivity. Exoglucanases can be specific for the reducing end (GH7; CBH-1) or non-reducing end (GH6; CBH-2) of cellulose (*20*). Endoglucanases hydrolyze internal glycosidic bonds in cellulose resulting in creation of new chain ends. Endoglucanases (GH5, GH6, GH7, GH12, GH45) contain a shallow active site cleft and are not processive (Figure 1.1). β-glucosidases hydrolyze soluble cello-oligosaccharides into glucose and can prevent product inhibition of the cellulases by cellobiose (*21*).

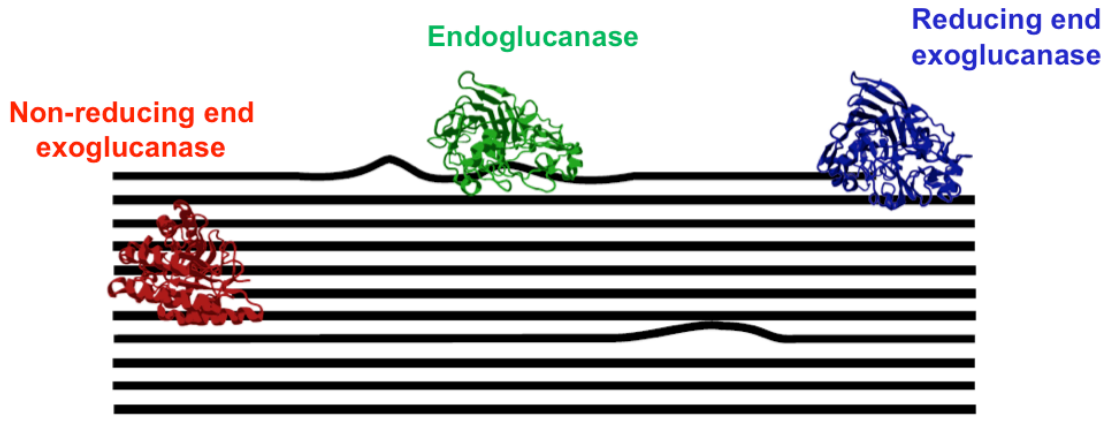

Figure 1.1: Hydrolytic model for cellulose degradation by cellulases. Cellulases gain access to a glucan chain and bring it into a cleft or tunnel active site where acid-base catalysis cleaves glycosidic bonds. Endoglucanases catalyze the cleavage of internal glycosidic bonds to generate new chain ends. Exoglucanases are specific to the reducing or non-reducing endo of cellulose and bind chain ends to release cellobiose as the primary product.

Each of these functionally different classes of enzymes cleaves cellulose through the hydrolysis of a glycosidic bond. The catalytic acid residues are spaced 5-11 Å apart depending on whether the mechanism of hydrolytic action is inverting or retaining with respect to product configuration at the anomeric carbon. Retaining glycoside hydrolases result in net retention of conformation and the product is the β-anomer. These hydrolases use a 2-step double displacement mechanism and form a covalent enzyme-substrate intermediate that is then broken by hydrolysis (Koshland mechanism). Inverting glycoside hydrolases result in inversion of conformation and the product is the α-anomer. Inverting glycoside hydrolases pass through an oxocarbenium ion-like transition state (*22*).

In addition to catalytic glycosyl hydrolase domains, many cellulases contain a glycosylated linker attached to a cellulose binding modulee that localizes the enzyme to the surface of cellulose. In fungi all cellulose-binding modules (CBM) belong to CBM family 1 and consist of 35-40 amino acids that form a beta-hairpin connected by two disulfide bonds. An NMR structure of the CBM1 from *T. reesei* CBH1 has been solved and mutagenesis, as well as molecular dynamics simulations, have investigated the molecular mechanism for cellulose binding (*23, 24*). Three conserved aromatic residues (Tyr or Trp) are located on a similar face and have been proposed to from hydrophobic interactions with cellulose and stack over the

glucose residues. Additional glutamine and asparagines are thought to be important for hydrogen bonding to cellulose as well (*25*). For many years glycosylation of the linker between the CBM and catalytic domains was hypothesized to provide increased stability to protease degradation.

While all known fungal cellulases act through a common hydrolytic mechanism, synergy between enzymes is an important theme in cellulase research and helps explain the benefit of having multiple enzymes that work via similar mechanisms. Synergy is the concept that the simultaneous addition of more than one enzyme to cellulose results in more efficient cellulose degradation than the sum of degradation achieved by each enzyme alone (*26*). Endo-exo synergy is the most commonly reported form of synergy. Endoglucanases hydrolyze internal glycosidic bonds in cellulose and exoglucanases bind these new chain ends to hydrolyze cellobiose (*27*). Exo-exo synergy has also been reported for exoglucanases that work from the reducing and non-reducing chain end. Endo-endo synergy has not been definitively shown raising the question as to why so many varieties of endoglucanases are secreted by many cellulolytic organisms (*28*).

Early investigations of cellulase synergy focused on calculating the degree of synergy between two individual components. It was from this analysis that it was first discovered that some enzymes have dual endo-exo activity. For example, CBH-2 from *H. insolens* was shown to have significant synergy with CBH-1, but not with a GH45 endoglucanase (*29*). This suggests that *H. insolens* CBH-2 may have both endo and exo activity. Recent analyses have capitalized on statistical design of experiments and high throughput assays to optimize complex mixtures of cellulases for optimal degradation of pure cellulose and other pretreated lignocellulosic substrates (*30, 31*). Many of these studies have resorted to production of fungal cellulases in *Pichia pastoris* to improve yield and throughput. This approach is flawed due to the different glycosylation and post-translational processing that occurs in yeast relative to filamentous fungi. Many of these posttranslational modifications have been shown to be required for efficient catalytic activity (*32*).

While the vast majority of resources have studied the role of hydrolases in cellulose degradation, some research has been done on the potential role of oxidative proteins in this process (*33*). Cellulolytic fungi in the phylum Ascomycota produce relatively few oxidative proteins while Basidiomycota produce many more. Cellobiose Dehydrogenase (CDH), an enzyme that catalyzes the oxidation of cellobiose to cellobionolactone, is one oxidative enzyme that is present in cellulolytic fungi in both Ascomycetes and Basidiomycetes. This enzyme is a secreted flavocytochrome that contains an N-terminal heme domain and a C-terminal flavin domain that is part of the larger glucose-methanol-choline oxidoreductase superfamily. The ferrous heme domain of CDH is able to reduce a wide variety of substrates including quinones, metal ions, and organic dyes (*34*). The observation that the ferrous heme domain can reduce iron has led to hypotheses that this enzyme could facilitate breakdown of lignocellulose using hydroxyl radicals. Such a model involves the generation of free ferrous iron chelates that react with hydrogen peroxide generated by CDH or another oxidase to form hydroxyl radicals by a Fenton reaction (*35*). The role of oxidative proteins in cellulose degradation was only recently elucidated and will be discussed further in chapters 3-5.

Functional Genomics of Cellulolytic Fungi

With the help of next generation sequencing technology, multiple transcriptomic and proteomic analyses of cellulolytic fungi have been performed in recent years (*36-40*). These analyses have led to an expansion in the number and types of enzymes that may be involved in cellulose degradation and utilization. These cellulolytic fungi can be divided into three main

groups: soft rot, brown rot, and white rot fungi. All known cellulolytic Ascomycetes are soft rot fungi and degrade cell wall polysaccharides but not lignin (Figure 1.2). Brown rot and white rot fungi are Basidiomycetes and are capable of modifying or completely degrading lignin.

Most work on Ascomycete soft rot fungi has focused on the industrial workhorse *Trichoderma reesei (*anamorph: *Hypocrea jecorina)*. The *T. reesei* genome contains just 10 cellulases and only 7 of these are expressed and secreted at detectable levels (*15*). A combination of antibodies and specific activity assays have been used to quantify the cellulases in *T. reesei* and results suggest that the exocellulases CBH-1 and CBH-2 are present as 60% and 20% of the total secreted protein, respectively. Endoglucanases EG-1 (GH7) and EG-2 (GH5) make up an additional ~10% with the remainder of protein constituting other low abundance proteins (*41*). A microarray of *T. reesei* grown on cellulose and extensive proteomic analyses by 2-dimensional SDS-PAGE has suggested a number of other accessory proteins may be important for cellulose degradation including: Cip1, Cip2, swollenin, and EG4 (GH61A) (*42*). The activity and biological function of many of these proteins remains unclear.

Analysis of other cellulolytic Ascomycetes has also been investigated quite extensively in recent years. The genome, transcriptome, and secretome of *Myceliopthora thermophila* and *Thielevia terrestris* was recently published enabling the investigation of cellulose degradation by thermophilic species (*40*). The major metabolic enzymes of these fungi are very similar to the mesophilic Ascomycetes that have been studied for biomass degradation. Work within the Energy Biosciences Institute has also utilized RNA-seq and LC-MS/MS to characterize *M. thermophila*. The development of a thermophilic expression host for enzyme production and the higher stability, and activity, of thermophilic enzymes are an important motivating force for these studies (*43*). Aside from the optimal growth temperature, these organisms are quite similar to mesophilic species.

Genomic, transcriptomic, and proteomic analysis of the Basidiomycetes *P. chrysosporium, P. placenta,* and *S. lacrymans* have revealed new and alternative mechanisms for cellulose degradation by filamentous fungi (*36, 38*). Basidiomycetes are phylogenetically separated from Ascomyetes by an estimated 500 million years and as a result these fungi display quite distinct life cycles. *P. placenta,* and *S. lacrymans* are brown rot fungi capable of degrading the polysaccharides in plant biomass but unable to degrade lignin. The genome of *P. placenta* completely lacks homologs for an exoglucanase (*37*) and RNA-seq of *S. lacrymans* showed that endoglucanases, oxidative enzymes, and proteins of unknown function were the primary proteins secreted during growth on biomass (*36*). The different combination of enzymes secreted by brown rot fungi implys that they might use a fundamentally different strategy for cellulose degradation when compared to Ascomycetes. Many groups have hypothesized that cellulose degradation in these organisms could occur by Fenton chemistry. While this model has been proposed and mentioned in many reports, there is limited evidence to support such a view.

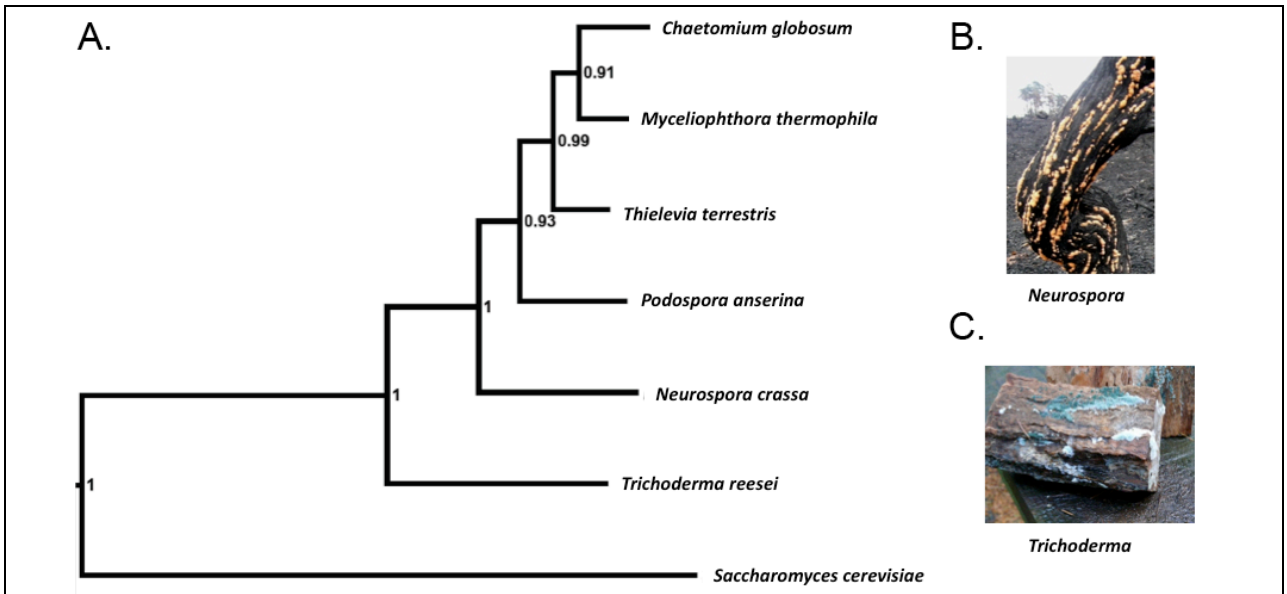

Figure 1.2. Phylogeny of select fungi within the Ascomycota phylum. A. Phylogeny was constructed using 18S ribosomal RNA sequences from the above listed species with *Saccharomyces cerevisiae* as an outgroup. *Trichoderma reesei* has been the focus of most research on cellulose degradation by fungi. Other species, including thermophilic isolates of *Thielevia* and *Myceliophthora*, have recently had their genomes sequence and have been the source of enzymes for improved cellulase cocktails. *Neurospora crassa* has long been a model organism for investigation of filamentous fungi. B. Photograph showing growth of *Neurospora* on a tree after a forest fire burn. C. Photograph of a species of *Trichoderma*.

Neurospora crassa as a Model Organism

Neurospora crassa is a filamentous fungus of the Ascomycete subphylum that has been studied for decades. *Neurospora* is easy to grow, has a haploid life cycle, and creates an ordered arrangement of products in meiosis facilitating genetic analysis (*44*). *Neurospora* was the model organism used when Beadle and Tatum proposed the one gene-one enzyme hypothesis, an idea that led them to the Nobel Prize in 1958. *N. crassa* was the first filamentous fungus to have its genome sequenced (*45*) and the *Neurospora* community publically provides microarrays and access to a nearly complete full genome gene deletion set.

In addition to its attractive properties as a model organism, *N. crassa* is also a proficient degrader of plant cell walls. *N. crassa* is commonly isolated from agricultural residues and woody biomass and is able to completely degrade pure cellulose in liquid culture. In 2010 the first systematic analysis of *N. crassa* during growth on cellulose and *Miscanthus* biomass was performed (*46*). This study exemplified the tremendous power of this model organism for understanding how filamentous fungi degrade and utilize plant cell walls. A whole genome microarray identified >400 candidate genes involved in the transcriptional response to biomass and proteomic analyses identified 23 proteins in the secretome including many of the cellulases found in other industrially relevant species like *T. reesei*. Phenotypic analysis of select gene deletion strains was also performed with notable phenotypes for deletion of genes encoding exoglucanases *cbh-1* and *gh6-2*, endoglucanase *gh5-1*, and the β-glucosidase *gh3-4*. The results of this work opened up opportunities for more detailed investigation of many important areas including: transcriptional regulation, signaling, sugar transport, and enzymatic degradation.

Thesis

Much of the work in the following document leveraged previous research devoted to developing *N. crassa* as a model organism. The use of *N. crassa* as a model organism for cellulose degradation was the result of a fruitful collaboration between the laboratories of Michael Marletta, Jamie Cate, and Louise Glass. Michael's expertise in enzyme mechanism and Louise's expertise in fungal biology and genetics were particularly influential in this effort. My research has specifically focused on degradation of cellulose because it is both the most abundant, and most recalcitrant, polysaccharide in the plant cell wall. Below, a strategy is outlined for the identification and quantification of the major proteins secreted by *N. crassa* in response to cellulose (Chapter 2). This work, coupled with data from the original systems analysis of *N. crassa* on cellulose, provided support for a hypothesis that accessory proteins must play a role in the degradation of crystalline cellulose. While this hypothesis was not new, the genetic and experimental strategies designed in *Neurospora* were either not possible or not attempted by previous groups in the field.

Our fundamental strategy was guided by the generation of transcriptomic and proteomic data to identify candidates for accessory roles in cellulose degradation (Figure 1.3). A bottom-up approach was used to purify all canonical cellulases with known functions in cellulose degradation including 2 cellobiohydrolases, an endoglucanase, and a β-glucosidase (Chapter 2). A complementary top-down strategy was used to investigate the deletion strains for individual genes predicted to be involved in cell wall degradation. This genetic approach was used to characterize all the proteins identified by quantitative mass spectrometry and an example of this approach is further described for deletion of a cellobiose dehydrogenase (Chapter 3). The deletion of the cellobiose dehydrogenase was particularly interesting and led to a series of experiments culminating in the discovery and characterization of a large class of copper-dependent metalloenzymes (Chapter 4). These enzymes were previously called glycosyl hydrolase family 61 proteins and were the topic of my qualifying proposal. Following the characterization of these copper metalloenzymes, a catalytic mechanism was proposed providing clear evidence that these proteins should be reclassified as polysaccharide monooxygenases (Chapter 5). The culmination of this body of work has resulted in an improved understanding of enzymatic cellulose degradation by filamentous fungi with an emphasis on the oxidative enzymes involved in this process.

In addition to characterizing the role of hydrolytic and oxidative enzymes secreted by *N. crassa* during growth on cellulose, I have also included a final chapter on the development of *N. crassa* as a host for recombinant expression. One of the primary tools limiting the characterization and improvement of lignocellulolytic enzyme cocktails is the lack of platforms for recombinant expression. Here, *N. crassa* was used as an expression host for production of GH5-1 as a proof of principle for further studies (Chapter 6).

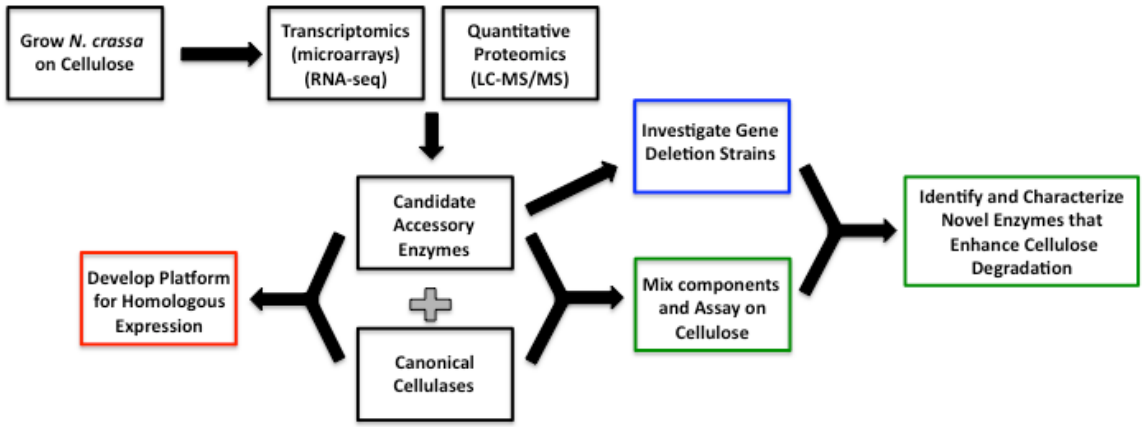

Figure 1.3. Research strategy for characterization of cellulose degradation in *N. crassa.* Chapter 2 (black boxes): A quantitative proteomic approach was used to identify secreted cellulases and candidate accessory enzymes involved in lignocellulose degradation. Chapter 3 (blue box): Gene deletion strains for candidate enzymes were investigated for phenotypes related to cell wall degradation. Chapters 4 and 5 (green boxes): Canonical cellulases and candidate enzymes of interest were purified, mixed, and assayed on cellulose. These enzymes were then biochemically characterized and a mechanism proposed for their action. Chapter 6 (red box): A platform for recombinant expression of secreted proteins was developed using *N. crassa* as a host.

CHAPTER 2: A quantitative proteomic approach to cellulose degradation

ABSTRACT

To better understand the biochemical route that filamentous fungi use to degrade plant biomass, we have taken a quantitative proteomics approach to characterizing the secretome of *Neurospora crassa* during growth on microcrystalline cellulose. Thirteen proteins were quantified in the *N. crassa* secretome using a combination of Absolute Quantification (AQUA) and Absolute SILAC to verify protein concentrations. Four of these enzymes including 2 cellobiohydrolases (CBH-1 and GH6-2), an endoglucanase (GH5-1), and a ß-glucosidase (GH3-4) were then chosen to reconstitute a defined cellulase mixture in vitro. These enzymes were assayed alone and in mixtures and the activity of the reconstituted set was then compared to the crude mixture of *N. crassa* secretome proteins. Results show that while these 4 proteins represent 63-65% of the total secretome by weight they account for just 43% of the total activity on microcrystalline cellulose after 24 hours of hydrolysis. This result, and quantitative proteomic data on other less abundant proteins secreted by *Neurospora,* suggest that proteins other than canonical fungal cellulases may play an important role in cellulose degradation by fungi.

INTRODUCTION

Filamentous fungi, such as *Neurospora crassa*, have evolved to secrete complex cocktails of enzymes that completely depolymerize cellulose and other plant cell wall polysaccharides (*46*). Several groups have focused on optimizing mixtures of cellulases in an effort to maximize hydrolysis of cellulosic substrates. These studies have relied upon statistical modeling and experimental data to determine the optimal combination of enzymes for hydrolysis (*30, 31, 47, 48*). An alternative approach would be to determine the relative abundances of the different enzymes produced by fungi and use this information to construct *in vitro* assays. In recent years, quantitative proteomics has emerged as a reliable technique to both identify and quantify proteins in complex mixtures. Some groups have used these proteomic approaches to determine the relative quantities of cellulases and other extracellular enzymes during growth on biomass using isotope labeling (*49-52*) or label-free approaches (*53*), however, these approaches have not allowed direct comparison of the concentrations of different secreted proteins.

Here, we use a quantitative proteomics approach (Figure 2.1) to create a defined cellulase system in *N. crassa*. A combination of absolute quantification (AQUA) (*54*) and absolute stable isotope labeling of amino acids in culture (Absolute SILAC) (*55*) was used to determine the absolute concentrations of 13 proteins in the secretome of *N. crassa* during growth on microcrystalline cellulose (Avicel®). Based on these results a defined cellulase system was assembled consisting of 4 proteins that comprise 63-65% of the total secretome by weight. These proteins were purified and their respective activities on cellulose were measured. Binary, ternary, and quaternary mixtures of these enzymes were made and optimized for degradation of cellulose. These purified enzymes coupled with the quantitative proteomics results facilitated a direct comparison of the *N. crassa* secretome with the reconstituted cellulase system and the results reveal the importance of low abundance proteins in cellulose hydrolysis by *N. crassa*.

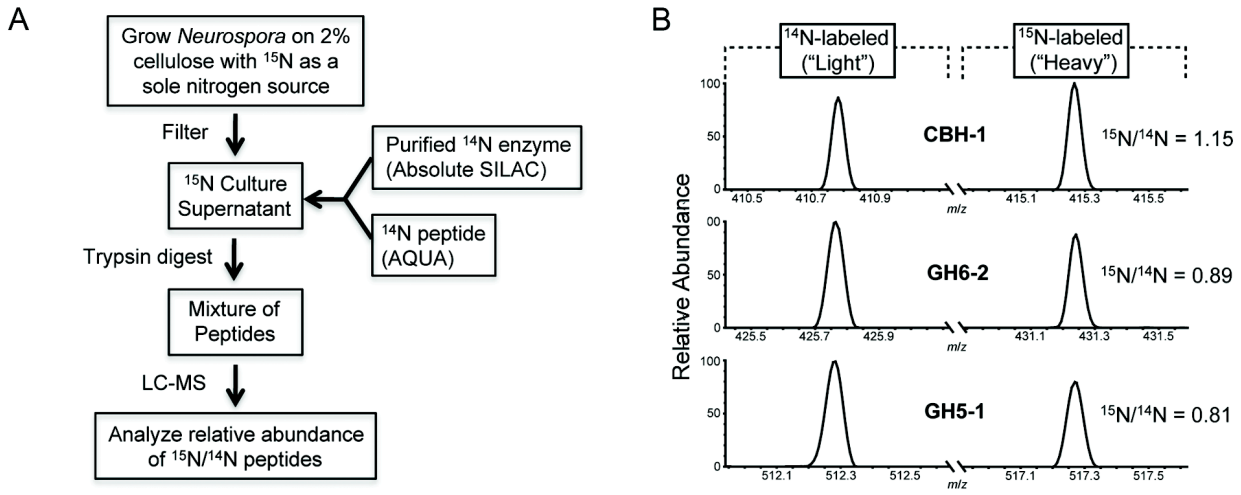

Figure 2.1. Workflow diagram and sample mass spectra of quantitative MS analysis. (A) To determine the absolute quantities of proteins secreted by *N. crassa*, the fungus was grown on Vogel's salts with 2% cellulose and $^{15}N^{2}$ ammonium nitrate as the sole nitrogen source. An ^{14}N-labeled internal standard, a peptide in the case of AQUA or a purified protein for Absolute SILAC, was added. The mixture of heavy supernatant and light internal standards was then digested with trypsin and the peptides analyzed by LC-MS. The mass spectral abundance ratios of heavy/light ions were then determined. (B) Sample mass spectra showing detail for heavy (^{15}N-labeled) and light (^{14}N-labeled) forms of peptide ions used for quantitative analysis, namely, the $(M + 2H)^{2+}$ ions of the peptides, VIFSNIK, TYINAIR, and IITDTDAFK, which correspond to residues 434-440 of CBH-1, 236-242 of GH6-2, and 186-194 of GH5-1. Absolute quantities of analyte proteins were determined from heavy:light ratios.

MATERIALS AND METHODS

Materials

Avicel® PH-101 (Sigma catalog #11-365), a form of microcrystalline cellulose, was used in all cellulase assays and growth experiments where cellulose was the sole carbon source. Acetonitrile (Fisher Optima grade, 99.9%) and formic acid (Pierce, 1 mL ampules, 99+%) were purchased from Fisher Scientific (Pittsburgh, PA) to prepare mobile phase solvents for liquid chromatography-mass spectrometry. All water was purified to a resistivity of 18.2 MΩ·cm (at 25 °C) using a Milli-Q Gradient ultrapure water purification system (Millipore, Billerica, MA).

Strains

All *Neurospora crassa* strains were obtained from the Fungal Genetics Stock Center (FGSC) including WT *N. crassa* (FGSC 2489). The gene deletion strain for *gh5-1* (FGSC 1647) was from the *N. crassa* functional genomics project(*44*). For preparation of conidia, strains were inoculated into 500 mL Erlenmeyer flasks containing 100 mL of Vogel's salts with 1.5% agar and 2% sucrose and grown for 3 days at 30 °C in the dark followed by 7 days at 25 °C in light.

Purification of core components

N. crassa CBH-1 was purified from WT *N. crassa* and GH6-2 was purified from a Δ*gh5-1* strain. A conidial suspension was then inoculated into Vogel's salts and 2% Avicel® at 25 °C in a 2.8 L ultrayield flask. Cultures were shaken at 200 rpm under constant light for 7 days post inoculum and then filtered over a 0.2 µm polyethersulfone (PES) filter. An affinity digestion was performed to purify and concentrate cellulose binding proteins based on their affinity for phosphoric acid swollen cellulose (*56*). Following digestion, samples were buffer exchanged into 25 mM Tris pH 8.5, 100 mM NaCl and proteins were purified by anion exchange chromatography. For purification of CBH-1 the affinity digest from the WT supernatant was directly loaded onto a MonoQ 10/100 GL column and eluted using a gradient from 100 mM to 1 M salt over 8 minutes. Purification of GH6-2 from the affinity digest of the Δ*gh5-1* strain was performed by loading the sample onto a Hiload 16/10 Q Sepharose HP column. GH6-2 in the flow through was collected, buffer exchanged into 25 mM Tris pH 8.5 and repurified over the MonoQ column using a shallow gradient from 0 to 100 mM NaCl over 10 minutes.

N. crassa GH5-1 with its native signal peptide for secretion and a C-terminal His tag for purification was homologously expressed and purified as described previously (*57*) with the following modifications. To decrease proteolysis of the His tag for constructs transformed with the pNeurA vector and to improve yields the TEV proteolysis site and GFP tag were removed using yeast recombineering (*58*). Further, the native *N. crassa* terminator, including 1 kb of sequence on the 5' end of the *gh5-1* ORF, in addition to the *Sc*ADH1 terminator were inserted following the *gh5-1* ORF and before the partial *his-3* sequence. This new vector, a derivative of pNeurA, was called pNevE-762. The recombinant rGH5-1 was shown to have equivalent or better activity than a natively purified GH5-1 (*57*).

N. crassa gh3-4 was amplified from cDNA from WT *N. crassa* during growth on Vogel's salts with 2% Avicel® as previously described (*59*) and was cloned into the pPicZαA vector which contains a signal peptide for secretion and a C-terminal 6xhis tag. This construct was then transformed into *P. pastoris* and expressed using the EasySelect Pichia Expression Kit (Invitrogen). The b-glucosidase was active and was shown to run at a similar molecular mass (75-80kDa) as the native enzyme (80kDa) (*46*).

Protein gel electrophoresis

Samples were added to 4x SDS Laemmli loading buffer, boiled 5 minutes, and loaded onto a Criterion 4-15% Tris-HCl polyacrylamide gel. Gelcode blue stain reagent (Thermo Scientific) was used for staining.

Isolation of secretome proteins for quantitative proteomics

A conidial suspension of WT *N. crassa* was then inoculated into 100 mL of Vogel's salts supplemented with 2% Avicel® in a 250 mL VWR Erlenmeyer flask. Vogel's salts contained $^{15}N_2$ ammonium nitrate (Cambridge Isostope Laboratories, CAS 43086-60-8) and this was used as the sole nitrogen source. After 7 days growth on Avicel® cultures were filtered over a 0.2 µm PES filter and concentrated to 2-3 mg/mL with a 10 kDa molecular weight cutoff spin concentrator using the Biorad Protein Assay with BSA as a standard. Cultures were grown in biological duplicate and these two distinct culture supernatants were analyzed for all quantitative mass spectrometry experiments.

Preparation of tryptic peptides for quantification

Thirty six milligrams of urea, 5 µL of 1 M Tris pH 8.5, and 5 µL of 100 mM DTT were added to 100 µL of 1 mg/mL ^{15}N culture supernatant and incubated at 65 °C for 60 minutes. Samples were then diluted with 700 µL 25mM ammonium bicarbonate and 140 µL methanol.

Fifty µL of 100 µg/mL trypsin (Promega sequencing grade) in 50 mM sodium acetate was then added to cleave peptide bonds on the carboxylic side of lysine and arginine residues. Samples were incubated overnight at 37 °C on a rocker. Following digestion, the samples were dried in a speed vac, washed with 300 µL MilliQ water 3 times and then desalted with OMIX microextraction tips. AQUA peptides (Biomer Technology, Pleasanton, CA) were ordered at >95% purity and were dissolved in 50% water:50% acetonitrile at a concentration of 0.04 mg/mL. AQUA peptides were added to samples following methanol addition to avoid solubility issues associated with adding some peptides. For Absolute SILAC, purified proteins were added to the 100 µL of 1 mg/mL ^{15}N culture supernatant before incubation at 65 °C.

Ultraperformance liquid chromatography

Trypsin-digested protein samples were analyzed using a tandem mass spectrometer that was connected in-line with an ultraperformance liquid chromatograph (UPLC). Peptides were separated using a nanoAcquity UPLC (Waters, Milford, MA) equipped with C_{18} trapping (180 µm × 20 mm) and analytical (100 µm × 100 mm) columns and a 10 µL sample loop. Solvent A was 99.9% water/0.1% formic acid and solvent B was 99.9% acetonitrile/0.1% formic acid (v/v). Sample solutions contained in 0.3 mL polypropylene snap-top autosampler vials sealed with septa caps were loaded into the nanoAcquity autosampler compartment prior to analysis. Following sample injection, trapping was performed for 5 min with 100% A at a flow rate of 3 µL/min. The injection needle was washed with 500 µL each of solvents A and B after injection to avoid cross-contamination between samples. The elution program consisted of a linear gradient from 5% to 40% B over 50 min, a linear gradient to 95% B over 0.33 min, isocratic conditions at 95% B for 5.67 min, a linear gradient to 1% B over 0.33 min, and isocratic conditions at 1% B for 13.67 min, at a flow rate of 500 nL/min. The analytical column and autosampler compartment were maintained at 35 ºC and 8 ºC, respectively.

Mass spectrometry and tandem mass spectrometry

The UPLC column exit was connected to a Universal NanoFlow Sprayer nanoelectrospray ionization (nanoESI) emitter that was mounted in the nanoflow ion source of a quadrupole time-of-flight mass spectrometer (Q-Tof Premier, Waters). The nanoESI emitter tip was positioned approximately 2 mm from the aperture of the sampling cone. The nanoESI source parameters were as follows: nanoESI voltage 2.3 kV, sample cone voltage 30 V, extraction cone and ion guide voltages 4 V, and source block temperature 80 ºC. No cone gas was used. The collision cell contained argon gas at a pressure of 8×10^{-3} mbar. The Tof analyzer was operated in "V" mode. Under these conditions, a mass resolving power(*60*) of 1.0×10^4 (measured at m/z = 771) was achieved, which was sufficient to resolve the isotopic distributions of the multiply charged peptide ions that were measured in this study. Thus, an ion's mass and charge could be determined independently, i.e., the charge state was determined from the reciprocal of the spacing between adjacent isotope peaks in the m/z spectrum. External mass calibration was performed prior to analysis using solutions of sodium formate(*61*). Mass spectra were acquired in the positive ion mode over the range m/z = 400-1500 using a 0.95 s scan integration and a 0.05 s interscan delay. In the data-dependent mode, up to five precursor ions exceeding an intensity threshold of 30 counts/second (cps) were selected from each survey scan for tandem mass spectrometry (MS/MS) analysis. Real-time deisotoping and charge state recognition were used to select 2+, 3+, 4+, and 5+ charge state precursor ions for MS/MS. Collision energies for collisionally activated dissociation (CAD) were automatically selected based on the mass and charge state of a given precursor ion. MS/MS spectra were acquired over the range m/z = 50-2000 using a 0.45 s scan integration and a 0.05 s interscan delay. Ions were

fragmented to achieve a minimum total ion current (TIC) of 30,000 cps in the cumulative MS/MS spectrum for a maximum of 3 s. To avoid the occurrence of redundant MS/MS measurements, real-time dynamic exclusion was used to preclude re-selection of previously analyzed precursor ions over an exclusion width of ± 0.2 *m/z* unit for a period of 180 s. Mass spectrometry data processing was performed using MassLynx software (version 4.1, Waters). Data resulting from LC-MS/MS analysis of trypsin-digested proteins were searched against the *N. crassa* protein database as described elsewhere (*46*).

Quantification of peptides was performed by manual integration of the peaks in the extracted ion chromatograms for the "heavy" (^{15}N-labeled) and "light" (^{14}N-labeled) forms of peptide ions. Mass spectral abundance ratios, heavy:light, were calculated from the peak areas of the heavy and light forms of the peptides. A standard curve plotting mass spectral abundance ratios, heavy:light, against the corresponding protein mixture ratios was generated, using intact CBH-1, to assess the linearity of the instrument response and to check for systematic error. The resulting curve exhibited a slope of 0.7975 and a linear correlation coefficient of 0.993 for the range, heavy:light ratio = 0.20 to 4.2 (data not shown).

Activity assays

All activity assays were performed in triplicate with 5 mg/mL Avicel® in 50 mM sodium acetate pH 5.0 at 40 °C. Assays of the binary and ternary cellulase mixtures were performed in 100 µL volumes in round bottom 96 well plates (Corning) and covered with aluminum sealing tape (Nunc). Each assay contained 1.0 µM total cellulase and 0.1 µM GH3-4. Wells contained one 3 mm glass bead each and were shaken at 200 rpm to provide sufficient mixing to keep the Avicel® from settling. At 24 hours microplates were centrifuged for 2 minutes at 4000 rpm to pellet the remaining Avicel® and 70 µL of assay mix was removed per well. Samples were incubated at 98 °C for 10 minutes then incubated with 7 µL of desalted, diluted Novozyme 188 (Sigma) for an additional 15 minutes at 40 °C. Assay supernatant (15 µL) was then analyzed for glucose using the glucose oxidase/peroxidase assay as described previously (*46*).

Assays comparing the activity of the *N. crassa* culture supernatant and the reconstituted cellulase mixture were performed as above with the following exceptions. Assays were performed in 1.5 mL microcentrifuge tubes with 1.0 mL total volume and were inverted 20 times per minute. Assays contained 0.1 mg/mL culture supernatant or 0.065 mg/mL reconstituted cellulase mixture containing CBH-1, GH6-2, GH5-1, and GH3-4 present in the ratio determined from the Absolute SILAC experiment (0.039 mg/mL CBH-1, 0.017 mg/mL GH6-2, 0.006 mg/mL GH5-1, 0.003 mg/mL GH3-4). One hundred µL assay mix was removed at 2, 6, and 24 hours. Samples were then centrifuged to remove Avicel® and supernatants were incubated at 98 °C for 10 minutes. Soluble sugars were measured by the glucose oxidase/peroxidase assay and the cellobiose dehydrogenase assays as described previously (*46*). Percent degradation was calculated based on the amounts of glucose and cellobiose measured relative to the theoretical conversion of 5 mg/mL Avicel®.

The ternary graph was constructed based on data representing a simple lattice of all possible combinations of CBH-1, GH6-2, and GH5-1 where each component was varied in 0.1 µM increments from 0 to 1.0 µM with the total concentration of cellulase held constant at 1.0 µM and the concentration of GH3-4 held constant at 0.1 µM for all 67 assays. The resulting data was then analyzed using Design-Expert software (version 8, Stat-Ease, Minneapolis, MN) and the best model was chosen (Adjusted R-squared = 0.895; Predicted R-squared = 0.8740). All activity assays were performed in triplicate with the exception of the data used to generate the ternary graph which was performed at least in duplicate.

RESULTS AND DISCUSSION

AQUA analysis of *N. crassa* secretome grown on cellulose

Absolute quantification (AQUA) of the *N. crassa* secretome was initiated by the selection of candidate proteins, and subsequently candidate peptides, to serve as internal standards for LC-MS analysis. Our previous work investigated the secretome of *N. crassa* during growth on cellulose and 25 proteins were initially identified followed by an additional 13 proteins after fractionation of cellulose binding and non-cellulose binding proteins(*46*). In the present study, 13 of those 38 total proteins were selected for AQUA analysis (Table 2.1). Selection of these 13 proteins was based on potential activity on cellulose (9 are predicted cellulases and 2 of the others contain a cellulose binding domain, CBM1) and relative abundance, as indicated by SDS-PAGE. None of these proteins were detected in the secretome following growth on glucose suggesting that they were specific to cellulose hydrolysis (data not shown). Tryptic peptides to be used for quantitative analysis were selected, for each of the proteins of interest, which were consistently detected during LC-MS/MS analysis. Peptides were further selected so as to minimize the possibility of post-translational or chemical modifications that could potentially complicate peptide quantification. A list of the peptides quantified in this study are present in the appendix (Table A2.2 and A2.3)

A workflow (Figure 2.1) was then developed in which *N. crassa* was grown on Vogel's salts with 2% cellulose and $^{15}N_2$ ammonium nitrate as a sole nitrogen source. After 7 days the culture was filtered, concentrated, and the synthetic ^{14}N-labeled peptides were added to the culture supernatant at a known concentration. This mixture of proteins was then reduced with DTT, digested overnight with trypsin, desalted, and analyzed by LC-MS. Sample mass spectra showing the ratios of heavy:light ions specific to CBH-1, GH6-2, and GH5-1 are shown in Figure 1B and from such ratios the absolute concentrations of multiple proteins in a sample were determined (Table 2.1). All measurements were made in biological duplicates and the range was typically 8% and no more than 13% for all sample duplicates. Further, the use of $^{15}N_2$ ammonium nitrate as the sole nitrogen source had no observable effect on the expression profile of secretome proteins as determined by SDS-PAGE (Figure 2.2). The total weight of secretome proteins for each sample was determined via quantitative amino acid analysis (UC-Davis Molecular Structure Facility) and the percentage of total weight attributed to each protein in the culture supernatant was then calculated (Figure 2.3).

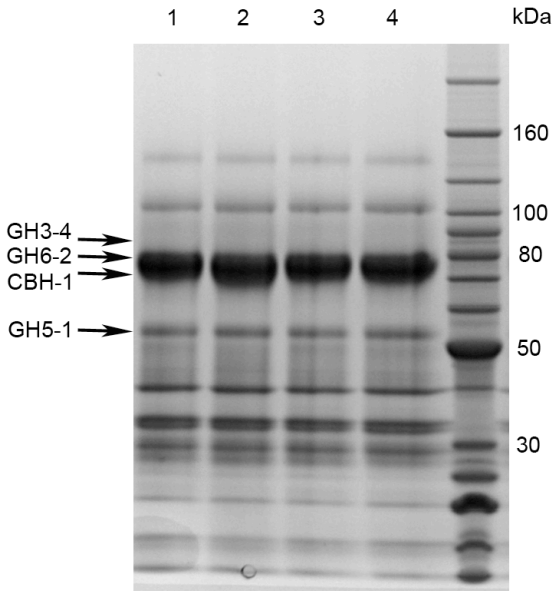

Figure 2.2. SDS-PAGE of *N. crassa* secretome on cellulose
N. crassa was grown in biological duplicate on Vogel's salts supplemented with 2% cellulose and $^{14}N^{2}$ ammonium nitrate (replicates shown in lanes 1 and 2) or $^{15}N^{2}$ ammonium nitrate (replicates shown in lane 3 and 4). After 7 days the cellulose was completely degraded and these culture supernatants were harvested and used for the quantitative proteomic analysis.

Analysis of the AQUA results revealed that 53% of the total supernatant protein could be attributed to 2 predicted cellobiohydrolases (CBH-1 and GH6-2). Both of these enzymes are ubiquitous throughout cellulolytic ascomycetes that cause soft rot and it is generally accepted that they act specifically from the reducing end (CBH-1) or non-reducing end (GH6-2) of the substrate (*20*). Moreover, these proteins are typically the two most abundant enzymes in most industrial cellulase cocktails (*41, 62*). Three predicted endoglucanases including GH5-1 (Endoglucanase II-like), GH7-1 (Endoglucanase I-like), and GH6-3 (Endoglucanase VI-like) were also detected and represent 13% of the total supernatant by weight. GH5-1 was the most abundant of the endoglucanases (5.9%) consistent with the observation that the Δ*gh5-1* strain results in a 70-80% reduction in the azo-CMC activity of the culture supernatant during growth on cellulose (*46, 57*). Finally, a predicted ß-glucosidase (GH3-4) accounted for 3.8% of the total protein and this was the only enzyme in the secretome predicted to contain this activity.

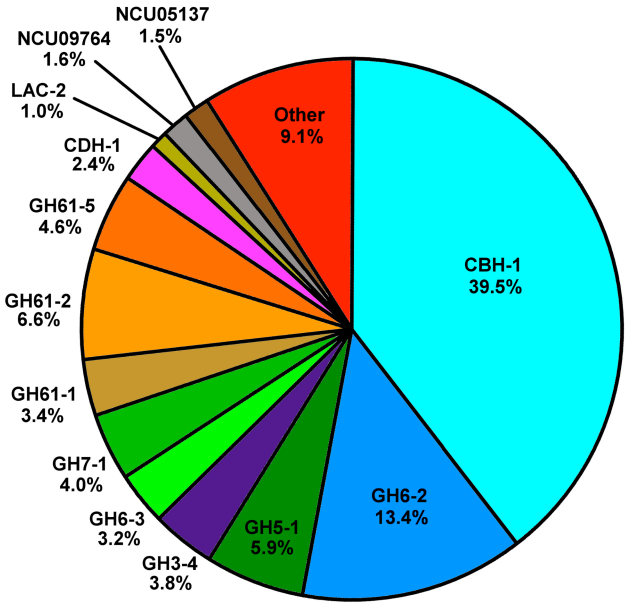

Figure 2.3. Chart showing the relative mass abundances of secreted proteins. To quantify proteins in the *N. crassa* secretome during growth on cellulose, peptides were synthesized and analyzed by the AQUA method. Thirteen proteins are predicted to comprise 91% of the weight of the culture supernatant protein during growth on cellulose with the remaining 9% likely consisting of other carbohydrate-active enzymes previously detected via LC-MS/MS.

In addition to these cellulases, a number of lower abundance accessory proteins were quantified. Three GH61 proteins (GH61-1, GH61-2, and GH61-5) were present in varying amounts and represented nearly 15% of the supernatant protein by weight. A fourth GH61 protein (GH61-4; NCU01050) was also detected consistently but was not successfully quantified in this study. A cellobiose dehydrogenase (CDH-1) containing a cellulose-binding module 1 (CBM1) and a type 2 lactonase (LAC-2) homologous to one recently characterized in *S. thermophile* (*63*) were also present at 2.4% and 1.0% of the secretome, respectively. Finally, two hypothetical proteins were present at less than 2% of the secretome weight including NCU09764, a CBM1-containing protein of unknown function, and NCU05137, a gene which when deleted led to an increase in cellulase expression (*46*).

All together these proteins accounted for 91% of the total secretome by weight with the remaining 9% likely attributed to other proteins previously detected via LC-MS/MS (3). The majority of the remaining proteins are predicted to be glycosyl hydrolases or esterases specific to non-cellulosic cell wall polysaccharides.

AQUA

Protein Name	Predicted Function	(µmol/g secretome) Average	Range[1]	Weight percent of supernatant
CBH-1	cellobiohydrolase	7.43	0.81	39.5%
GH6-2	cellobiohydrolase	2.73	0.05	13.4%
GH5-1	endoglucanase	1.46	0.11	5.9%
GH3-4	beta-glucosidase	0.50	0.06	3.8%
GH6-3	endoglucanase	0.81	0.07	3.2%
GH7-1	endoglucanase	0.89	0.06	4.0%
GH61-1	cellulase enhancing protein	1.07	0.07	3.4%
GH61-2	cellulase enhancing protein	2.72	0.21	6.6%
GH61-5	cellulase enhancing protein	1.44	0.13	4.6%
CDH-1	cellobiose dehydrogenase	0.28	0.02	2.4%
LAC-2	lactonase	0.26	0.03	1.0%
N/A	hypothetical with cbm1	0.41	0.00	1.6%
N/A	hypothetical	0.21	0.02	1.5%

ABSOLUTE SILAC

Protein Name	Predicted Function	(µmol/g secretome) Average	Range[1]	Weight percent of supernatant
CBH-1	cellobiohydrolase	7.27	0.47	38.6%
GH6-2	cellobiohydrolase	3.46	0.70	16.7%
GH5-1	endoglucanase	1.59	0.16	6.4%
GH3-4	beta-glucosidase	0.43	0.00	3.3%

1 - Range represents range of biological replicates.

GH, glycoside hydrolase; cbm, cellulose binding domain.

Table 2.1. Quantification of secreted *N. crassa* proteins during growth on cellulose

Absolute SILAC as verification of AQUA results

While AQUA analysis serves as an expedient method to quantify proteins based on a synthetic peptide standard, there are disadvantages associated with quantifying intact proteins based on the measurement of a single peptide. To evaluate the accuracy of the AQUA results, Absolute SILAC was used to provide a more robust technique for quantification. In addition to facilitating the quantification of multiple peptides, the use of intact protein requires a complete tryptic digest of the ^{15}N-labeled internal standard as well as the ^{14}N-labeled secretome sample (*64*). Here, Absolute SILAC was carried out on four purified proteins, CBH-1, GH6-2, GH5-1, and GH3-4. For each protein, four peptides were selected and quantified (Table 2.1 and Table A2.2).

There was excellent agreement between the results obtained using AQUA and Absolute SILAC, with differences ranging from 2% for CBH-1 to 22% for GH6-2 (Figure 3). The relative standard deviations of heavy:light ratios for the four different peptides from a given protein were less than 12% in all cases. This Absolute SILAC analysis showed that these four proteins account for 65% of the total secretome on cellulose and are present at a relative molar ratio of 6.0 (CBH-1) : 2.6 (GH6-2) : 1.0 (GH5-1) : 0.5 (GH3-4).

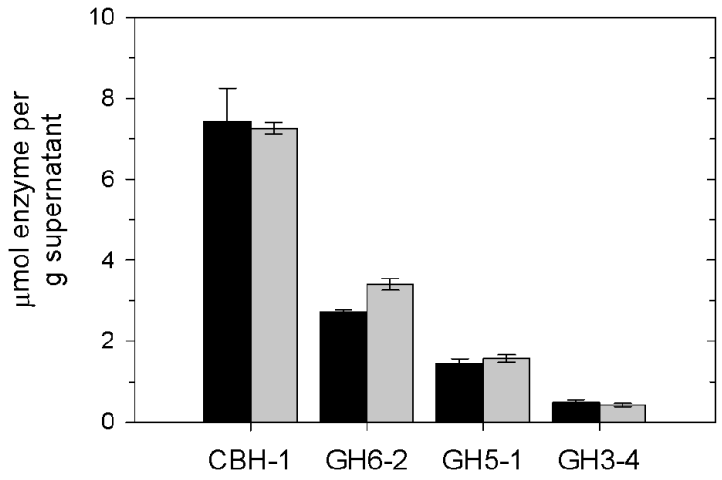

Figure 2.4. Comparison of results from AQUA and absolute SILAC. To evaluate the accuracy of the quantifications made by AQUA analysis, Absolute SILAC was carried out for CBH-1, GH6-2, GH5-1, and GH3-4, in which intact purified proteins were used as internal standards. Four peptides from each of the proteins were quantified to eliminate any bias associated with using a single peptide. Results from AQUA (black) were then compared with Absolute SILAC (gray). All experiments were performed in biological duplicates. There was good agreement between the results obtained using Absolute SILAC and AQUA. In total, these four proteins accounted for 65% of the secretome by weight. The error bars represent the range of biological duplicates for both methods.

Reconstitution and characterization of a defined cellulase system

Utilizing the knowledge gained from the quantitative mass spectrometry, coupled with a basic understanding of fungal cellulose degradation, the design of a minimal, defined cellulase system that would contain all the necessary activities required for cellulose hydrolysis was attempted. CBH-1, GH6-2, GH5-1, and GH3-4 were chosen as the core components of this system. CBH-1 and GH6-2 represented more than half of the total supernatant by weight and the respective specificity differences for the chain ends of cellulose are thought to be required for efficient cellulose hydrolysis. Endoglucanase GH5-1 was chosen because it was the most abundant endoglucanase and is responsible for most of the Azo-CMC activity in the culture supernatant (*57, 59*). Finally, GH3-4 was the only ß-glucosidase detected and was included to decrease product inhibition of the other cellulases (*21, 65*). These four enzymes are highly conserved in cellulolytic fungi and their homologs have been consistently identified in secretome analyses of fungi performed during growth on plant biomass. They are absolutely conserved throughout cellulolytic Ascomycetes and have been detected in the secretome of *Trichoderma reesei (62)*, *Aspergillus fumigatus* (*66*), and the plant pathogens *Botrytis cinerea (67, 68) and Fusarium graminearum (69)*. Many basidiomycetes also contain homologs of these four enzymes including the white rot fungi *Phanaerochaete chrysosporium (70),* though CBH-1 and a GH6 cellobiohydrolase are notably absent in the brown rot fungus *Postia placenta (37, 70)*.

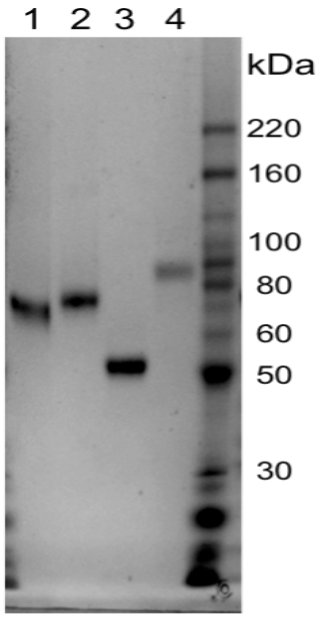

Figure 2.5. SDS-PAGE of purified *N. crassa* proteins
CBH-1 (lane 1) and GH6-2 (lane 2) were isolated from culture supernatant of *N. crassa* after 7 days of growth on cellulose. They were purified using the affinity digestion method followed by separation over Q HP and MonoQ ion exchange columns. GH5-1 (lane 3) and GH3-4 (lane 4) were expressed and secreted in *N. crassa* and *P. pastoris*, respectively, with C-terminal His tags and were subsequently purified using Ni^{2+} affinity chromatography. All purified proteins were identified via LC-MS/MS as the only proteins present in the respective purified samples.

CBH-1, GH6-2, GH5-1, and GH3-4 were purified to investigate the activity of this defined cellulase system (Methods and Figure 2.5). The activities of the individual cellulases as well as binary and ternary mixtures of the cellulases in the presence of the ß-glucosidase GH3-4 were assayed on microcrystalline cellulose (Avicel®). Analysis of binary mixtures of the three cellulases (Figure 4A-C) revealed both cellobiohydrolase-endoglucanase and cellobiohydrolase-cellobiohydrolase synergy as all titrations showed activity greater than expected in the absence of interaction. The combination of the two cellobiohydrolases (Figure 2.6C) gave the best activity (20-23% degradation after 24 hours hydrolysis). All combinations of these two enzymes were significantly more active than either enzyme alone while the same was not true for combinations of the cellobiohydrolases with the endoglucanase GH5-1 (Figure 2.6A and 2.6B). The importance of CBH-1 and GH6-2 was further emphasized in ternary mixtures of all three cellulases in the presence of ß-glucosidase. A ternary diagram of the results confirms that *N. crassa* endoglucanase GH5-1 has little effect on the total cellulase activity at 24 hours (Figure 2.6D). Further, the optimal ratio of these enzymes as determined by quantitative MS is similar, though distinct, from the optimal ratio predicted in the ternary diagram.

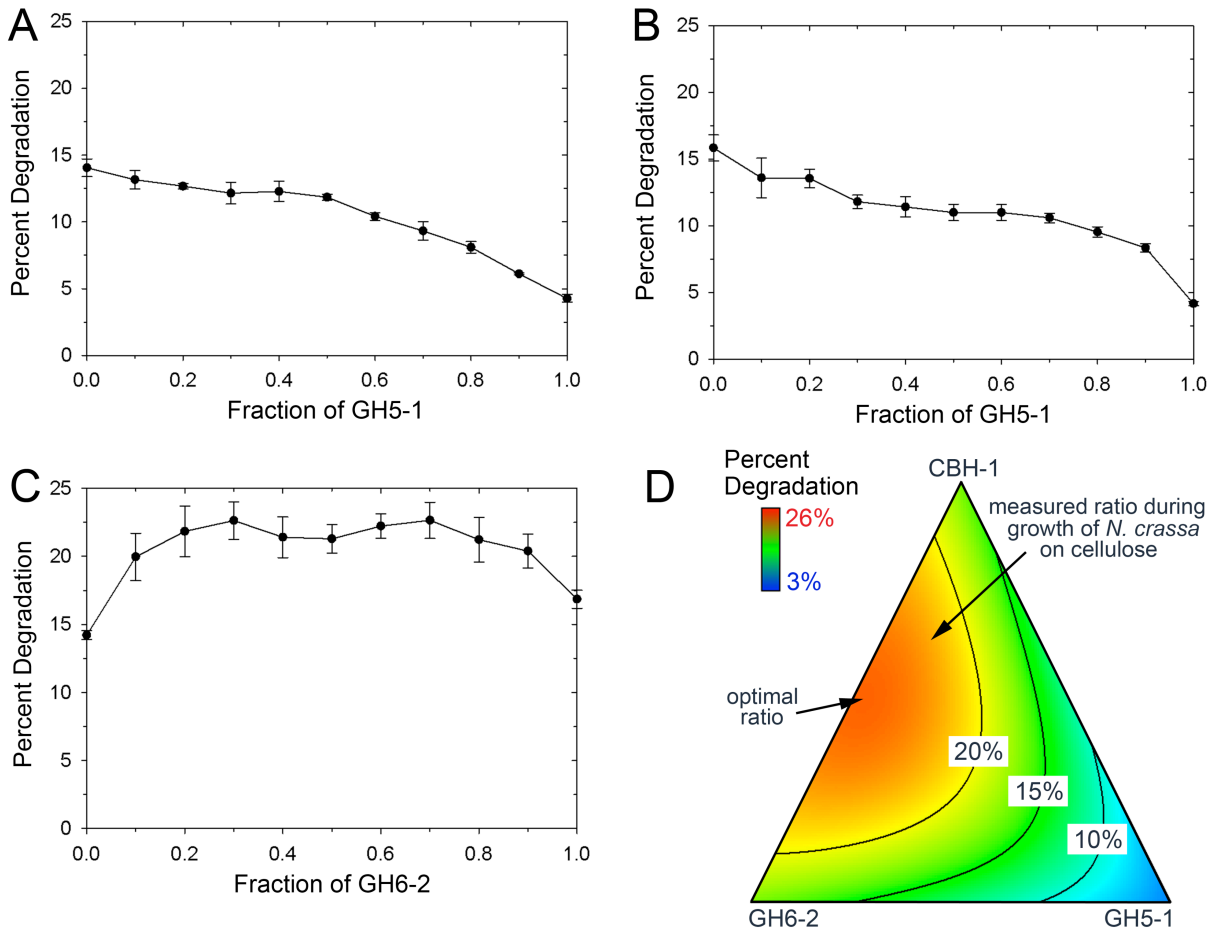

Figure 2.6. Binary and ternary mixtures of *N. crassa* cellulases. Cellulase assays contained 5 mg/mL cellulose, 50 mM sodium acetate pH 5.0, 1.0 µM total cellulase and 0.1 µM GH3-4 to prevent cellobiose accumulation. After 24 hours mixing at 40 °C the percent degradation was calculated by measurement of the total glucose in the supernatant with the glucose oxidase/peroxidase assay. Binary mixtures were as follows: (A) CBH-1 and GH5-1, (B) GH6-2 and GH5-1, and (C) CBH-1 and CBH-2. (D) Ternary mixtures of the three cellulases were also performed and a ternary diagram was generated to predict the optimal ratio for conversion of cellulose. The optimal ratio as identified in this assay and the ratio of these 3 proteins during growth of *N. crassa* on cellulose are shown. All binary assays were performed in triplicate (error bars indicate the standard deviations) and each ternary assay was performed at least in duplicate.

Contribution of accessory proteins in cellulose hydrolysis

Utilizing these purified components, the contribution of the defined system to the total cellulase activity present in the *N. crassa* secretome was determined. A cellulase assay was carried out where the absolute concentrations of CBH-1, GH6-2, GH5-1 and GH3-4 in the defined system were identical to that of the *N. crassa* secretome. The defined mixture comprised 63-65% of the total secretome (Table 1) by weight and contained the four primary activities associated with fungal cellulose degradation. The activity of the reconstituted mixture achieved 43% of the activity of the *N. crassa* secretome on cellulose after 24 hours (Figure 2.7), suggesting that additional proteins in *Neurospora* enhance the degradation of cellulose.

Despite the evidence suggesting that these cellulases are among the most conserved in fungal cellulose degradation, they only partially reconstituted the activity of the *N. crassa* secretome in assays on cellulose. This is in contrast to a similar study where the activity of the *T. reesei* supernatant on filter paper was completely reconstituted with just four cellulases including two cellobiohydrolases (CBHI and CBHII) and two endoglucanases (EGI and EGIII) (*41*).

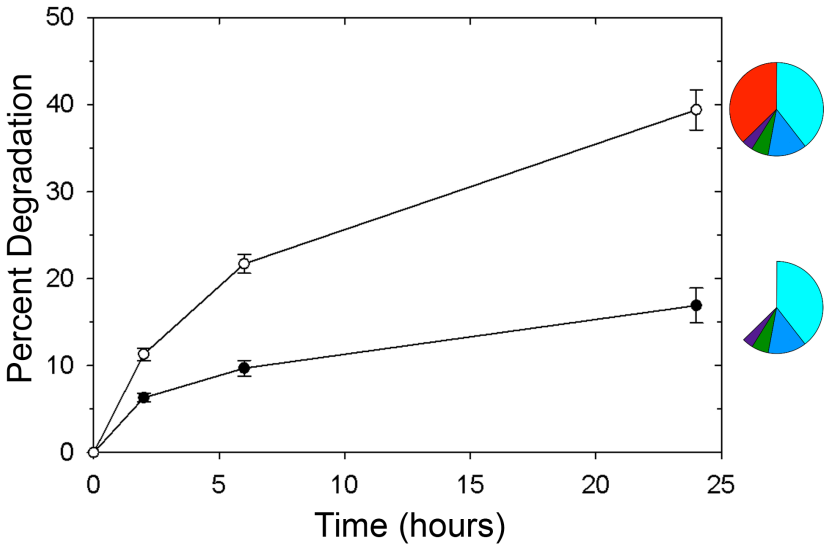

Figure 2.7. Cellulase assay of ternary mixture versus culture supernatant. A cellulase assay with 5 mg/mL cellulose comparing the activity of a defined mixture of CBH-1, GH6-2, GH5-1, and GH3-4 (filled circles) versus that of the *N. crassa* culture supernatant grown on cellulose (open circles). The relative ratio of the quaternary mixture is equivalent to that predicted by Absolute SILAC and the total loading was 0.065 mg/mL. The triangles represent a supernatant loading of 0.1 mg/mL where CBH-1, GH6-2, GH5-1, and GH3-4 are present at the same concentration as the defined mixture with additional proteins constituting the other 0.035 mg/mL. While the defined mixture comprises 65% of the culture supernatant by weight, it has just 43% of the total cellulase activity at 24 hours. All assays were performed in triplicate with the standard deviations indicated by error bars.

It is likely that one or many of the other enzymes identified and quantified by AQUA are responsible for the substantially higher activity of the total secretome of *Neurospora* relative to the defined mixture. One hypothesis is that the putative endoglucanases GH7-1 and GH6-3 could be responsible for an increase in activity. However, given the results of the ternary diagram (Figure 4D), in which endoglucanase activity does not appear to be limiting, it is unlikely that these two proteins account for the full 2.3-fold increase in hydrolysis. Despite this observation, it is possible that alternative endoglucanases may be important in accessing different faces or subsites on the cellulose surface and these different specificities could lead to improved activity.

An alternative hypothesis is that one or more of the remaining proteins identified in the secretome is capable of stimulating hydrolysis by the primary cellulases. Recently, the GH61 proteins were described as metalloproteins having cellulase-enhancing activity despite having no

inherent hydrolytic activity (*71*). This effect was only seen with assays on pretreated corn stover and not on pure cellulose leading the authors to suggest that the cellulase enhancing activity of GH61 may be limited to substrates containing hemicellulose and/or lignin. It is tempting to speculate that the stimulating effect could occur on pure cellulose given that GH61-1, GH61-2, and GH61-5 comprised nearly 15% of the *N. crassa* secretome on a weight basis during growth on pure cellulose. Further, the GH61 family of proteins is significantly larger in the *N. crassa* genome which contains 14 GH61 family proteins, relative to *T. reesei* which contains just two (*15*). This may provide an alternative explanation for the different results obtained when the purified *T. reesei* cellulases were compared to the *T. reesei* culture supernant grown on cellulose (*41*). In regard to the GH61 proteins *T. reesei* may be the outlier, as many fungi including several *Aspergillus* species*, P. chrysosporium*, *Chaetomium globosum*, and multiple other fungi have significantly expanded sets of GH61 proteins (*15*) whose production under cellulolytic growth has been confirmed in secretome studies as well.

Another potential candidate for an accessory role in cellulose degradation is the CDH-1 protein, a cellobiose dehydrogenase linked to a CBM1, that is absent in *T. reesei,* but present in the secretome of *P. chrysosporium (70)*. This protein oxidizes cellobiose and other cello-oligomers to sugar lactones and for many years these dehydrogenases have been hypothesized to play a role in cell wall degradation, though the biological function of this enzyme family remains uncertain (*72*). Three remaining candidates quantified here include a lactonase (*63*) and two proteins of unknown function, one of which contains a CBM1.

To evaluate the role that GH61 proteins have in cellulose degradation, the culture supernatant of *N. crassa* was assayed in the presence and absence of 1 mM EDTA (Figure 2.8). Previous analyses have shown that a divalent metal is required for GH61 activity and that EDTA can be used to prevent its cellulase enhancing effect (*71*). Assays were setup as previously described with 0.1 mg/mL supernatant and 5 mg/mL Avicel. The addition of EDTA to cellulase assays had a significant inhibitory effect resulting in 42% lower cellulase activity than the supernatant alone after 24 hours incubation. Purified *N. crassa* cellulases are not inhibited by EDTA. This strongly supports the notion that metals or metalloproteins are important for cellulose degradation and results from the quantitative proteomics suggest a probable role for the GH61 family of proteins.

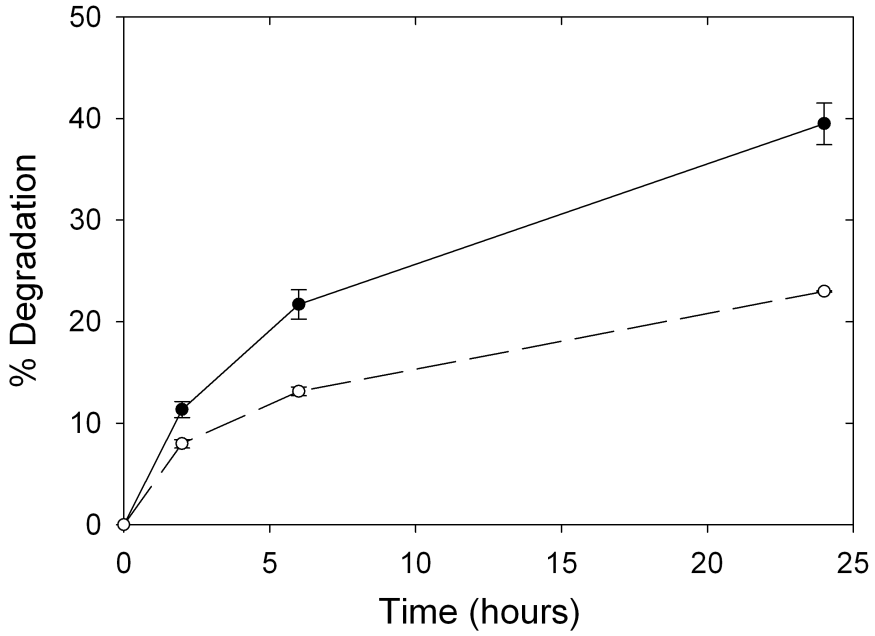

Figure 2.8. EDTA Inhibition of *N. crassa* cellulases. Effect of EDTA on cellulase activity of wild-type *N. crassa* culture filtrate. Cellulase activity of the wild-type *N. crassa* culture filtrate (•) in the presence of 1.0 mM EDTA ( ). Values are the mean of three replicates. Error bars are the SD between these replicates.

CONCLUSIONS

In this report, a quantitative proteomic approach was taken to reconstitute the cellulase activity of the *N. crassa* secretome *in vitro* through the expression and purification of four abundant enzymes believed to be at the core of fungal cellulose degradation. A combination of AQUA and Absolute SILAC was taken to quantify 13 proteins secreted by *N. crassa* during growth on pure cellulose and four of these proteins were then purified and used to create a defined cellulase system consisting of 2 cellobiohydrolases (CBH-1 and GH6-2), an endoglucanase (GH5-1), and a β-glucosidase (GH3-4). Together these four proteins comprised 65% of the total secretome by weight. An in vitro assay coupled with statistical modeling of this data suggests that the optimal cellulase activity would be achieved with a mixture of 48.0% CBH-1, 49.4% GH6-2, and 2.6% GH5-1. This ratio is similar to the ratio seen in *N. crassa* supernatants grown on cellulose in that the two cellobiohydrolases (CBH-1 and GH6-2) are significantly more abundant than the endoglucanase GH5-1, but it differs in its lack of preference for CBH-1 over GH6-2. Despite the evidence suggesting that these three cellulases are among the most abundant in fungal cellulose degradation, these three cellulases coupled with the primary ß-glucosidase (GH3-4) were only able to partially reconstitute the activity of the *N. crassa* secretome in assays on cellulose. Further, EDTA was shown to decrease the activity of the N. crassa secretome supporting a propable role for metalloproteins like GH61.

These results, coupled with the increasing number of genomic, transcriptomic, and proteomic analyses of filamentous fungi (*37, 49-51, 59, 62, 70, 73*) highlight important

opportunities for characterizing understudied proteins implicated in cellulose degradation by fungi. Through investigating mechanisms beyond the traditional understanding of cellulose degradation by cellobiohydrolases and endoglucanases, it may be possible to capitalize on the diversity of fungal enzymes secreted for efficient conversion of plant biomass.

PREVIOUSLY PUBLISHED MATERIAL

This chapter was modified from a previously published article co-authored by Anthony T. Iavarone and Michael A. Marletta. Thanks to the co-authors and publishers at the Journal of Proteome Research for allowing use of this material.

NCU number	Protein name	Predicted function	Residues	Peptide sequence
NCU07340	CBH-1	cellobiohydrolase	434-440	VIFSNIK
NCU09680	GH6-2	cellobiohydrolase	236-242	TYINAIR
NCU00762	GH5-1	endoglucanase	186-194	IITDTDAFK
NCU04952	GH3-4	beta-glucosidase	54-64	VNIVTGVGWNK
NCU07190	GH6-3	endoglucanase	193-200	EGIAFAIK
NCU05057	GH7-1	endoglucanase	407-413	VTFSNIK
NCU02240	GH61-1	cellulase enhancing protein	67-77	IITVNAGSTVK
NCU07898	GH61-2	cellulase enhancing protein	202-215	TPSSGLVSFPGAYK
NCU08760	GH61-5	cellulase enhancing protein	137-144	IFEDTWAK
NCU00206	CDH-1	cellobiose dehydrogenase	675-686	AAVVQGIVNLQK
NCU07143	LAC-2	lactonase	176-188	FMLVPDLGADLIR
NCU09764	N/A	hypothetical with cbm1*	113-121	VFYHFSLMR
NCU05137	N/A	hypothetical	453-460	AFLDNGIR

GH, glycoside hydrolase; cbm, cellulose binding domain

Table 2.2. Peptides used for quantitative analysis using the AQUA technique.

NCU number	Protein name	Predicted function	Residues	Peptide sequence
NCU07340	CBH-1	cellobiohydrolase	115-124	GSYSTNIGSR
			303-311	FTVVTQFIK
			356-366	TAFGDIDDFNK
			434-440	VIFSNIK
NCU09680	GH6-2	cellobiohydrolase	166-174	VPTFQWLDR
			184-190	STLEEIR
			236-242	TYINAIR
			244-252	LLIEYSDIR
NCU00762	GH5-1	endoglucanase	126-133	SQGYNIFR
			134-140	VGFAMER
			186-194	IITDTDAFK
			306-314	IVGATAWLR
NCU04952	GH3-4	beta-glucosidase	54-64	VNIVTGVGWNK
			373-387	LAIIGSSSVVNPAGR
			550-556	LPYTIAK
			630-644	ADLWETVATVTAVVK

GH, glycoside hydrolase

Table 2.3. Peptides used for quantitative analysis using the Absolute SILAC technique.

CHAPTER 3: Characterization of a Δ*cdh-1* strain

ABSTRACT

Deletion of *cdh-1,* the major cellobiose dehydrogenase (CDH) of *Neurospora crassa,* reduces cellulase activity in the culture filtrate of the Δ*cdh-1* strain to levels 37-49% lower than in the wild-type strain. Addition of purified CDHs to the Δ*cdh-1* strain culture filtrate resulted in a 1.6 to 2.0-fold stimulation in cellulase activity, which restored activity to wild-type levels, while addition of CDH to a mixture of purified cellulases showed no stimulatory effect. Domain truncations of a full length CDH showed that the heme domain is required for the observed stimulatory effects on cellulase activity. The stimulatory effect of CDH requires the presence of molecular oxygen and likely other metalloproteins.

INTRODUCTION

The filamentous ascomycete, *Neurospora crassa,* is a well-known genetically tractable organism that proficiently degrades plant cell walls (*44, 59*). *N. crassa* secretes more than 30 different enzymes during growth on pure cellulose. Many of these enzymes are similar to cellulases and hemicellulases that have been extensively studied in other organisms, but there are also a significant number of enzymes with poorly defined or no known biological functions. In addition to hydrolytic enzymes, *N. crassa* also produces large amounts of cellobiose dehydrogenase (CDH) (*74-76*). CDH-1 is the major oxidoreductase secreted by *N. crassa* during growth on crystalline cellulose, and accounts for approximately 1-3% of the total secreted protein, suggesting a potential role in the degradation process.

CDH was first described over 35 years ago and since then has been identified in phylogenetically diverse fungi (*77*), but is notably absent from the industrial workhorse *Hypocrea jecorina (anamorph Trichoderma reesei).* The CDH from the white-rot fungus, *Phanerochaete chrysosporium,* has been extensively studied biochemically and by x-ray crystallography (*78-80*). CDH catalyzes the oxidation of cellobiose and longer cellodextrins to the corresponding 1-5-δ-lactones. All CDH enzymes contain an N-terminal heme domain and a C-terminal flavin domain. The flavin domain is part of the larger glucose-methanol-choline (GMC) oxidoreductase superfamily (*81*), which is widespread throughout all domains of life, while orthologs of the heme domain are only found in fungi (*82*). Oxidation of cellobiose takes place in the flavin domain with subsequent electron transfer to the heme domain. The biological electron acceptor for CDH is unknown, but the reduced heme is able to reduce a wide variety of substrates including quinones, metal ions, and organic dyes. Reduced CDH can also react with molecular oxygen, but at a 10-20 fold slower rate than organic dyes and metal ions (*83*).

Several hypotheses have been proposed for the function of CDH including the oxidative degradation of cellulose or lignin via hydroxyl radical production (*80, 84-86*), reduction of feedback inhibition of cellulases by cellobiose (*87*) or support of ligninolytic enzymes by quinone and/or manganese reduction (*88*). The most prominent hypothesis is that involving the generation of hydroxyl radicals formed via oxidation of cellobiose followed by heme domain reduction of an extracellular ferric complex, most likely Fe(III)-oxalate (*80*). Ferrous iron can then take part in a Fenton reaction in the presence of hydrogen peroxide produced by CDH or

another oxidase. While the scope of these reactions is possible, control of hydroxyl radical reactivity would be particularly challenging.

In this study, we have determined the contribution of CDH to cellulose degradation in *N. crassa* using a combination of genetic and biochemical techniques. CDH enhances the degradation of cellulose by the cocktail of enzymes secreted by *Neurospora* nearly 2-fold, but this enhancement is not dependent on low molecular weight ferric ion complexes. This enhancement of activity is also not seen when CDH is added to purified *N. crassa* cellulases. Taken together, our results show that in *N. crassa*, CDH is a central component in cellulose degradation and works in conjunction with other factors to facilitate the degradation of crystalline cellulose by cellulases.

MATERIALS AND METHODS

Strains. All *Neurospora crassa* strains were obtained from the Fungal Genetics Stock Center (FGSC) including wild-type *N. crassa* (FGSC 2489) and the Δ*mus-51* (FGSC 9717) used for generating gene deletions. The Δ*gh5-1* (FGSC 1647) was from the *Neurospora* functional genomics project.

Preparation of Δ*cdh-1* strains. The DNA cassette used to delete *cdh-1* was provided by the *Neurospora* functional genomics project. Details about how the cassette was generated are available online at (http://www.dartmouth.edu/~neurosporagenome/protocols.html). FGSC 9717 was grown on Vogel's minimal media (*89*) slants for 21 days at room temperature. Conidia from the FGSC 9717 slant were transformed by electroporation with 1 μg of the Δ*cdh-1* (ΔNCU00206) cassette and plated onto media containing hygromycin. Positive transformants were then crossed with wild-type *N. crassa*. Ascospores were germinated on media containing hygromycin and several hygromycin resistant transformants were harvested and screened for production of CDH. The genotypes of three transformants that showed good growth on cellulose and lacked CDH activity were confirmed by PCR using primers specific to *cdh-1* and the hygromycin resistance cassette.

Growth and harvest of *N. crassa* culture filtrates. Wild-type or Δ*cdh-1 N. crassa* was inoculated onto slants of Vogel's minimal media and grown for 3 days at 30 °C in the dark followed by 7 days at room temperature. A conidial suspension was then inoculated into 100 mL of Vogel's salts supplemented with 2 % Avicel® PH101 in a 250 mL Erlenmeyer flask. After 7 days of growth on Avicel®, cultures were filtered over a 0.2 μm polyethersulfone (PES) filter.

Cellulase assays. All cellulase assays were performed in triplicate with 10 mg/mL Avicel® PH101 (Sigma) in 50 mM sodium acetate pH 5.0 at 40 °C. Assays were performed in 1.7 mL microcentrifuge tubes with 1.0 mL total volume and were inverted 20 times per minute. Each assay contained 0.05 mg/mL culture filtrate or 0.05 mg/mL reconstituted cellulase mixture containing CBH-1, GH6-2, GH5-1, and GH3-4 present in a ratio of 6:2.5:1:0.5. The concentration of heme domain used in stimulatory assays was 1.0 μM as determined by absorption at 430 nm of the fully reduced protein.

Assays were centrifuged for two minutes at 4000 rpm to pellet the remaining Avicel® and 20 μL of assay mix was removed per well. Samples were incubated with 100 μL of desalted, diluted Novozyme 188 (Sigma) at 40 °C for 20 minutes to hydrolyze cellobiose and then 10-30

μL of the Novozyme 188 treated cellulase assay supernatant was analyzed for glucose using the glucose oxidase/peroxidase assay as described previously (*59*). Percent degradation was calculated based on the amount of glucose measured relative to the maximum theoretical conversion of 10 mg/mL Avicel®.

Metal chelating reaction. To determine the requirement for small molecules and metals, wild-type or Δ*cdh-1* culture filtrate was buffer exchanged more than 10,000-fold in a 10 kDa MWCO spin concentrator (Sartorius). The culture filtrate was then incubated with 100 μM EDTA for 2 hours followed by the addition of 1 volume of 2 mM metal ($CaCl_2$, $MgSO_4$, $ZnSO_4$, $CoSO_4$, $Fe(NH_4)_2(SO_4)_2$, $MnSO_4$, or $CuSO_4$) for 12 hours. EDTA or metal reconstituted culture filtrate was then assayed as described above.

Anaerobic assays. Anaerobic cellulase assays were performed as above except all assays were conducted in an anaerobic chamber (Coy) at room temperature. Buffers were sparged with nitrogen for 1 hour and culture filtrates were concentrated more than 20-fold to volumes of less than 300 μL before introduction into the anaerobic chamber. All solutions were left open in the anaerobic chamber, and buffer solutions were stirred vigorously for 72 hours before use to fully remove dissolved oxygen. Aerobic reactions were prepared in the anaerobic chamber in 3 mL reactivials and then removed from the anaerobic chamber, exposed to air, sealed, and returned to the anaerobic chamber. At specified timepoints, assays were centrifuged in the glove bag and 100 μL of assay mix was removed and analyzed by the glucose-oxidase peroxidase assay as described above.

Protein purification. For isolation of *Myceliophthora thermophila* (ATCC 46424) CDH-1 and CDH-2, 10 day old *M. thermophila* conidia were inoculated into 1.0 liter of Vogel's salts supplemented with 40 g/L cotton balls in 2.8 liter Fernbach flasks. After 6 days of growth at 48 °C and 200 RPM shaking, fungal biomass and residual cotton was removed by filtration using 0.2 μm PES filters. The culture filtrate was then passed over CaptoQ resin (GE Healthcare) at 20 mL/min. CDH-1 and CDH-2 were eluted from the CaptoQ resin with buffer containing 500 mM sodium chloride and 25 mM HEPES pH 7.4. The pooled CaptoQ concentrate was then desalted into 25 mM HEPES pH 7.4 using a HiPrep 26/10 desalting column. The protein was further purified on a 10/100 GL MonoQ column and eluted with a linear gradient from 0 to 500 mM sodium chloride. CDH-1 elutes from the column between 180 and 220 mM sodium chloride; CDH-2 elutes between 280 and 320 mM sodium chloride. CDH-1 was then further purified by binding to 1.0 grams of Avicel® in 50 mM sodum acetate buffer pH 5.0 for 5 minutes at 50 °C. The Avicel® was removed by centrifugation in 50 mL conical tubes then washed with 50 mL of acetate buffer three times. CDH-1 was eluted from the Avicel® by addition of 50 mL of 50 mM pH 11.3 phosphate buffer. The eluted CDH-1 was concentrated using 10,000 molecular weight cutoff (MWCO) PES spin concentrators and stored at -80 °C. CDH-2 was further purified by gel filtration chromatography using a 16/60 Sephacryl S200 column with a mobile phase of 25 mM HEPES pH 7.4 and 150 mM sodium chloride. The flavin domain of CDH-2 was isolated by treatment of the full length enzyme with papain (*83*). After papain cleavage the fragments were separated by gel filtration chromatography using a 16/60 Sephacryl S100 column with a mobile phase of 25 mM HEPES pH 7.4 and 150 mM sodium chloride. The fractions enriched in flavin domain were then further purified using a 10/100 GL MonoQ column and eluted with a linear gradient from 0 to 500 mM sodium chloride.

N. crassa CDH-1 was partially purified from wild-type *N. crassa*. A conidial suspension was inoculated into 500 mL of Vogel's salts supplemented with 2% Avicel® at 25 °C in two liter Erlenmeyer flasks. Cultures were shaken at 200 RPM under constant light for 7 days. Fungal biomass was removed by filtration using 0.2 μm PES filters. Phosphoric acid swollen cellulose (PASC) was then added (20 mL) to the culture filtrate at 4 °C and mixed for 10 minutes. The PASC was then removed from the culture filtrate by centrifugation for 10 minutes at 4,000 RPM. Next 724 g/L ammonium sulfate was added to the culture filtrate and stirred at 4 °C for one hour. The precipitated proteins were then isolated by centrifugation at 8,000 RPM for 25 minutes. The pellet was resuspended in a minimal volume of water and then buffer exchanged into 25 mM TRIS pH 8.5 using a HiPrep 26/10 desalting column (GE Healthcare). The buffer exchanged proteins were then loaded onto a 10/100 GL MonoQ column and eluted with a linear gradient from 0 to 500 mM sodium chloride. CDH-1 elutes from the column between 50 and 100 mM sodium chloride and is ~80% pure by SDS-PAGE.

N. crassa CBH-1 (NCU07340) was purified from wild-type *N. crassa* and GH6-2 (NCU09680) was purified from a Δ*gh5-1* strain. A conidial suspension was inoculated into Vogel's salts and 2 % Avicel® at 25 °C in a 2.8 L ultrayield flask. Cultures were shaken at 200 RPM under constant light for 7 days post inoculum and then filtered over a 0.2 μm PES filter. An affinity digestion was performed to concentrate cellulose binding proteins based on their affinity for PASC (*56*). Following dialysis into 25 mM Tris pH 8.5, 100 mM sodium chloride was added to the samples and proteins were purified by anion exchange chromatography. For purification of CBH-1 the affinity digest from the wild-type culture filtrate was directly loaded onto a Mono Q 10/100 GL column and eluted using a gradient from 100 mM to 1 M sodium chloride over 8 minutes. Purification of GH6-2 from the affinity digest of the Δ*gh5-1* strain was performed by loading the sample onto a Hiload 16/10 Q Sepharose HP column. GH6-2 in the flow through was collected, buffer exchanged into 25 mM Tris pH 8.5 and repurified over the Mono Q column using a shallow gradient from 0 to 100 mM sodium chloride over 10 minutes.

N. crassa GH5-1 (NCU00762) was homologously expressed with a C-terminal His tag and purified on a Ni-NTA column essentially as described previously (*57*) with the following modifications. To decrease proteolysis of the His tag for constructs transformed with the pNeurA vector and improve yields, the TEV proteolysis site and GFP tag were removed using yeast recombineering. Further, the native *N. crassa* terminator, including 1 kb of sequence on the 5' end of the *gh5-1* ORF, in addition to the ScADH1 terminator were inserted following the *gh5-1* ORF and before the partial *his-3* sequence. This new vector was called pNevE-762.

DNA encoding for *N. crassa* GH3-4 (NCU04952) and the *M. thermophila* CDH-2 heme domain were amplified by PCR with gene specific primers from cDNA isolated from *N. crassa* and *M. thermophila* during growth on Vogel's salts supplemented with 2% Avicel® as previously described (*59*). The genes were cloned into the pPicZαA vector using standard techniques and then transformed into *P. pastoris* and expressed according to the EasySelect *Pichia* Expression Kit instructions (Invitrogen).

Protein gel electrophoresis. Samples were treated with 4x SDS Laemmli loading buffer, boiled 5 minutes, and loaded onto a Criterion 4-15% Tris-HCl polyacrylamide gel (Biorad). Gelcode blue stain reagent (Thermo Scientific) was used for staining.

Protein identification by tandem mass spectrometry. All natively purified proteins were positively identified by carrying out in-solution tryptic digests of purified proteins and then analyzing samples by LC-MS/MS as previously described (*59*).

Protein quantification and enzyme assays: Total extracellular protein content was determined using the Biorad Protein Assay (Biorad) according to the manufacturer's instructions. CDH activity assays were performed at room temperature by the addition of an appropriate amount of CDH or culture filtrate to a mixture containing 1.0 mM cellobiose, 200 μM DCPIP, and 100 mM sodium acetate pH 5.0. Reduction of DCPIP was monitored spectrophotometrically by the decrease in absorbance at 530 nm. One unit is equivalent to the number of micromoles of DCPIP reduced per minute. Endoglucanase activity was determined by mixing appropriately diluted culture filtrate to the azo-CMC reagent (Megazyme SCMCL), according to the manufacturer's instructions. The rate of hydrolysis of 4-Methylumbelliferyl β-D-lactoside (MULAC) was determined by monitoring the increase in fluorescence (excitation λ=360nm; emission λ=465nm) upon addition of appropriately diluted culture filtrate to 1.0 mM MULAC.

CDH binding to Avicel®. Purified CDH-1 or CDH-2 (20 μg) was added to 1.0 mL of 10 mg/mL Avicel® in 50 mM sodium acetate buffer pH 5.0. After incubation for 5 minutes at room temperature, the Avicel® was spun down by centrifugation at 10,000 RPM. The supernatant was removed and the Avicel® pellet was washed with 1.0 mL of fresh 50 mM sodium acetate buffer pH 5.0. The washing step was repeated three times and then the Avicel® pellet was boiled in SDS loading buffer. After boiling, the Avicel® was spun down and the supernatant loaded onto a 10% Tris-HCl polyacrylamide gel.

Product analysis by HPLC. Cellulase samples were taken at 2, 12, and 24 hours then immediately mixed with 1 volume of 0.1 M NaOH to stop the reaction. Samples were diluted appropriately and stored at 4 °C until analyzed on a Dionex ICS-3000 HPLC. Cello-oligosaccharides were separated on a PA-200 HPAEC column using a gradient of 0.1 M NaOH to 0.1 M NaOH plus 80 mM sodium acetate over 8 minutes. The flow rate was set to 0.4 mL/min, the column was maintained at a temperature of 30 °C, and samples were detected on an electrochemical detector. Standards of glucose, cellobiose, glucono-δ-lactone and cellobiono-δ-lactone were simultaneously analyzed and peaks areas were calculated to determine the concentration. Cellobiono-δ-lactone was synthesized as previously described (*90*).

RESULTS

Production of a strain of *N. crassa* containing a deletion of NCU00206, *cdh-1*

The *Neurospora* functional genomics project has generated knockout strains for most of the genes in the *N. crassa* genome using targeted gene replacement through homologous recombination (*91*). A heterokaryon strain of Δ*cdh-1* is available through the Fungal Genetic Stock Center (FGSC), but despite numerous attempts, a homokaryon strain could not be generated due to an ascospore-lethal linked mutation. To obtain a clean deletion of *cdh-1,* a *N. crassa* strain deficient in non-homologous end joining recombination was transformed with a cassette provided by the *Neurospora* functional genomics project (*92*). Heterokaryon transformants showing hygromycin resistance were genotyped using PCR to confirm the deletion of *cdh-1*. Transformants were crossed with wild-type *N. crassa* and several hygromycin resistant

progeny were then screened for the production of CDH during growth on cellulose. The strains that showed the best growth on Avicel®, a microcrystalline cellulose, and that were also deficient in CDH activity in the culture filtrate were genotyped. Multiple homokaryon strains in which *cdh-1* was deleted were confirmed by PCR.

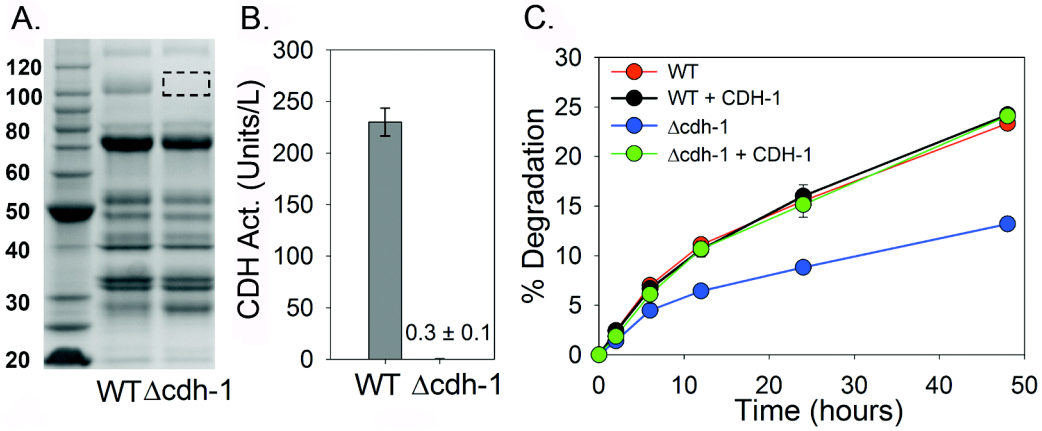

Figure 3.1. Characterization of Δ*cdh-1* strain. (A) SDS-PAGE of *N. crassa* WT (left) and Δ*cdh-1* strains. MW markers in kDa are to the left, and a box indicates the expected position of CDH-1. (B) CDH volumetric activity in the culture filtrate of WT and Δ*cdh-1* cultures grown on Avicel®. (C) Cellulase assays with the WT and Δ*cdh-1* strains. Assays contained 10 mg/mL Avicel® and 0.05 mg/mL secretome protein. CDH-1 from *Myceliophthora thermophila* was added at 0.004 mg/mL.

Growth of the Δ*cdh-1* strains in liquid culture on Vogel's salts supplemented with 2% sucrose was identical to that of wild-type. There was only a slight growth defect on cellulose. Both the wild-type and Δ*cdh-1* strains completely degraded all the cellulose in the culture after 6-7 days of growth, as determined by light microscopy. The proteins present in the culture filtrate were analyzed by SDS-PAGE and the extracellular proteins secreted by the Δ*cdh-1* strains were very similar to those of the wild-type, with the exception of the loss of the CDH-1 band between 100 and 120 kDa (Fig. 3.1A). The total secreted protein in the Δ*cdh-1* strains varied from ~40% lower than the wild-type strain to equal to the wild-type strain for the different transformants. CDH activity in the culture filtrate of the Δ*cdh-1* strains was 800 ± 300-fold lower than in the wild-type culture filtrates (Fig. 3.1B). Cellulase-specific activities of the Δ*cdh-1* strains and the wild-type were then compared. The endoglucanase activity and cellobiohydrolase activity, as measured by the azo-CMC and MULAC assays, respectively, were similar for the wild-type and Δ*cdh-1* strains when equal levels of total protein were added. Cellulase activity was 37-49% lower in the Δ*cdh-1* strain culture filtrates than in those from wild-type when added on an equal protein basis (Fig. 3.1C). HPLC analysis of hydrolysis products after 24 hours of reaction time showed that in the Δ*cdh-1* strain culture filtrate, glucose (>90%) was the main sugar produced followed by cellobiose. Glucose remained the dominant product (>80%) in assays of wild-type culture filtrate, followed by cellobiose, cellobionic acid and trace amounts of gluconic acid. No additional peaks were present in the chromatograms.

Stimulation of cellulose degradation by CDH

To more directly assess the contribution of CDH-1 to the degradation of cellulose, *in vitro* complementation assays were undertaken using purified CDHs. CDH-1 is difficult to purify from *N. crassa* culture filtrates, and only a partially purified preparation of *N. crassa* CDH-1 could be isolated (Figure 3.2). The orthologous protein in the closely related thermophilic fungus, *Myceliophthora thermophila* (*83*), can be purified to homogeneity and was used for most of the complementation assays (Figure 3.1). *M. thermophila* and *N. crassa* CDH-1 share 70% sequence identity, the same domain architecture and a C-terminal fungal cellulose binding domain. CDH-1 from *M. thermophila* had no activity on cellulose, while the partially purified *N. crassa* CDH-1 had a slight contaminating hydrolytic activity.

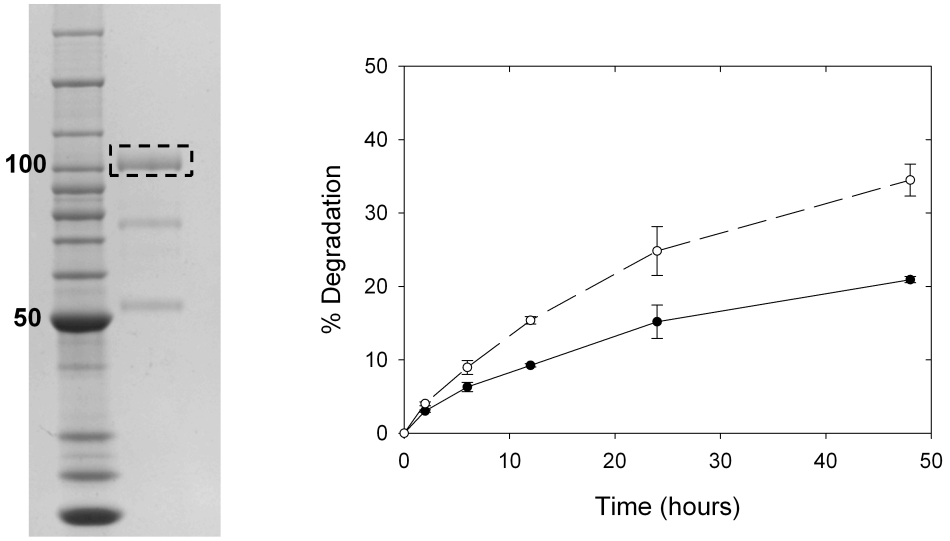

Figure 3.2. Complementation of a Δ*cdh-1* strain with *N. crassa* CDH-1. Stimulation of cellulose degradation by the addition of partially purified *N. crassa* CDH-1 to the Δ*cdh-1* culture filtrate. (A) SDS-PAGE of partially purified *N. crassa* CDH-1. (B) Cellulase activity of the Δ*cdh-1* culture filtrate. (◦) Represent experiments where 400 μg *N. crassa* CDH-1 per gram of cellulose was added. (•) Represent experiments where no exogenous CDH was added. Values are the mean of three replicates. Error bars are the SD between these replicates.

Addition of *M. thermophila* CDH-1 or partially purified *N. crassa* CDH-1 to the culture filtrate of the Δ*cdh-1* strains stimulated cellulose hydrolysis substantially (Figure 3.1 and 3.2). The cellulase activity was 1.6- to 2.0-fold higher than the Δ*cdh-1* culture filtrate alone. Addition of *M. thermophila* CDH-1 to wild-type culture filtrate had no stimulatory effect on cellulose hydrolysis (Figure 3.1). Further, CDH-1 was unable to stimulate a mixture of purified cellulases (Figure 3.3) from *N. crassa* including 2 cellobiohydrolases (CBH-1 and GH6-2), an endoglucanase (GH5-1), and a ß-glucosidase (GH3-4). SDS-PAGE and LC-MS/MS was used to confirm that these proteins were >90% pure (Figure 3.4).

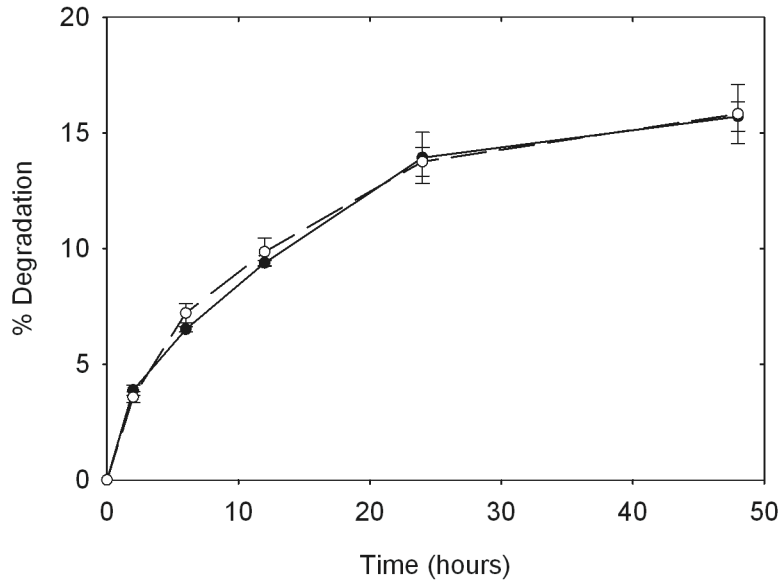

Figure 3.3. Addition of CDH-1 to Purified Cellulases. *M. thermophila* CDH-1 was added to a mixture of purified cellulases (CBH-1, GH6-2, GH5-1, GH3-4) from *N. crassa* and assayed on cellulose. (•) No exogenous CDH added (◦) 400 μg *M. thermophila* CDH-1 per gram of Avicel® added. Values are the mean of three replicates. Error bars are the SD between these replicates.

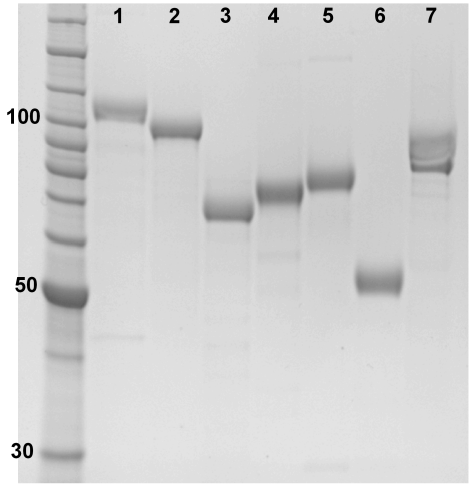

Figure 3.4. SDS-PAGE of purified proteins. Proteins were loaded at 5 μg per lane in the following order: (1) *M. thermophila* CDH-1, (2) *M. thermophila* CDH-2, (3) *M. thermophila* CDH-2 flavin domain, (4) *N. crassa* CBH-1, (5) *N. crassa* GH6-2, (6) *N. crassa* GH5-1, (7) *N. crassa* GH3-4.

M. thermophila also produces a second CDH during growth on cellulose, CDH-2, which does not contain a fungal cellulose binding module (Figure 3.5A). The cellulose-binding propensity of *M. thermophila* CDH-1 and CDH-2 was determined using pull down experiments

with cellulose (Figure 3.5B). *M. thermophila* CDH-1 binds strongly to cellulose, while *M. thermophila* CDH-2 has only a very weak affinity. Aside from the different affinities for cellulose, *M. thermophila* CDH-1 and CDH-2 have very similar steady-state kinetic properties (*83*). At a CDH loading of 0.4 mg/g cellulose, CDH-2 was able to stimulate the hydrolysis of cellulose to the same extent as CDH-1 (Figure 3.5C).

To further investigate the role of the cellulose-binding module on the ability of CDH to stimulate cellulose hydrolysis, a titration experiment was performed (Figure 3.5D). CDH-1 was able to stimulate the activity of the Δ*cdh-1* strain culture filtrate at a 10-fold lower loading than CDH-2. A stimulatory effect on cellulase activity in the Δ*cdh-1* culture filtrate was observed at a loading of 5 μg of CDH-1 per gram of cellulose, while 50 μg of CDH-2 was required for a similar stimulation (Figure 3.5D). At 4 mg CDH/g cellulose, both *M. thermophila* CDH-1 and CDH-2 have an inhibitory effect on cellulase activity relative to the lower loadings.

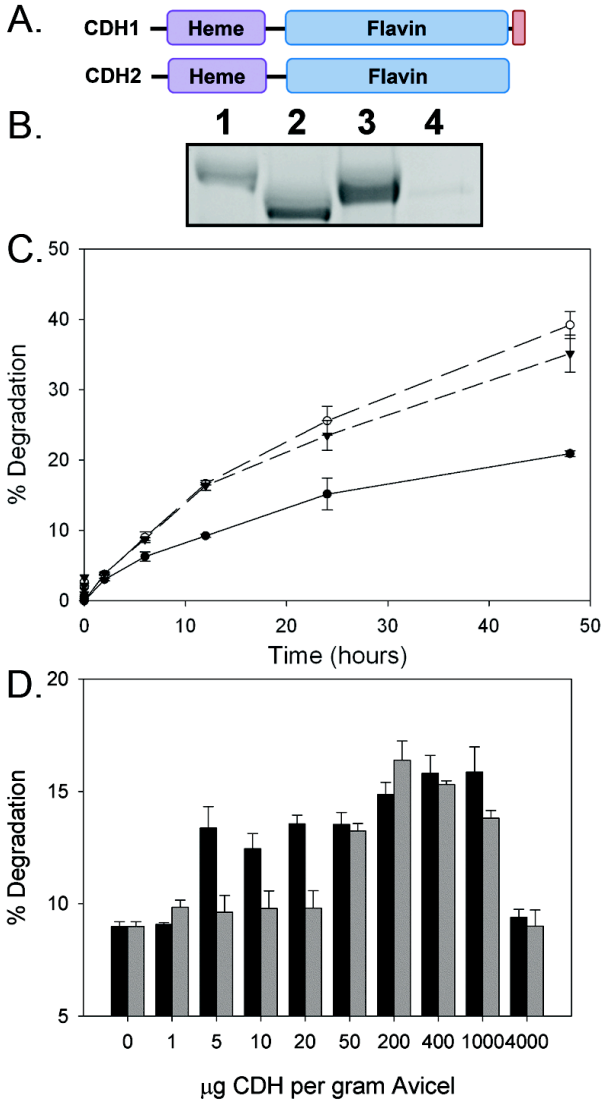

Figure 3.5. Stimulation of cellulose degradation by isoforms of CDH. (A) Domain architectures of *M. thermophila* CDH-1 and CDH-2. Red C-terminal domain on CDH-1 is a fungal cellulose-binding domain (CBM1). (B) Cellulose binding assay for *M. thermophila* CDH-1 and CDH-2. Lane 1 *M. thermophila* CDH-1, Lane 2 *M. thermophila* CDH-2, Lane 3 CDH-1 bound to Avicel®, Lane 4 CDH-2 bound to Avicel®. (C) Stimulation of cellulose degrading capacity of the Δ*cdh-1* culture filtrate (•) by addition of CDH-1 (◦), or CDH-2 (◆). (D) Effect of the concentration of *M. thermophila* CDH-1 (black) and *M. thermophila* CDH-2 (gray) on cellulase activity of the Δ*cdh-1* culture filtrates. Values are the mean of three replicates. Error bars are the SD between these replicates.

The flavin and heme domains of *M. thermophila* CDH-2 can be separated by cleavage with papain (*83*). To determine the contribution of the heme domain to the stimulation of activity, *M. thermophila* CDH-2 was cleaved with papain and the flavin domain isolated by size exclusion chromatography. The flavin domain oxidizes cellobiose at the same rate as the full length enzyme when 2,6-dichlorophenolindophenol (DCPIP) is used as an electron acceptor, but has no activity with cytochrome c, reflecting on the importance of the heme domain for transfer to 1 electron acceptors (*83*). The flavin domain, when added on an equal activity basis as the full length CDH-2, is unable to stimulate the hydrolysis of cellulose when added to the Δ*cdh-1* culture filtrate, despite production of cellobionic acid (Figure 3.6). Even at a loading 10-fold higher than the full length CDH-2, the flavin domain is still unable to stimulate cellulose hydrolysis, suggesting that the heme domain is essential for the stimulatory effect.

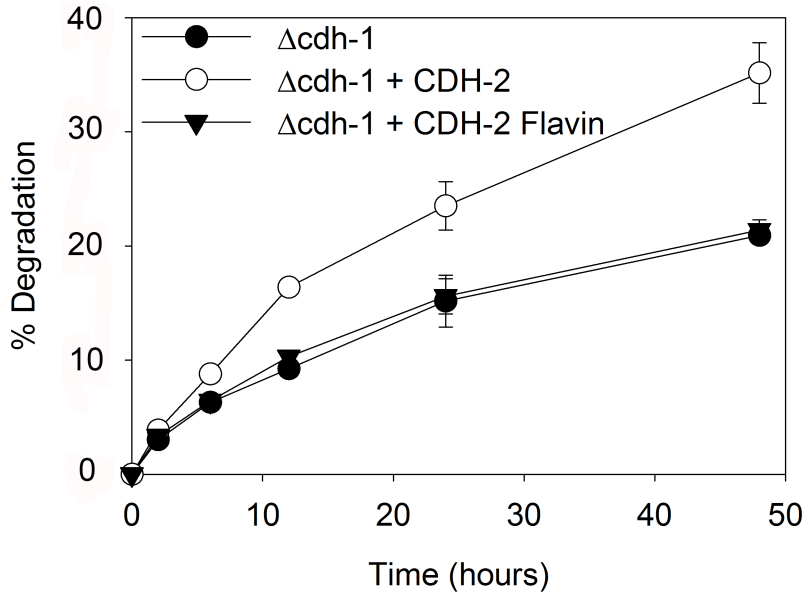

Figure 3.6. CDH flavin domain. Stimulation of cellulose degrading capacity of the Δ*cdh-1* culture filtrate by addition of full length CDH-2 or the CDH-2 flavin domain. Values are the mean of three replicates. Error bars are the SD between these replicates.

The heme domain of *M. thermophila* CDH-2 could not be sufficiently purified from the papain digestion of the full length protein and was thus recombinantly expressed in the yeast *Pichia pastoris*. The heme domain from CDH-2 was purified by nickel metal affinity chromatography and has the same spectral properties of the full length CDH-2 (SI Fig. 3). The recombinant heme domain was then tested for the ability to stimulate cellulose hydrolysis of the Δ*cdh-1* strain culture filtrate (Figure 3.7). Addition of the ferric heme domain at the same molar concentration as the full length CDH-2 required for maximum stimulation had no stimulatory effect.

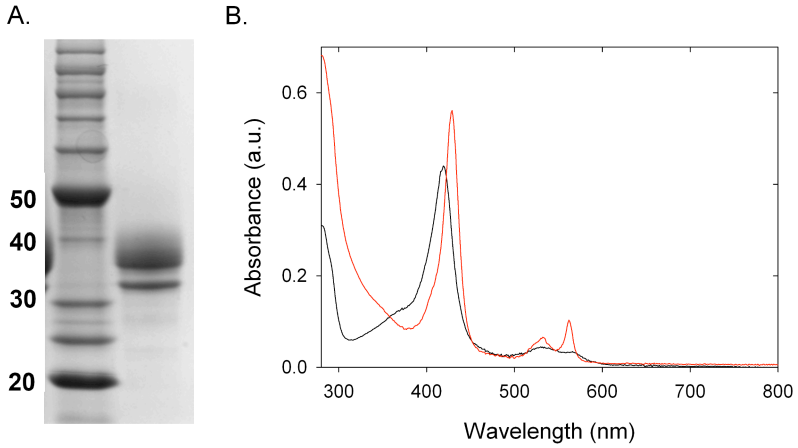

Figure 3.7. Purity and spectral properties of recombinant CDH-2 heme domain. CDH-2 heme domain was expressed in *Pichia pastoris*. (A) SDS-PAGE of purified recombinant CDH-2 heme domain. (B) UV-vis spectra of the oxidized (black) and reduced (red) CDH-2 heme domain.

Oxygen and metal ion dependence on the stimulation of cellulose degradation by CDH

A prevalent hypothesis for the biological function of CDH states that electrons from the heme domain of CDH are transferred to ferric complexes, quinones, molecular oxygen, or other redox mediators which lead to the production of radical species that can non-specifically degrade cellulose or lignin. Experiments were carried out to address if the stimulation of activity observed with CDH addition to the Δ*cdh-1* culture filtrate was due to a direct reaction with the cellulose or an indirect effect where metals or small molecules became reduced by CDH and subsequently contributed to the degradation.

To test for the effect of small molecules in the Δ*cdh-1* culture the culture filtrate was buffer exchanged 10,000-fold using 10,000 MWCO spin concentrators. After this treatment, CDH-1 was still able to stimulate the activity of the Δ*cdh-1* culture filtrate to the same extent. To test if there was a metal dependence for the stimulation, buffer exchanged culture filtrates from the Δ*cdh-1* cultures were incubated with 100 μM EDTA for 1 hour, and then assayed for cellulase activity. EDTA had no effect on the cellulase activity of the Δ*cdh-1* culture filtrate; however, when *M. thermophila* CDH-1 was added to the EDTA treated Δ*cdh-1* culture filtrate, no stimulatory effect was observed (Fig. 3.8A). Previous results had shown that wild-type culture filtrate reduced cellulase activity by ~50%. Taken together, these results suggest that there is a protein bound metal ion essential for the stimulation of cellulose degradation by CDH.

Overnight incubation of *M. thermophila* CDH-1 with 1.0 mM EDTA had no effect on the oxidation of cellobiose with DCPIP or cytochrome c as electron acceptors.

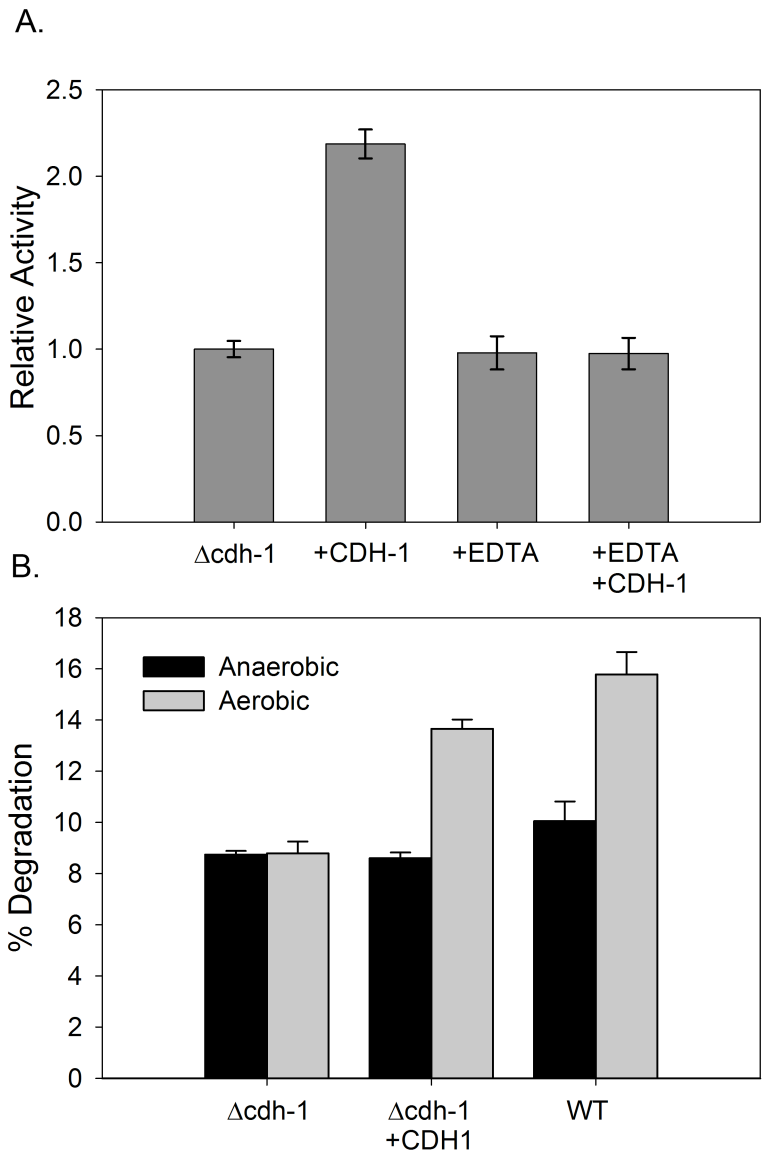

Figure 3.8. Contribution of metals or small molecules to the CDH dependent stimulation. (A) Cellulase activity of 10,000-fold buffer exchanged Δ*cdh-1* secretome in the presence or absence of 0.004 mg/mL CDH-1. For reactions containing EDTA, 100 μM EDTA was preincubated with the sample for 2 hours and then assayed. (B) Oxygen dependence of the stimulation of cellulase activity by CDH. Black bars indicate experiments conducted anaerobically, gray bars indicate experiments conducted aerobically. Values are the mean of three replicates. Error bars are the SD between these replicates.

Finally, the role of molecular oxygen on the stimulation of activity by CDH-1 in the Δ*cdh-1* culture filtrate was explored. Cellulase activity of the Δ*cdh-1* culture filtrates is not affected by the absence of molecular oxygen, while in wild-type culture filtrates activity is

reduced by ~40%. When purified *M. thermophila* CDH-1 was added to the Δ*cdh-1* culture filtrate under anaerobic conditions no stimulatory effect on cellulase activity was observed (Fig. 3.8B).

DISCUSSION

The chemical makeup of the plant cell wall makes it a highly recalcitrant source of nutrients for animals and microbes. The structural backbone of the plant cell wall is the crystalline polysaccharide, cellulose, which typically constitutes 30-40% of the dry weight of terrestrial plants (*93*). During growth on pure cellulose, *N. crassa* increases the expression of more than 100 different genes and secretes more than 30 different proteins (*59*). Many of these proteins have high sequence homology to known hydrolytic enzymes, but there are also proteins predicted to be involved in oxidative reactions and proteins of unknown function. CDH-1 is the most abundant secreted oxidoreductase produced by *N. crassa* during growth on cellulose, constituting as much as 3% of the total secreted protein. Using a combination of genetic and biochemical techniques, we report here that CDH-1 is a major contributor to the depolymerization of cellulose by *N. crassa*. The deletion of CDH-1 lowers the aggregate cellulase activity of the culture filtrates by 37-49%. Addition of purified CDH-1 back to the Δ*cdh-1* culture filtrate stimulates the cellulase activity back to the wild-type level. A stimulatory effect was seen with an addition of CDH-1 equivalent to only 0.1% of the total protein in the culture filtrate.

In the cellulolytic Sordariales sequenced thus far, all species have two copies of CDH (*75*), one containing a C-terminal fungal cellulose binding domain (CBM), and one without a CBM. In *N. crassa,* only the CBM-containing CDH-1 is produced in significant amounts during growth on cellulose. However, in the closely related thermophilic fungus, *M. thermophila,* both CDHs are produced at high levels during growth on cellulose (*83*). Both CDHs from *M. thermophila* have been previously shown to have very similar steady-state kinetic properties with soluble substrates (*83*), and we now show that both enzymes can stimulate hydrolysis of cellulose to the same extent. A key difference between the two CDHs is that CDH-1 was functional at a 10-fold lower concentration than CDH-2. Cellulose binding modules are known to increase the local concentration of cellulases on the surface of cellulose, and the results here are consistent with the stimulatory effect being due to a reaction taking place on or near the surface of the cellulose.

The isolated and catalytically active flavin domain of CDH-2 is unable to stimulate hydrolysis of cellulose, whereas the CDH-2 heme domain was able to stimulate cellulose hydrolysis to the same extent as full length CDH-2, at a 20 to 50-fold higher concentration. The iron in the heme domain of CDH is ligated by absolutely conserved methionine and histidine residues. Neither of these two residues can be displaced by cyanide, azide when ferric, or carbon monoxide when ferrous (*94*), supporting the hypothesis that the heme domain is likely involved in outer sphere electron transfer reactions. The results presented here suggest that 1-electron transfer, mediated through the heme domain, is essential for the stimulatory effect. The stimulatory effect of the ferric heme domain was unexpected, as it would have no electron source. However, the Δ*cdh-1* culture solution contains a trace CDH activity, due to a very low level expression of CDH-2. Full length CDH-2 is able to reduce free CDH heme domains in the presence of cellobiose and likely accounts for the stimulation in activity by the free heme domain.

Proteins with sequence homology to the heme domain of CDH are widespread throughout the fungal kingdom. As more fungal genome sequences have become available, CDH-like heme domains have been found in proteins with diverse domain architectures. In addition to a canonical CDH, the basidiomycete, *Phanerochaete chrysosporium* also produces a secreted CDH-like heme domain with a C-terminal fungal cellulose-binding domain (*95*). In the *N. crassa* genome there are three genes encoding proteins predicted to contain stand alone CDH-like heme domains with N-terminal signal peptides; however, previous transcriptional profiling of *N. crassa* did not show them upregulated during growth on cellulose. These free heme domains are conserved throughout the Sordariales with sequenced genomes and all are predicted to have the same methionine and histidine axial iron ligation.

The prevailing hypothesis for the biological function of CDH in the degradation of lignocellulose involves flavin oxidation of cellobiose with sequential electron transfer to the heme and then heme reduction of a one electron acceptor, speculated to be an Fe(III)-oxalate complex (*80*). This ferrous iron is then proposed to take part in a Fenton reaction with peroxide generated by CDH or other extracellular oxidases to generate hydroxyl radicals which non-specifically degrade plant cell wall polysaccharides. Fenton chemistry requires ferrous iron and peroxide, and has been routinely used in DNA footprinting experiments (*96*). After a 10,000-fold buffer exchange of the Δ*cdh-1* culture filtrate, the free iron in solution is less than 1 nM; however, CDH was still able to fully stimulate cellulase activity. Treatment of the culture filtrate with EDTA completely blocks the stimulation by CDH, although EDTA should not prevent ferrous iron from participating in Fenton reactions. In fact, iron-EDTA chelates are often used to generate hydroxyl radicals (*96*). These results do not support the involvement of Fenton chemistry in the stimulation of cellulase activity by CDH in *Neurospora*. The requirement of molecular oxygen for the stimulation in activity; however, suggests that oxidation reactions may play an important role.

Our results are consistent with the heme domain of CDH contributing to the degradation of cellulose through interaction with other metalloproteins that are larger than 10,000 daltons. Potential candidates include metal-dependent glycosyl hydrolase family 61 proteins or other metal-dependent proteins of unknown function present in the culture filtrate. GH61 family proteins were recently shown to stimulate the hydrolysis of pretreated corn stover when added to a cocktail of industrial cellulases (*97*). The stimulation by GH61 proteins is completely inhibited by addition of EDTA. This inhibition of activity by EDTA has been ascribed to the removal of an essential surface exposed divalent metal ion from the protein, and can be rescued by addition of divalent metal ions to the reaction. Interestingly, no stimulation of activity by GH61 proteins was observed on pure cellulosic substrates (*97*). The requirement for a divalent metal is peculiar in that recent work has shown that multiple different metals work equally well. This is further complicated by the variety of metals found in structures of GH61 proteins including Zn, Mg, and Ni. Neither zinc nor magnesium is redox active calling into question the notion that GH61 proteins are involved in an oxidative mechanism. Transition metals are generally required for activation of oxygen.

CBP21, a protein structurally related to GH61 proteins, from the chitinolytic bacterium *Serratia marcescens*, was recently shown to stimulate the hydrolysis of crystalline chitin (*98, 99*), presumably by the same mechanism as GH61 proteins. CBP21 was shown to require divalent metal ions (Zinc or Magnesium) for activity, as well as the presence of molecular oxygen (*100*). Addition of CBP21 to chitin in the presence of molecular oxygen and ascorbic acid leads to the formation of oxidized chito-oligosaccharides by an unknown mechanism. If

fungal GH61 proteins stimulate hydrolysis by the same mechanism as CBP21, it is likely that CDH is functioning as an extracellular reductant. The *N. crassa* genome contains fourteen genes encoding predicted extracellular GH61 proteins, of which, at least nine are upregulated during growth on cellulose (*59*). There are also multiple hypothetical proteins secreted by *Neurospora* which could be involved in the CDH stimulated degradation pathway.

The discovery that cellobiose dehydrogenase plays a major role in pure cellulose degradation by some fungi is a significant shift from previous models centered on the degradation of cellulose by a mixture of glycoside hydrolases. The well understood genetics and resources available in *Neurospora* should facilitate the discovery of CDH's other partners so that the full system can be reconstituted *in vitro*.

PREVIOUSLY PUBLISHED MATERIAL

Parts of this chapter were from a previously published article co-authored by William T. Beeson, Jamie H. Cate, and Michael A. Marletta. Thanks to the co-authors and publishers at the ACS Chemical Biology for allowing use of this material.

CHAPTER 4: Cellobiose dehydrogenase and a copper-dependent polysaccharide monooxygenase potentiate cellulose degradation

ABSTRACT

Here, we show that cellobiose dehydrogenase enhances cellulose degradation by coupling the oxidation of cellobiose to the reductive activation of copper-dependent polysaccharide monooxygenases (PMOs), previously called GH61 proteins, that catalyze the insertion of oxygen into C-H bonds adjacent to the glycosidic linkage. Three of these PMOs were characterized and shown to have different regiospecifities resulting in oxidized products modified at either the reducing or non-reducing end of a glucan chain. In contrast to previous models where oxidative enzymes were thought to produce reactive oxygen species that randomly attacked the substrate, the data here supports a direct, enzyme-catalyzed oxidation of cellulose. Cellobiose dehydrogenases and proteins related to the polysaccharide monooxygenases described are found throughout both ascomycete and basidiomycete fungi suggesting that this model for oxidative cellulose degradation may be widespread throughout the fungal kingdom. When added to mixtures of cellulases, these proteins enhance cellulose saccharification, suggesting that they could be used to reduce the cost of biofuel production.

INTRODUCTION

In the previous chapter, we used a gene deletion of CDH-1 in *Neurospora crassa* to show the importance of oxidative enzymes in fungi. Addition of CDH from *M. thermophila* was then used to complement the Δ*cdh-1* strain and it was shown that metalloprotein(s) and molecular oxygen were required for the CDH dependent stimulation of cellulase activity. While cellulose degradation has traditionally been modeled as hydrolytic degradation by cellulases, CDH is involved in a process that is oxidative. Many previous groups have proposed that Fenton chemistry might be important though our previous work suggested that this model is unlikely (*35*). One alternative would be the direct, enzymatic oxidation of cellulose by a combination of oxidative proteins (Figure 4.1). To test this model, we hoped to identify the metalloprotein that was required for CDH dependent oxidative degradation of cellulose

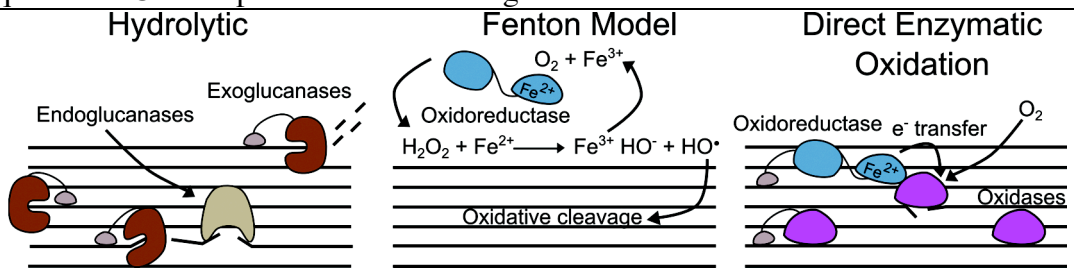

Figure 4.1. Schematic of hydrolytic and oxidative mechanisms proposed for cellulose breakdown. (Left) Hydrolytic chemistry: Cellulases must gain access to a glucan chain and bring it into a cleft or tunnel active site where acid base catalysis is used to cleave glycosidic bonds. (Center) Fenton chemistry: Hydroxyl radicals produced via the Fenton reaction from reduction of extracellular metal ions randomly oxidize cellulose. (Right) Enzymatic oxidation: Direct enzyme catalyzed oxidation by a combination of oxidases and oxidoreductases. Unlike hydrolases, oxidases could cleave glycosidic bonds without the energetically costly step of abstracting a glucan chain from crystalline cellulose.

One likely hypothesis suggested that enzymes erroneously classified as glycosyl hydrolase family 61 (GH61) enzymes were involved. These enzymes are present in the genomes of nearly all cellulolytic filamentous fungi secreted to date and of the 14 present in the *Neurospora* genome, 10 were upregulated in response to avicel or *Miscanthus* (Figure 4.2) (*46*). Additionally, the work to quantitatively characterize the protein secreted by *N. crassa* by quantitative mass spectrometry revealed that 3 of these GH61 enzymes constituted more than 15% of the secretome by mass.

GH61 enzymes were originally purified and identified as endoglucanases (EG4) due to their very low hydrolytic activity on cellulose (*101*). The hydrolytic activity demonstrated by these enzymes has been a matter of debate and recent studies have suggested that this activity may be due to contamination and is quite low on all the polysaccharide substrates tested (*71*). It was not until recently that the number of genomic sequences and transcriptomic efforts began to reveal the importance of this class of enigmatic proteins in fungi. GH61 proteins were present in *T. reesei* and expressed in response to cellulose but only 3 of these proteins are found in the genome (*15*). This is surprising given that many species of cellulolytic fungi have significantly more GH61 proteins than they do cellulases. *N. crassa* has 14 GH61 proteins in its genome and other diverse cellulolytic species, like *M. thermophile*, *P. anserina*, *S. commune*, and others, have more than 20 to 30 isoforms. In the white rot fungus, *P. chrysosporium,* and the brown rot fungus, *S. lacrymans* expression profiling experiments revealed that a PMO is the most highly upregulated protein in response to growth on biomass (*36, 70*).

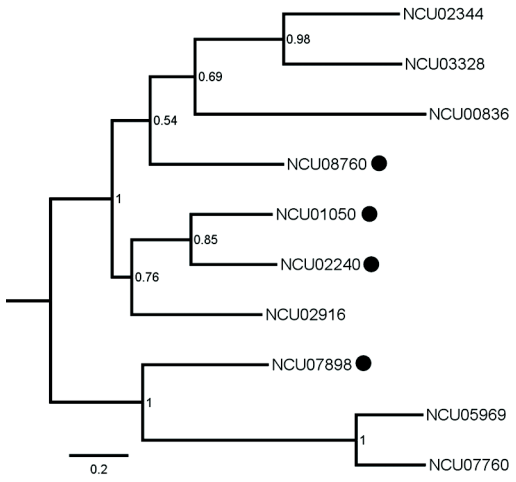

Figure 4.2. Phylogeny of GH61 proteins in *N. crassa*. Shown are the upregulated GH61 proteins. Of the 14 GH61 proteins in the *N. crassa* genome, 10 are upregulated >2-fold in response to growth on cellulose relative to sucrose (*39*). Proteins identified via proteomics and purified here are marked (•).

These GH61 proteins have been shown to increase the activity of cellulases acting on pretreated corn stover, but not pure cellulose, through an unknown mechanism. The structure of GH61B from *H. jecorina* was solved in 2008 revealing a highly conserved flat surface, unlike the tunnel or cleft active site found in most cellulases. Notably, this protein lacked the conserved acid residues that could catalyze hydrolytic cleavage (*102*). These enzymes have a highly conserved metal binding site that includes two histidine residues. One of the histidines is the N-

terminal residue and functions as a bidentate ligand involving the amine and ring N2. Crystal structures of GH61 proteins with nickel (*102*), magnesium, zinc (*103*), or copper (*104*) have been reported. Here, we have used a fractionation strategy to identify that GH61 enzymes are actually copper-dependent oxidases that act synergistically with cellobiose dehydrogenase to oxidatively cleave cellulose.

MATERIALS AND METHODS

Growth of *N. crassa*.

Wild-type or Δ*cdh-1 N. crassa* was inoculated onto slants of Vogel's minimal media and grown for 3 days at 30 °C in the dark followed by 7 days at room temperature with ambient lighting. A conidial suspension was then inoculated into 100 mL of Vogel's salts supplemented with 2% Avicel® PH101 (Sigma) in a 250 mL Erlenmeyer flask. After 7 days of growth on Avicel®, cultures were filtered over 0.2 μm polyethersulfone (PES) filters.

Copper stoichiometry of apo-PMOs.

Apo-PMO stocks of NCU01050, NCU07898, and NCU08760 were diluted to a final concentration of 1.0 mg/mL in 10 mM Tris pH 8.5 buffer and incubated with 200 μM copper sulfate at room temperature for 16 hours. After reconstitution, the protein was diluted 5-fold into 10 mM Tris pH 8.5 and desalted using a 26/10 desalting column to remove unbound copper. The desalted protein was concentrated to a final volume of 2.5 mL using 3,000 MWCO PES spin concentrators. The absorption at 280 nm was recorded for each sample and used to determine the concentration of the protein. The concentration of copper in the sample was measured using a Perkin Elmer 7000 series ICP-AES. The wavelengths used for copper quantification were 327.393 and 324.752 nm.

Cellulase assays on PASC.

Phosphoric acid swollen cellulose (PASC) was prepared by addition of 10g Avicel® to 500 mL 85% phosphoric acid and blended for 30 minutes. Cellulose was precipitated by the addition ice cold water and washed with water multiple times. The concentration of PASC was determined by the phenol-sulfuric acid assay. Assays contained 5.0 μM PMO, 0.5 μM CDH-2, and 9 mg/mL PASC in 10 mM ammonium acetate pH 5.0 and were performed at 40 °C unless otherwise noted. In some assays, 2 mM ascorbic acid was used in place of CDH-2.

Product analysis by HPAEC.

Cellulase assays were mixed with 1 volume of 0.1 M NaOH to quench the reaction and then centrifuged to remove the supernatant. Samples were analyzed on a Dionex ICS-3000 HPAEC-PAD. Products were separated on a PA-200 HPAEC column using 0.1 M NaOH in the mobile phase with the concentration of sodium acetate increasing from 0 to 140 mM (14 min), 140-300 mM (8 min), 300 to 400 mM (4 min) and then held constant at 500 mM (3 min) before re-equilibration in 0.1 M NaOH (4 min). The flow rate was set to 0.4 mL/min, the column was maintained at a temperature of 30 °C, and samples were detected on an electrochemical detector. Authentic standards of glucose, cellodextrins, glucono-δ-lactone and cellobiono-δ-lactone were used to determine retention times and for quantification. Cellobiono-δ-lactone was synthesized as previously described (*90*).

Product analysis by LC-MS.

Samples were analyzed by an Agilent HPLC (1200 series) connected to an electrospray ionization emitter in a linear ion trap mass spectrometer (LTQ XL, Thermo Scientific). Carbohydrates were separated using a SeQuant ZIC®-HILIC column (150 x 2.1 mm, 3.5 μM 100Å) with a SeQuant ZIC®-HILIC guard column (20 x 2.1 mm, 5 μm). Solvent A was 5 mM ammonium acetate pH 7.2 and solvent B was 90% acetonitrile and 10 mM ammonium acetate pH 6.5. Samples were prepared by centrifugation of the assay mixture followed by the addition of 1 volume of 100% acetonitrile and 1% formic acid to the supernatant. Sample injection was set to 5 μL. The elution program consisted of a linear gradient from 80% B to 20% B over 14 minutes followed by 5 minutes at 20% B then re-equilibration for 2 minutes at 80% B. The column temperature was maintained at 25 °C and the flow rate was 0.2 mL/minute. Mass spectra were acquired in negative ion mode over the range m/z = 310-2000. Data processing was performed using Xcalibur software (version 2.2, Thermo Scientific).

Metal dependence of PMO activity.

Apo-PMO was prepared by treatment of as purified PMO with 10 mM EDTA for 24 hours. Protein was then concentrated in a 3 kDa spin concentrator and loaded onto a Sephacryl S100 column with 10 mM Tris pH 8.0 and 100 μM EDTA in the mobile phase. Following elution, Sigma TraceSELECT grade buffers, metals, and water were used for all assays and only extensively washed and rinsed plastics were used due to problems with copper contamination. The protein was buffer exchanged >100-fold into 10 mM sodium acetate (Sigma Cat # 59929 and #07692) in water (Sigma Cat # 14211) to a final concentration of >40 μM PMO. Cu- or Zn-bound PMO was then produced by reconstitution with a 2-fold molar excess of $CuSO_4$ (Sigma Cat #: 203165) or $ZnSO_4$ (Sigma Cat #: 204986).

Assays to quantify CDH activity in the presence or absence of PMO protein were performed in the presence of 1.0 mM cellobiose, 50 mM sodium acetate pH 5.0 and 200 nM CDH-2. NCU01050 (5 μM) or NCU01050 reconstituted with Zn or Cu was added to the reaction and after 30 minutes, assays were quenched by addition of 0.1M NaOH and analyzed for cellobionic acid production by Dionex HPAEC. PASC Assays to determine the metal dependence of NCU08760 activity were performed as described above except TraceSelect grade buffer and water were used with equimolar amounts of apo-, Zn-, or Cu-bound PMO. Before the assay, PASC was mixed in a large volumetric excess of 100 uM EDTA for 48 hours. The PASC was then washed multiple times with Traceselect water until the concentration of residual EDTA was < 1nM.

Protein gel electrophoresis and quantification.

Samples were mixed with SDS Laemmli loading buffer, boiled for 5 minutes, and loaded onto a Criterion 4-15% Tris-HCl polyacrylamide gel (Biorad). Gelcode Blue stain reagent (Thermo Scientific) was used for staining. Total extracellular protein content was determined using the Biorad Protein Assay (Biorad) according to the manufacturer's instructions.

Cellulase assays on Avicel®.

Cellulase assays were performed in triplicate with 10 mg/mL Avicel® PH101 in 50 mM sodium acetate pH 5.0 at 40 °C. Assays were performed in 1.7 mL microcentrifuge tubes with 1.0 mL total volume and were inverted 20 times per minute. Each assay contained 0.05 mg/mL culture filtrate or 0.05 mg/mL reconstituted cellulase mixture containing CBH-1, GH6-2, GH5-1,

and GH3-4 present in a ratio of 6:2.5:1:0.5 (*105*). CDH addition to assays was at a concentration of 0.004 mg/mL unless otherwise noted. CDH-2 flavin domain was added on an equal activity basis relative to full-length CDH-2 as measured by the cellobiose dependent reduction of DCPIP.

To measure the percent degradation, Avicel® assays were centrifuged, and 20 μL of assay mix was removed per well. Samples were incubated with 100 μL of desalted, diluted Novozyme 188 (Sigma) at 40 °C for 20 minutes to hydrolyze cellobiose and then 10-30 μL of the Novozyme 188 treated cellulase assay supernatant was analyzed for glucose using the glucose oxidase/peroxidase assay as described previously (*59*). Percent degradation was calculated based on the maximum theoretical conversion of 10 mg/mL Avicel®.

Phylogeny of *N. crassa* PMO proteins.

Amino acid sequences were processed to remove signal peptides so that every sequence started with histidine 1. The C-terminus of each protein was also truncated to remove linkers or cellulose binding modules present on some PMOs. Multiple sequence alignments were performed locally using T-COFFEE (*106*). A maximum likelihood phylogeny was determined using PhyML version 3.0 with 500 bootstraps through the Phylogeny.fr webserver (*107*).

Protein purification.

N. crassa PMO proteins were purified from the *N. crassa* Δ*cdh-1* strain. Culture filtrates from multiple flasks were pooled and concentrated 100-fold using a tangential flow filtration system with a 5,000 MWCO PES membrane (Millipore). The concentrated culture filtrate was then buffer exchanged into 10 mM Tris pH 8.5 using a HiPrep 26/10 desalting column. The concentrated and buffer exchanged protein was then fractionated using an AKTAexplorer FPLC system (GE Healthcare) and a 10/100 GL MonoQ column. The mobile phases for the anion-exchange fractionation were buffer A: 10 mM Tris pH 8.5 and buffer B: 10 mM Tris pH 8.5 with 1.0 M sodium chloride. For each run on the MonoQ column approximately 100 mg of total secretome protein was loaded and eluted from the column with a linear gradient from 0 to 50% buffer B over six column volumes. NCU08760 and NCU01050 do not bind the column under these conditions and are present in the flow through. NCU02240 and NCU07898 elute from the column between 4-9 mS/cm. Fractions containing the target proteins were pooled and treated with 1.0 mM EDTA overnight to strip bound metals. The EDTA treated samples were then concentrated using 3,000 MWCO PES spin concentrators and desalted into 10 mM Tris pH 8.5 using a 26/10 desalting column. Removal of the bound metal ion increases the affinity of the PMOs for the anion-exchange resin and causes them to elute at higher salt concentrations. For NCU08760 and NCU01050, removal of bound metal ion causes the proteins to bind to the MonoQ column. The apo NCU01050 and NCU08760 are then eluted from the column using the same buffers as above with a linear gradient from 0 to 3.5% buffer B over 3 column volumes. NCU01050 elutes at ~1.6 mS/cm and NCU08760 at ~2.2 mS/cm conductivity. The apo forms of NCU02240 and NCU07898 elute from the MonoQ column between 7-9 mS/cm. The purity of the PMOs can be further improved by reconstituting the apo PMOs with Zn(II) and repeating the anion-exchange fractionation. Other proteins in the secretome do not change their affinity for the resin in the presence or absence of metal ions and can be effectively removed from PMOs by cycles of stripping the metal, fractionating, reconstituting, and fractionating again. NCU01050 and NCU08760 can then be separated from one another by size exclusion chromatography using a Sephacryl S100 column with a mobile phase of 10 mM Tris pH 8.5 with 150 mM sodium chloride. NCU02240 and NCU07898 are separated from one another using the same method as

used for NCU01050 and NCU08760. The four natively purified PMOs from *N. crassa* are stable for several months at 4 °C.

Metal chelating reaction.

To determine the requirement for small molecules and metals, wild-type or Δ*cdh-1* culture filtrate was buffer exchanged more than 10,000-fold in a 10 kDa MWCO PES spin concentrator (Sartorius). The culture filtrate was incubated with 100 μM EDTA for 2 hours. The culture filtrate was then assayed as described above in the presence or absence of CDH-1.

Anaerobic assays.

Anaerobic cellulase assays were performed as above except all assays were conducted in an anaerobic chamber (Coy) at room temperature. Buffers were sparged with ultra high purity argon (Praxair, UN 1006) for 1 hour and all enzymes were concentrated to volumes of less than 300 μL before introduction into the anaerobic chamber. All solutions were left open in the anaerobic chamber, and buffer solutions were stirred vigorously for 72 hours before use to fully remove dissolved oxygen. Aerobic reactions were prepared in the anaerobic chamber in 3 mL Reacti-Vials and then removed from the anaerobic chamber, exposed to air, sealed, and returned to the anaerobic chamber. After 24 hours of reaction, assays were centrifuged in the glove bag and 100 μL of assay mix was removed for analysis by the glucose oxidase/peroxidase assay or HPLC and LC-MS.

Screen to identify PMO proteins.

The *Δcdh-1* culture filtrate was fractionated over a 10/100 GL MonoQ column as described above. An appropriate concentration of the load, flow-through, and all fractions were added to a mixture of 0.03 mg/mL purified *N. crassa* cellulases (CBH-1, GH6-2, and GH3-4) and assayed on Avicel® for 12 hours. Fractions that had increased cellulase activity in the presence of CDH were kept and analyzed by SDS PAGE and LC-MS/MS.

Analysis of copper and zinc in the secretome by ICP-AES

The *N. crassa Δcdh-1* strain was grown on 2% w/v Avicel® as previously described with an additional 5 μM copper sulfate, and 30 μM zinc sulfate supplemented in the minimal media. The culture filtrate was concentrated using tangential flow filtration and buffer exchanged into 10 mM Tris pH 8.5. The concentrated and buffer exchanged culture filtrate was loaded onto a 10/100 GL MonoQ column and separated into 5 fractions with a linear salt gradient. Each fraction was then analyzed for the presence of copper or zinc. Metal analysis was performed using a Perkin Elmer inductively coupled plasma atomic emission spectrometer (ICP-AES) The wavelengths used for quantification for copper were 327.393 or 324.752 nm, and for zinc, 213.857 or 206.200 nm. Samples were also checked for the presence of magnesium, calcium, manganese, iron, and cobalt, none of which were enriched in the concentrated culture filtrate relative to flow through from the spin concentrators.

RESULTS

Identification of a copper metalloenzyme.

To identify the additional metalloprotein(s) involved in the CDH dependent enhancement of cellulose degradation, we devised a fractionation strategy of the *N. crassa* Δ*cdh-1* supernatant.

Analysis of the secretome showed that copper and zinc were the only metals present. Upon further analysis, it was also noted that the concentration of copper in the minimal media was low at just 1 μM. The concentration of copper and zinc in the media was increased by a factor of 5 and following ICP analysis copper was 10-fold more abundant than zinc (Figure 4.3). However, no *N. crassa* proteins secreted during growth on cellulose were known to bind copper.

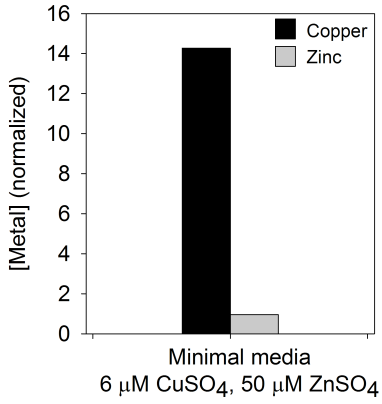

Figure 4.3. ICP-AES metal analysis of the Δ*cdh-1* secretome. Minimal media was supplemented with 5 μM of $CuSO_4$ and 30 μM $ZnSO_4$ and after seven days of growth on Avicel® the fungal biomass was removed by filtration. The secretome was concentrated using 3,000 MWCO spin concentrators and then buffer exchanged into 10 mM TRIS pH 8.5 using a 26/10 desalting column. The micromoles of metal were then normalized to the total protein concentration in the secretome as determined by the Biorad protein assay.

Fractionation of the secretome (Figure 4.4) resulted in two fractions that enhanced the cellulase activity of purified cellulases in a CDH-dependent fashion. Tryptic digests and subsequent LC-MS/MS analysis showed that each fraction contained two members of the GH61 enzyme family. Further purification showed fractions containing GH61 proteins were also enriched in copper (Figure 4.5). The GH61 proteins encoded by NCU01050, NCU02240, NCU07898, and NCU08760 were purified (Figure 4.6A). Three of these were analyzed by inductively coupled plasma–atomic emission spectroscopy (ICP-AES) and found to bind copper with a 1:1 stoichiometry (Figure 4.6B). NCU02240 was not present in sufficient purity or yield for further characterization.

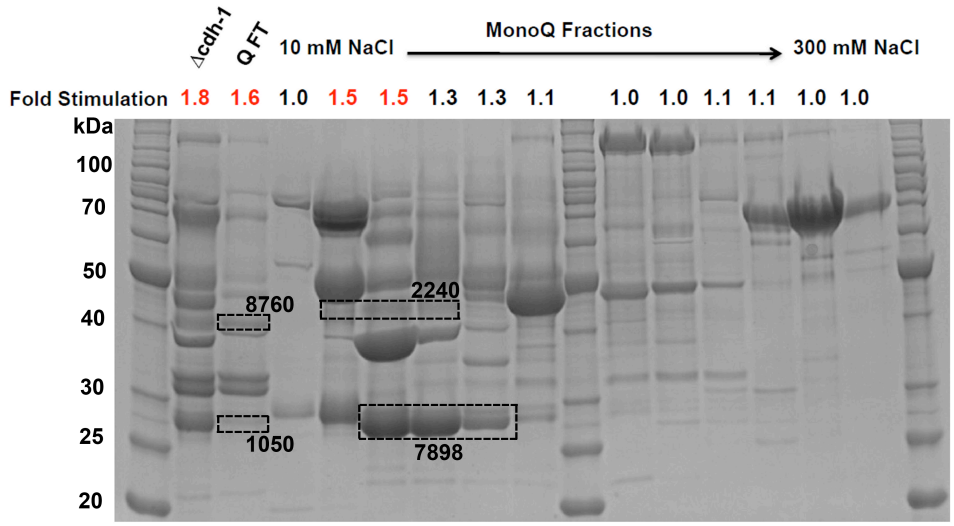

Figure 4.4. Fractionation of the Δ*cdh-1* secretome. A screen was designed to identify other factors involved in CDH dependent enhancement of cellulase activity. Shown is an SDS-PAGE analysis of fractions from MonoQ separation of the Δ*cdh-1* secretome. Above each lane is the fold stimulation of the fraction when added to a mixture of purified *N. crassa* cellulases in the presence or absence of CDH-1. Fractions highlighted in red were analyzed by mass spectrometry and showed the presence of four glycosyl hydrolase family 61 proteins.

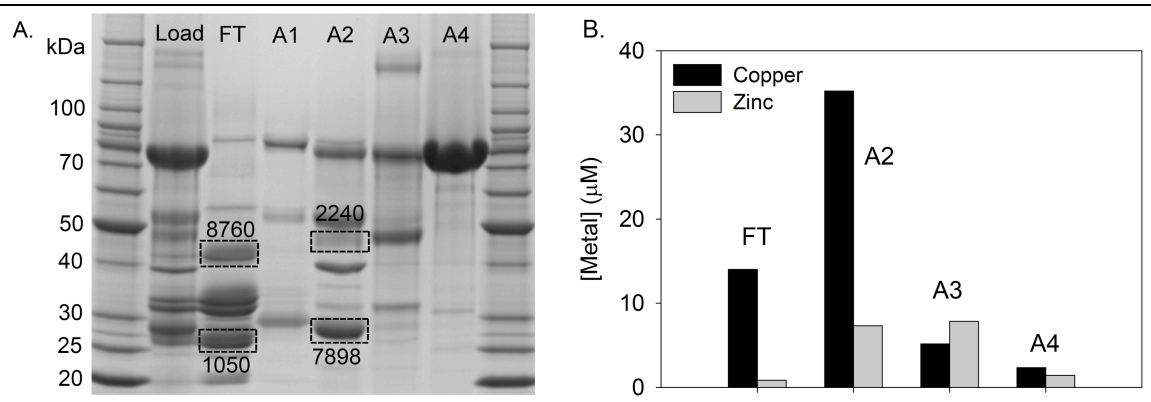

Figure 4.5. ICP-AES metal analysis of MonoQ fractions. The secretome of the Δ*cdh-1* strain was desalted and fractionated with a linear gradient of sodium chloride and analyzed by ICP-AES. (A) Concentrations of copper and zinc in fractions from the MonoQ column. (B) SDS-PAGE analysis of the MonoQ fractions analyzed by ICP-AES.

Since copper is the metal natively bound to GH61 proteins from *N. crassa*, the correlation of activity with metal binding was investigated. In the presence of copper bound GH61, CDH activity increased nearly 10-fold, whereas apo or zinc bound GH61 only enhanced turnover 2-fold (Fig. 4.6C). This suggests that GH61, and in particular GH61 bound to copper, can accept electrons from reduced CDH, thus increasing the oxidation of cellobiose. Hence, the copper in GH61 proteins could act as the biological electron acceptor for CDH. Two other proteins that contain bidentate N-terminal histidine ligands were found in the protein databank. One of them, CopC, is part of the cop operon involved in copper resistance in bacteria and has been shown to bind Cu(II) with picomolar affinity (Fig. 4.6D) (*108*). The other, particulate methane monooxygenase (pMMO), uses a trinuclear copper site to oxidize methane (*109*). Combining our experimental results with the similar ligation in CopC and pMMO, we conclude that copper is the native metal in GH61 proteins.

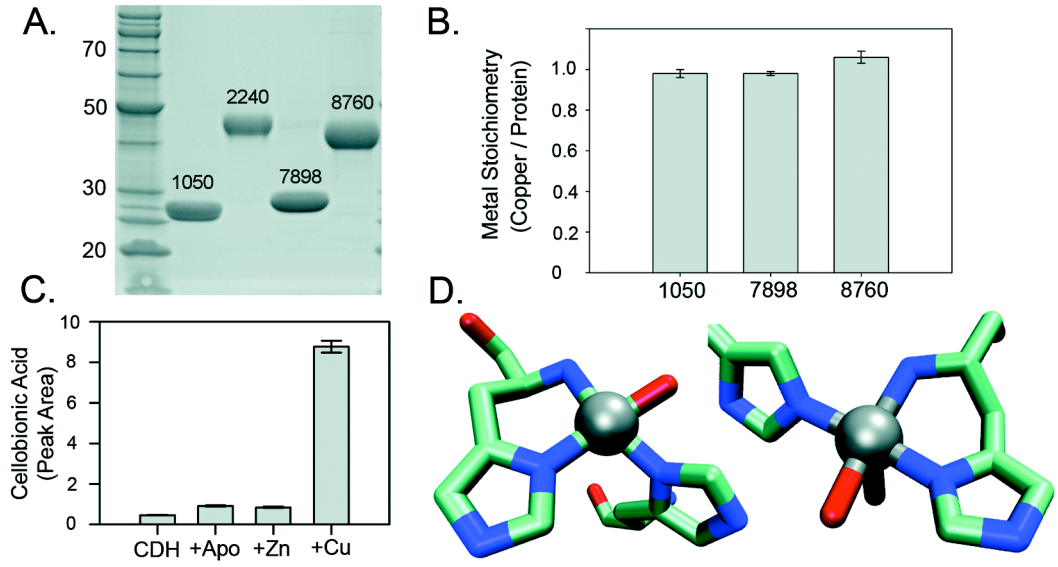

Figure 4.6. Purity and metal analysis of GH61 proteins. (A) SDS-PAGE of purified *N. crassa* GH61 proteins. (B) The number of bound copper molecules for each purified GH61 as determined by ICP-AES. (C) Effect of GH61 metal state on CDH activity. CDH-2 (200 nM) was mixed with 5.0 μM of apo or metal reconstituted NCU01050 and 1.0 mM cellobiose. The reaction was incubated for 1 hour at 40 °C and products analyzed by HPAEC. (D) Comparison of the metal binding sites in CopC(left) and GH61E(right) from *Thielavia terrestris*. Copper is bound in the CopC structure and zinc is bound in GH61E.

Product analysis of oxidative cellulose cleavage.

The phylogenetic diversity of 10 *N. crassa* GH61s whose transcripts are upregulated during growth on cellulose (*39*) suggests that these enzymes may target a wide array of substrates in lignocellulose, or generate different products (Figure 4.2). To investigate the reaction products of the purified GH61s, assays were performed on phosphoric acid swollen cellulose (PASC). When PASC was treated with GH61 and CDH, a series of aldonic acids two to nine glucose residues in length (A2-A9) were identified by high performance anion exchange chromatography (HPAEC). In addition to aldonic acids, the combination of CDH and GH61s NCU01050 or NCU07898 produced peaks at a later retention time (Figure 4.7A). Product

analysis by liquid chromatography-mass spectrometry confirmed the presence of aldonic acids (Gx+15 a.m.u.), as well as masses of Gx + 13 a.m.u. and Gx + 31 a.m.u (Figure 4.7B). The Gx +13 mass is consistent with a doubly oxidized cellodextrin. Cellulose cleavage by these GH61s likely results in oxidation at the non-reducing end followed by oxidation at the reducing end by CDH. Given the necessity to cleave a 1,4-glycosidic bond, these products are likely oligosaccharides with a 4-keto sugar at the non-reducing end. The Gx + 31 mass is consistent with the hydrate of this product, a ketal. Ketoaldoses are unstable in aqueous solution and are known to decompose spontaneously into many different species (*110*). The third purified GH61, NCU08760, did not form the late eluting peak on the HPAEC, or Gx + 13 and Gx + 31 species (Figure 4.7A and 4.7B), consistent with oxidation exclusively at the reducing end on C1 to form aldonic acids. Incubation of PASC with GH61 alone led to the formation of low amounts of hydrolytic products (Figure 4.8). The formation of hydrolytic products could be due to low levels of cellulase contamination.

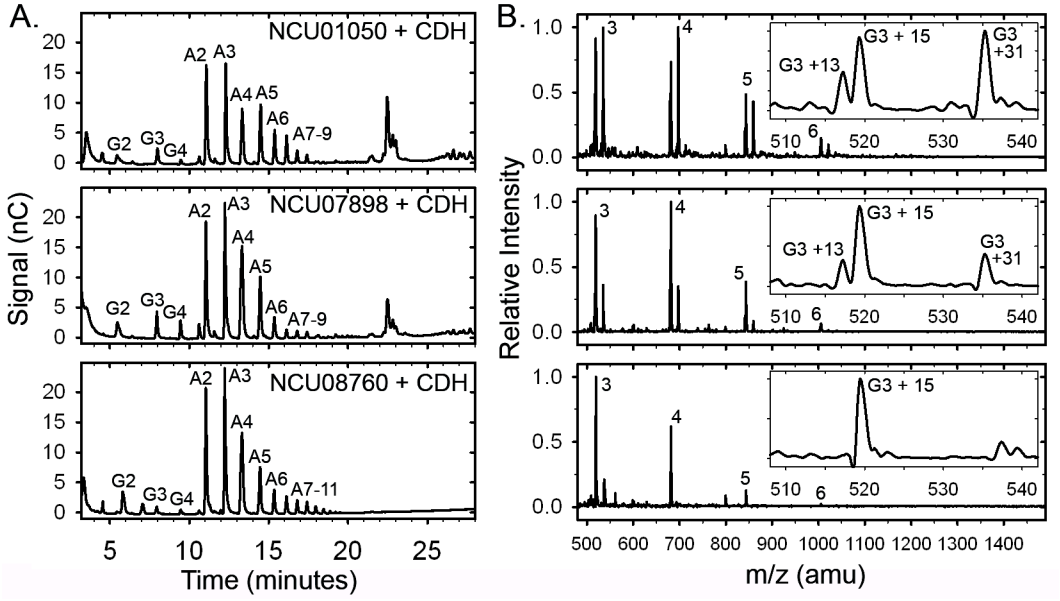

Figure 4.7. Comparison of the products of cellulose cleavage by GH61 enzymes. GH61 (5.0 μM) and 0.5 μM CDH-2 were incubated with 5 mg/mL phosphoric acid swollen cellulose for 2 hours in 10 mM ammonium acetate pH 5.0 at 40°C. Products of CDH-2 in combination with each GH61 protein (NCU01050-top, NCU07898-middle), or NCU08760-bottom)) were analyzed by HPAEC (A) and LC-MS (B). HPAEC standards were used to determine retention times of cellodextrins (G1-G6) and the respective aldonic acid derivatives (A2-A9). LC-MS of reaction mixtures in negative ion mode shows reaction mixtures comprised of masses consistent with a ladder of aldonic acids (Gx + 15 a.m.u.) separated by an anhydroglucose unit. Inset is a zoom around the G3 series. NCU01050 and NCU07898 show additional masses consistent with a keto-aldonic acid (Gx + 13 a.m.u.) or the hydrate of that product, a ketal-aldonic acid (Gx + 31 a.m.u.).

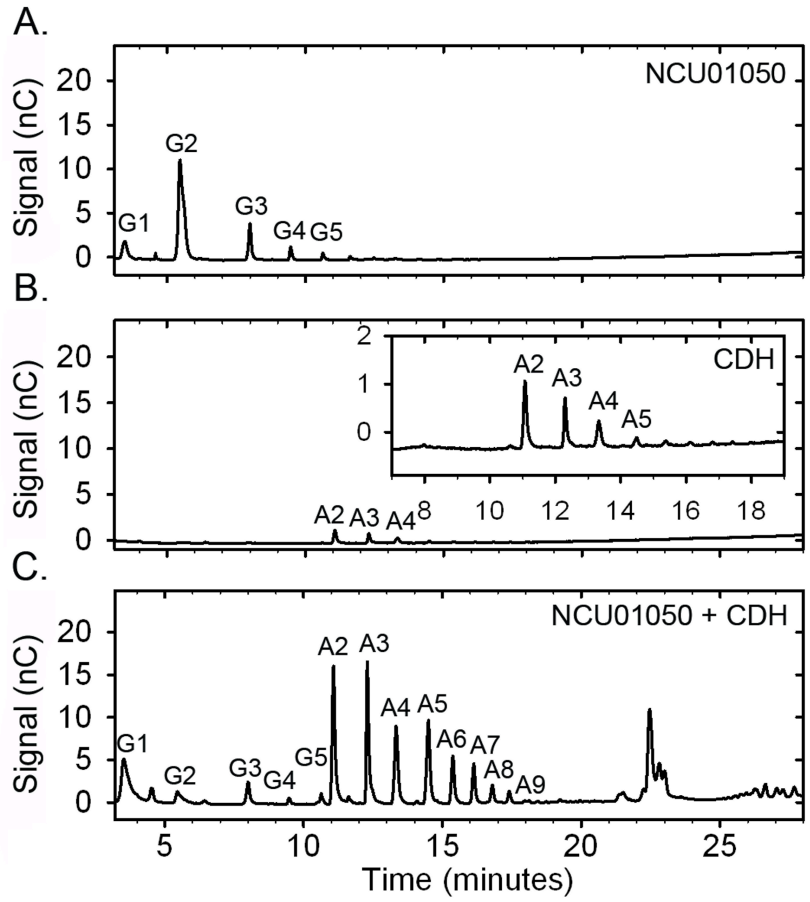

Figure 4.8. HPAEC analysis of CDH-2 and NCU01050 products. (A) GH61 (5.0 μM) (NCU01050), (B) 0.5 μM CDH-2, or (C) a combination of the two were incubated with 5 mg/mL phosphoric acid swollen cellulose (PASC) for 2 hours in 10 mM ammonium acetate pH 5.0 at 40°C. Products were analyzed by HPAEC and standards were used as references to label cello-oligosaccharides (G1-G5) and the respective aldonic acid derivatives (A2-A9). Inset in (B) indicates the presence of low abundance aldonic acids following treatment with CDH-2 alone. Peaks with retention times of 22-25 minutes correlate with the presence of the Gx + 13 and Gx + 31 species in the LC-MS.

Since CDH is known to oxidize the C1 position of cellodextrins, a reaction with NCU08760 was carried out with ascorbic acid substituted for CDH. In the presence of ascorbic acid and copper, NCU08760 produced a ladder of aldonic acids (Figure 4.9 and Figure 4.10). Under identical conditions, NCU01050 produced a ladder of products with a later retention time when analyzed by HPAEC and 100-fold less aldonic acid than NCU08760 (Figure 4.9B).

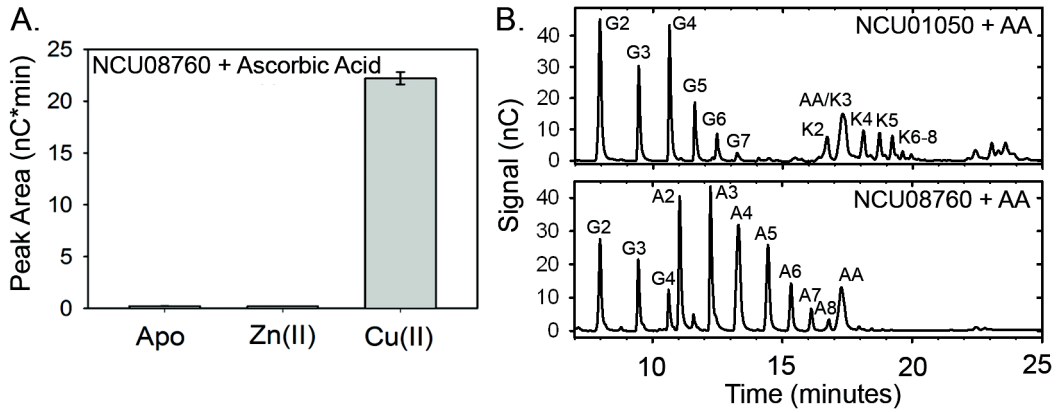

Figure 4.9. Product analysis of GH61 enzymes with ascorbic acid. (A) Incubation of 5.0 μM apo-, Zn-bound, or Cu-bound NCU08760 with 2 mM ascorbic acid confirms that Cu-bound GH61 is required for generation of oxidative products. Error bars represent standard deviation of assays performed in triplicate (B) Ascorbic acid (2 mM) and 5.0 μM GH61 were assayed on PASC and analyzed by HPAEC. Products of NCU01050 include a ladder of cello-oligosaccharides (G2-G7) and a ladder of later eluting products that are likely oxidized at the non-reducing end to generate 4-keto sugars (K2-8). Products of NCU08760 include a ladder of cello-oligosaccharides (G3-G6) and aldonic acids (A2-A7). Trace amounts of aldonic acids were produced by NCU01050 but these are 100-fold less abundant than those produced by NCU08760 suggesting different regiospecificities for the 2 proteins. AA designates the peak due to ascorbic acid.

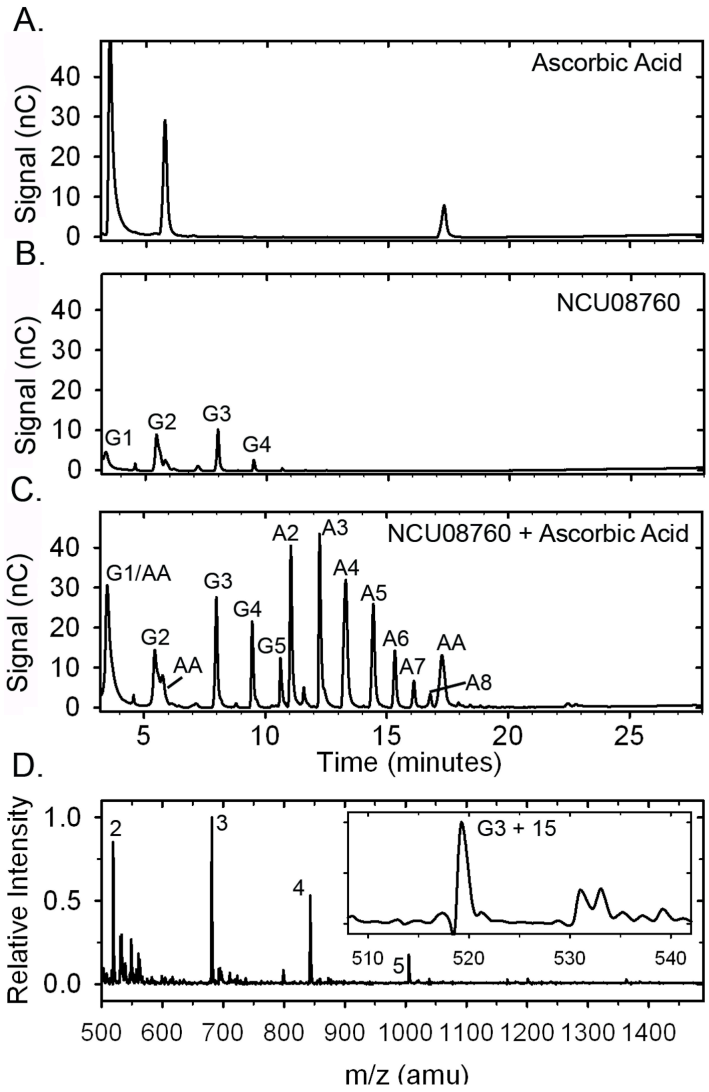

Figure 4.10. HPAEC and LC-MS analysis of NCU08760 products. Ascorbic acid (2 mM), 5.0 μM GH61 (NCU08760) or a combination of the two were incubated with 5 mg/mL phosphoric acid swollen cellulose (PASC) for 2 hours in 10 mM ammonium acetate pH 5.0 at 40°C. (A-C) Products were analyzed by HPAEC and standards were used as references to label cello-oligosaccharides (G1-G5) and the aldonic acid derivatives (A2-A8). Peaks in the sample containing ascorbic acid only were also present in control reactions where no PASC was present. (D) LC-MS of the reaction containing both ascorbic acid and NCU08760 confirms the production of masses consistent with an aldonic acid. Inset is a zoom around the G3 series.

Proposed mechanism of polysaccharide monooxygenases.

The generation of oxidized sugars by the GH61s was oxygen dependent, suggesting that GH61s are oxidases (Figure 4.11). Peroxide is not able to shunt the reaction in the absence of CDH, and catalase showed no inhibitory effect (Figure 4.12). Evidence that GH61s are copper enzymes requiring electron transfer from CDH to cleave cellulose in an oxygen dependent manner provides the basis to propose a chemical mechanism for a new group of enzymes acting

as polysaccharide monooxygenases (PMOs) (Figure 4.13). Precedent is drawn from the well-studied copper monooxygenases (*111, 112*). The work reported here supports one electron reduction of PMO-Cu(II) to PMO-Cu(I) by the CDH heme domain followed by oxygen binding and internal electron transfer to form a copper superoxo intermediate. Hydrogen atom abstraction by the copper superoxo at the 1-position (by NCU08760) or the 4-position (by NCU01050 or NCU07898) of an internal carbohydrate then takes place, generating a copper hydroperoxo intermediate and a substrate radical. The 2nd electron from CDH then facilitates O-O bond cleavage releasing water and generating a copper oxo radical that couples with the substrate radical, thereby hydroxylating the polysaccharide at the 1- or 4-position. The additional oxygen atom destabilizes the glycosidic bond leading to elimination of the adjacent glucan and formation of a sugar lactone or ketoaldose. This elimination would be facilitated by a general acid, possibly a third absolutely conserved histidine that is located on the surface of all fungal PMO proteins near the metal binding site (*102*). It is possible that a 2-electron reduction of oxygen to a Cu-OOH intermediate could abstract the hydrogen.

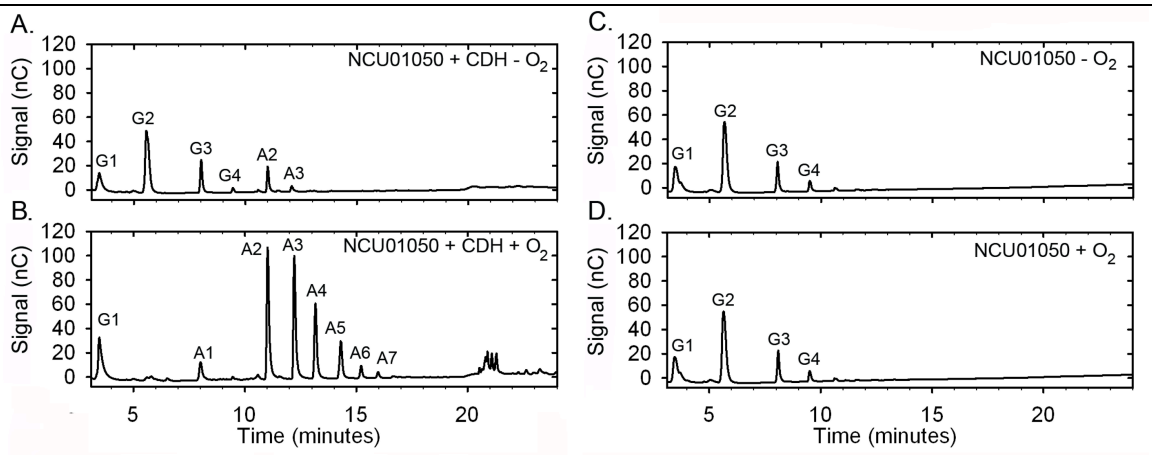

Figure 4.11. Oxygen dependence of GH61 activity. GH61 (5.0 μM) (NCU01050) and 0.5 μM CDH-2 were incubated with PASC for 24 hours in 10 mM ammonium acetate pH 5.0 under aerobic (A) or anaerobic (B) conditions. In the absence of oxygen, the aldonic acid peaks are significantly reduced in size. Further, the late eluting peak that was consistent with a ladder of 4-keto-aldonic acids is completely absent under anaerobic conditions. The hydrolytic activity observed by NCU01050 alone was not affected by the presence (C) or absence (D) of oxygen.

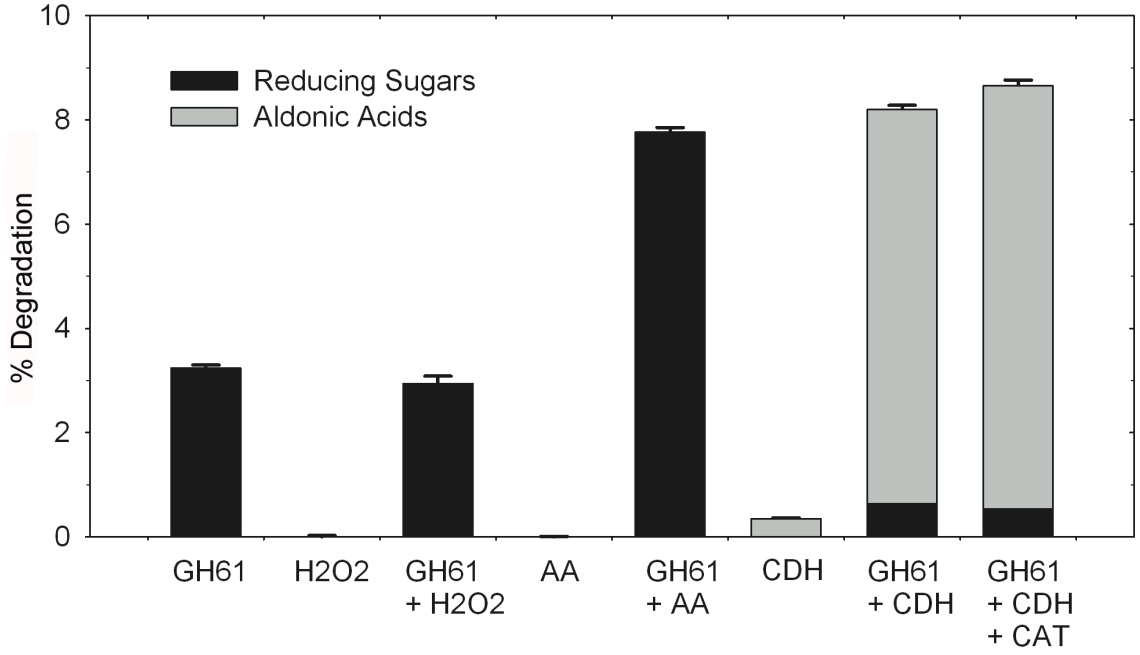

Figure 4.12. GH61 cannot be shunted with hydrogen peroxide. GH61 (5.0 μM) (NCU01050) was assayed alone, with 2 mM peroxide, 2 mM ascorbic acid, or 0.5 μM CDH-2. Assays were performed on 5 mg/mL PASC in 10 mM ammonium acetate pH 5.0 with a 24-hour endpoint. Assays containing catalase (*A. niger*) were supplemented with 0.01 mg/mL enzyme. Percent degradation was calculated based on the HPAEC chromatogram and data is shown as a stacked bar graph. Values are the mean of three replicates. Error bars are the SD between these replicates.

DISCUSSION

The evidence presented above shows that oxidative enzymes are key components of the enzyme cocktails secreted by fungi for plant cell wall degradation and have proposed a chemical mechanism for the action of a new family of metalloenzymes, the polysaccharide monooxygenases. While this manuscript was in preparation, similar results were published showing that an *H. insolens* CDH and a GH61 from *T. aurantiacus* act synergistically to depolymerize cellulose (*113*). Shortly thereafter, the same group reported an x-ray crystal structure of *T. aurantiacus* GH61A bound to copper(II) with a similar ligation to that previously described. Interestingly, the N-terminal histidine of this protein was methylated at ring N3. In the presence of non-protein reductants, GH61A generated oxidized sugars modified at the reducing or non-reducing end, and non-reducing end modification was proposed to occur at C6; however, no evidence was provided to support this (*104*). Hydroxylation at C6 could lead to breakage of the glycosidic bond via elimination to form a 4,5-unsaturated aldehyde. No evidence for a dehydrated product was observed, though it is possible that water addition could occur following elimination. Oxidation at the 4-position could lead to cleavage of the glycosidic bond via the same general mechanism as that proposed for cellulose cleavage by oxidation at C1 (Figure 4.13).

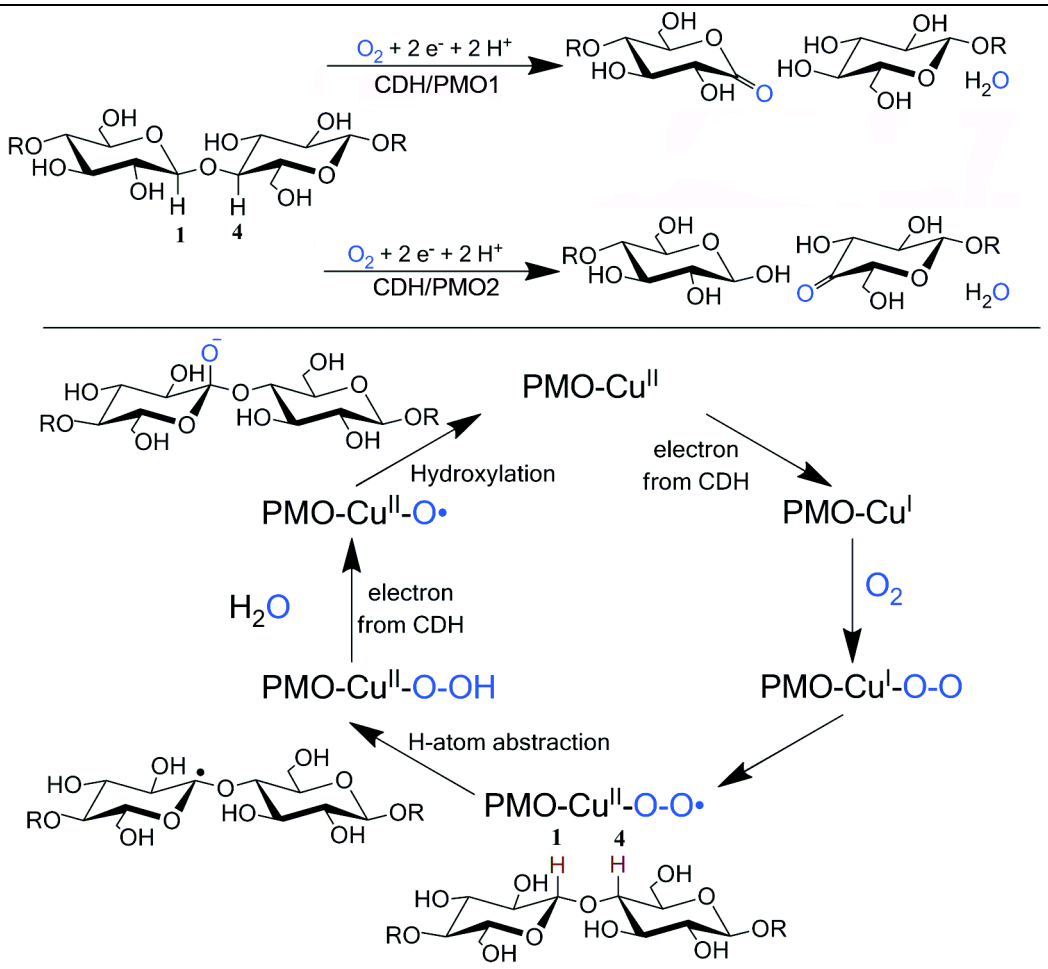

Figure 4.13. PMO reactions and proposed mechanism. (Top) Type 1 PMOs abstract a hydrogen atom from the 1 position leading to formation of sugar lactones. Type 2 PMOs catalyze hydrogen atom abstraction from the 4 position leading to formation of ketoaldoses. (Bottom) PMO mechanism: An electron from the heme domain of CDH reduces the PMO Cu(II) to Cu(I) and then O_2 binds. Internal electron transfer takes place to form a copper superoxo intermediate, which then abstracts a H• from the 1 or 4 position on the carbohydrate. A second electron from CDH leads to homolytic cleavage of the Cu-bound hydroperoxide. The copper oxo species (Cu-O•) then couples with the substrate radical, hydroxylating the substrate. Addition of the oxygen atom destabilizes the glycosidic bond and leads to elimination of the adjacent glucan.

In contrast to the widely discussed Fenton model, our data supports a direct enzymatic oxidation of cellulose leading to glycosidic bond cleavage. The genetic and biochemical experiments reported here with CDH show that in *N. crassa,* CDH-1 functions as the sole extracellular enzyme that exhibits reductase activity towards PMO's, and that the heme domain of CDH is required for enhancement of cellulose degradation. Previous expression profiling studies showed that expression of at least 10 of the PMOs was induced during growth on cellulose. In fact there are more PMOs expressed in *N. crassa* than there are cellulases.

In addition to their prevalence in nature, supplementation of cellulase cocktails with PMOs can significantly reduce the enzyme loading required for saccharification of

lignocellulose. Because several different PMOs are produced by fungi, and PMOs work through a mechanism completely orthogonal to that of cellulases, it is likely that addition of multiple PMOs to cellulase cocktails will further reduce enzyme loadings. Additional mechanistic insights into this large family of enzymes may facilitate their development for commercial applications.

PREVIOUSLY PUBLISHED MATERIAL

This chapter was adapted from a previously published article co-authored by William T. Beeson, Jamie H. Cate, and Michael A. Marletta. Thanks to the co-authors and publishers at the ACS Chemical Biology for allowing use of this material.

CHAPTER 5: Mechanistic insights into cellulose cleavage by polysaccharide monooxygenases

ABSTRACT

Fungal-derived copper-dependent polysaccharide monooxygenases (PMOs) formerly known as GH61 proteins, have been recently shown to catalyze the O_2 dependent oxidative cleavage of recalcitrant polysaccharides. Different PMOs isolated from *Neurospora crassa* were found to generate oxidized cellodextrins modified at the reducing or non-reducing ends when incubated with cellulose and cellobiose dehydrogenase. Here it is shown that the non-reducing end product formed by a *N. crassa* PMO is a 4-keto-aldose. Together with isotope labeling experiments, further support is provided for a mechanism involving oxygen insertion and subsequent elimination to break glycosidic bonds in crystalline cellulose.

INTRODUCTION

For cellulase-catalyzed hydrolysis to occur, a cellulose chain must be separated from the crystalline surface and then drawn into the active site of the enzyme where Asp or Glu residues function in general acid/base catalysis. The separation of the glucan chain from crystalline cellulose has been proposed to be the slow step in enzymatic hydrolysis of cellulose (*114*).

Recently, oxidative enzymes have been shown to be important for enzymatic degradation of cellulose and have been identified in multiple transcriptomic and proteomic analyses (*36, 38-40, 105, 115*). Polysaccharide monooxygenases (PMO), previously called GH61 proteins, are a recently discovered class of copper-dependent metalloenzymes that oxidatively cleave glycosidic bonds on the surface of cellulose, without requiring separation of a glucan chain (*102-104, 113, 116*). These enzymes require molecular oxygen and reducing equivalents from cellobiose dehydrogenase.(*113, 116*) A chemical reductant can also be used to drive the reaction (*104, 116*). PMOs have been shown to augment the hydrolysis of cellulose by cellulases (*103, 113, 116*), and a deeper mechanistic understanding of these enzymes could be used to further reduce costs of cellulosic biofuels.

The oxidative chemistry catalyzed by fungal PMOs will likely lead to incorporation of molecular oxygen into the products. We proposed a mechanism by which PMOs insert molecular oxygen into C-H bonds adjacent to the glycosidic linkage leading to elimination of the adjacent carbohydrate moiety (*116*). Two classes of PMOs were described. Type 1 PMOs generate products oxidized at C1, probably initially in the lactone form, which is then hydrolyzed spontaneously or enzymatically (*63*) to yield an aldonic acid. Type 2 PMOs generate products oxidized at the non-reducing end. Formation of a 4-keto-aldose could result from oxidative cleavage proceeding by the same general mechanism proposed for oxidation at C1. Another report with *T. aurantiacus* GH61A also observed oxidation at C1 and on the non-reducing end, proposed to be at C6 (*104*). No data has been reported that identifies the position on the carbohydrate of the non-reducing end oxidation catalyzed by type 2 PMOs. Here, evidence is shown to further elucidate the mechanism of PMO action through the use of isotope labeling experiments and definitive identification of the non-reducing end product of a type 2 PMO.

MATERIALS AND METHODS

General PMO assay conditions

N. crassa PMOs NCU01050 and NCU08760 and CDH-2 from *Myceliophthora thermophila* (*Mt*CDH-2) were purified natively from culture filtrates as previously described.(*116*) Assays contained 5.0 μM PMO, 0.2 μM *Mt*CDH-2, and 5.0 mg/mL PASC and were mixed with a stir bar in a water bath at 40 °C. Phosphoric acid swollen cellulose (PASC) was also prepared as previously described (*116*). In some assays, 2.0 mM ascorbic acid was used in place of *Mt*CDH-2. LC-MS assays of cellulose degradation products were performed after 1 hour of reaction in 50 mM ammonium bicarbonate pH 7.8 or ammonium acetate pH 5.0 buffer. Assays for product identification were performed for 10 hours in 50 mM sodium acetate pH 5.0.

Reactions in ^{18}O or ^{16}O gas

^{18}O labeled molecular oxygen was purchased from Sigma (99 atom % ^{18}O). For experiments with $^{18}O_2$, all reagents were made anaerobic by incubation in an anaerobic glove bag for at least 48 hours. Reactions were setup in the glove bag (Coy) in oxygen impermeable vials with double faced PTFE/silicone septa. The sample was then attached to a Schlenk line, then vacuum applied followed by $^{18}O_2$ delivery to the headspace of the sample.

Hypoiodite oxidation of PMO reaction products

Residual PASC was removed from the PMO reaction by centrifugation and the supernatant was recovered for further characterization. For hypoiodite oxidation, a fresh Lugol's solution was prepared by mixing 100 mM iodine with 250 mM potassium iodide. PMO reaction product solution (250 μL) was then mixed over the course of 30 minutes with equal volumes of 0.1 M sodium hydroxide and Lugol's solution (90 μL). The sodium hydroxide and Lugol's solutions were added 4.5 μL at a time with mixing. After the 30 minute mixing period, residual iodine was removed by addition of excess silver carbonate (100 mg). The silver carbonate was then removed by centrifugation and the products analyzed by Dionex HPAEC. The hypoiodite oxidized products were then hydrolyzed using trifluoroacetic acid (TFA), as described below.

Reduction with sodium borohydride

PMO reaction supernatant (100 μL) was mixed with freshly prepared 20 mg/mL sodium borohydride in 1.0 M ammonium hydroxide (100 μL). The reaction was allowed to proceed for 2 hours at room temperature with occasional mixing. Glacial acetic acid was added until bubbling ceased (25 μL). Next, 200 μL of a 9:1 methanol:acetic acid mixture was added to the reaction and the samples were then dried under a stream of nitrogen at 40 °C. The resulting sample was hydrolyzed by TFA as described below.

TFA Hydrolysis

Samples were incubated with 2.0 M TFA at 121 °C on a heating block for 1 hour. The samples were then removed from the heat block, cooled on ice, centrifuged briefly, and dried under a stream of nitrogen at 40 °C. After drying the sample was washed with 300 μL of isopropanol and dried under a stream of nitrogen twice. Dried samples were then dissolved in 1.0 mL of water for analysis on a PA-20 column (Dionex) or 1.0 mL 0.1 M sodium hydroxide for analysis on a PA-200 column (Dionex).

Dionex HPAEC

Samples were analyzed on a Dionex ICS-3000 HPAEC-PAD. The products of oxidation and TFA hydrolysis or TFA hydrolysis alone were separated on a PA-200 HPAEC column as previously described (*116*). The products of sodium borohydride reduction and TFA hydrolysis were separated isocratically on a PA-20 column. Products were eluted with 10 mM potassium hydroxide for 20 minutes followed by a 5 minute wash with 100 mM potassium hydroxide and a

5 minute equilibration at 10 mM potassium hydroxide. Standards for glucose, galactose, sorbitol, gluconic acid, and glucuronic acid were purchased from Sigma.

Product analysis by LC-MS. Samples were analyzed on an Agilent HPLC (1200 series) connected to an electrospray ionization emitter in a linear ion trap mass spectrometer (LTQ XL, Thermo Scientific) as described previously (*116*) with the following modifications. To limit the exchange of bulk water into the oxidized products, the mobile phases were changed to contain 10 mM ammonium bicarbonate pH 8.0 in both solvent A and solvent B. Following centrifugation of the assays and removal of the supernatant, 1 volume of 100% acetonitrile was added to the samples. Samples were immediately injected into the LC-MS and the injection was set to 5 µL. The elution program consisted of a linear gradient from 80% B to 20% B over 7 minutes followed by 5 minutes at 20% B then re-equilibration for 2 minutes at 80% B.

RESULTS AND DISCUSSION

To show oxygen insertion from O_2, reactions were prepared anaerobically that contained 5.0 µM of a type 1 PMO from *Neurospora crassa* (NCU08760), 2.0 mM ascorbic acid, 50 mM ammonium bicarbonate pH 7.8, and 5.0 mg/mL phosphoric acid swollen cellulose (PASC). The solutions were sealed in 1.0 mL vials and then the headspace was replaced with $^{18}O_2$ on a Schlenk line or opened to atmospheric oxygen. Reactions were allowed to proceed at 40 °C for 1 hour and analyzed by LC-MS as previously described (*116*). Cellulase and PMO reactions are typically carried out at pH 5.0. A more basic pH was chosen here in order to limit the exchange of bulk water into the products. Figure 5.1 shows the mass spectra confirming incorporation of 1 atom of ^{18}O into the aldonic acid products, providing evidence that the enzyme functions as a monooxygenase. Similar experiments were performed where the ascorbic acid was substituted with *Myceliophthora thermophila* cellobiose dehydrogenase 2 (*Mt*CDH-2) (Figure 5.2). ^{18}O incorporation into the products was also observed at both pH 5.0 and pH 7.8. A type 2 non-reducing end PMO (NCU01050) did not produce products labeled with ^{18}O; however, the predicted 4-keto-aldose or di-aldose products are present as hydrates in aqueous solutions and would rapidly exchange with bulk water (*117, 118*).

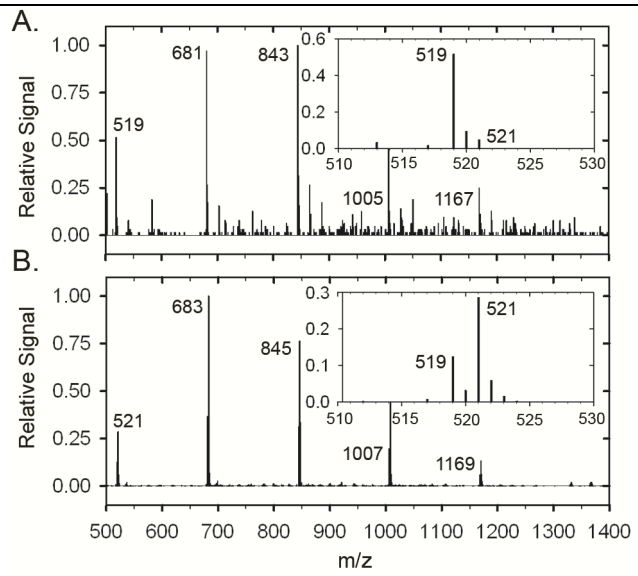

Figure 5.1. Mass spectra of PMO products from reaction in $^{18}O_2$ with ascorbic acid. Mass spectra illustrating the incorporation of ^{18}O from $^{18}O_2$ into the aldonic acid products of a type 1 PMO (NCU08760). Assays were performed with $^{16}O_2$ (A) or $^{18}O_2$ (B) and the products were analyzed by LC-MS. Shown is a ladder of aldonic acid products (DP 3-7). The inset is an expanded region around the mass of the cellotrionic acid ion.

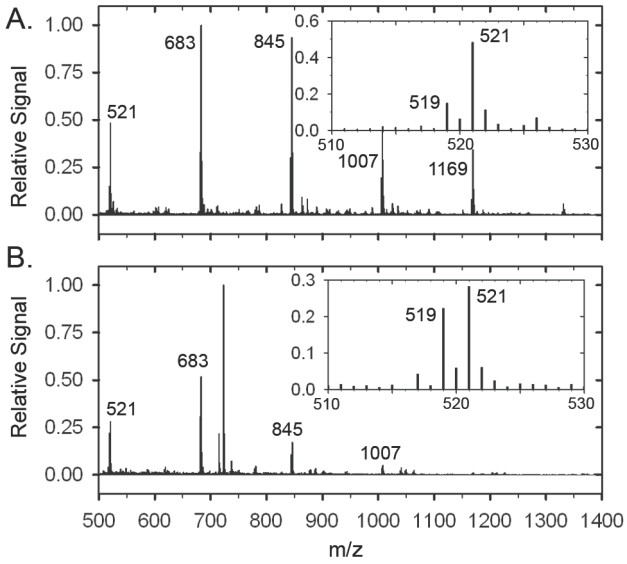

Figure 5.2. Mass spectra of PMO products from reaction in $^{18}O_2$ with CDH-2. Mass spectra illustrating the incorporation of ^{18}O from $^{18}O_2$ into the aldonic acid products of a type 1 PMO (NCU08760) with *Mt*CDH-2 as the reductant. Assays were performed with NCU08760 and MtCDH-2 in $^{18}O_2$ at pH 7.8 (A) or pH 5.0 (B) and the products were analyzed by LC-MS. Assays were incubated at 40 °C for 10 hours and contained 5.0 mg/mL PASC, 5.0 μM NCU08760, 0.5 μM CDH-2 and 50 mM ammonium acetate pH 5.0 or ammonium bicarbonate pH 7.8. Shown is a series of aldonic acid products (A3-A7). Peaks in the series are separated by 162, the mass of an anhydro-glucose unit. The inset shows an expanded region around the cellotrionic acid ion.

The identity of the non-reducing end product generated by the type 2 PMO (NCU01050) was then investigated. Both C6 and C4 oxidation have been proposed to be the non-reducing end modification catalyzed by some PMOs (*104, 116*); however, no evidence beyond mass measurements has been provided to support these hypotheses. To distinguish between these two possible products, a chemical modification strategy was used (Figure 5.4A). It is well established that carbohydrates containing a C6 aldehyde can be oxidized to the corresponding uronic acids upon treatment with mild oxidants like Br_2 or I_2 (*119, 120*). If the non-reducing end product contained a C6 aldehyde, oxidation with hypoiodite would convert it to a carboxylic acid. After chemical hydrolysis with trifluoroacetic acid (TFA), three monosaccharide products would be produced: glucuronic acid, derived from the non-reducing end; glucose, from internal carbohydrates; and gluconic acid, from oxidation at the reducing end. NCU01050 (5.0 μM) was incubated with 0.2 μM *Mt*CDH-2, 5.0 mg/mL PASC, and 50 mM sodium acetate buffer pH 5.0 at 40 °C for 10 hours to generate non-reducing end products. PASC was removed by centrifugation and the products were then oxidized with hypoiodite as previously described (*120*). After oxidation, residual iodine was removed by addition of excess silver carbonate.

Precipitated material was removed by centrifugation and TFA was added to a concentration of 2.0 M. Oxidized oligosaccharides were heated at 121 °C for 1 hour and then dried under a stream of nitrogen and washed twice with isopropanol. Products were then dissolved in 0.1 M sodium hydroxide and analyzed by Dionex HPAEC as previously described (Figure 5.4B). The absence of glucuronic acid rules out a PMO product containing a C6 aldehyde.

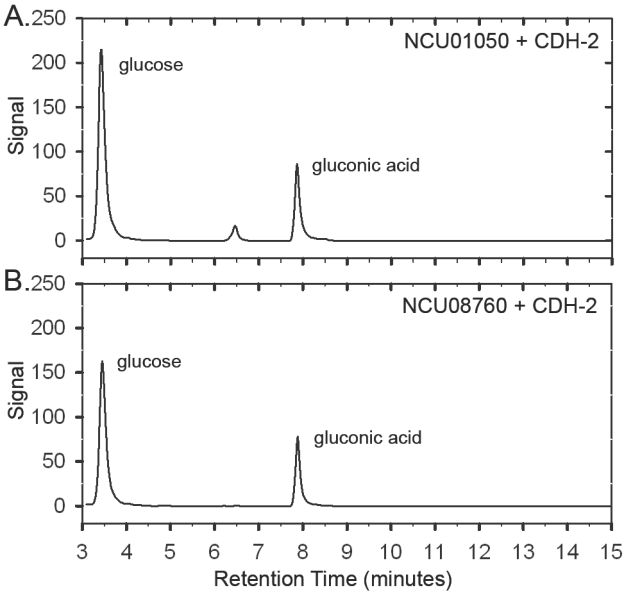

Figure 5.3. TFA hydrolysis of PMO reaction products. The products of PASC degradation by MtCDH-2 and a type 1 PMO (NCU08760) (A) or a type 2 PMO (NCU01050) (B) were hydrolyzed by TFA for 1 hour and analyzed by HPLC (Dionex PA-200). Both reactions produced a mixture of glucose and gluconic acid. Gluconic acid is formed from the reaction of MtCDH-2 on the reducing ends of cellodextrins and is also a product of NCU08760. The NCU01050 reaction contained an additional peak with a retention time of 6.4 minutes.

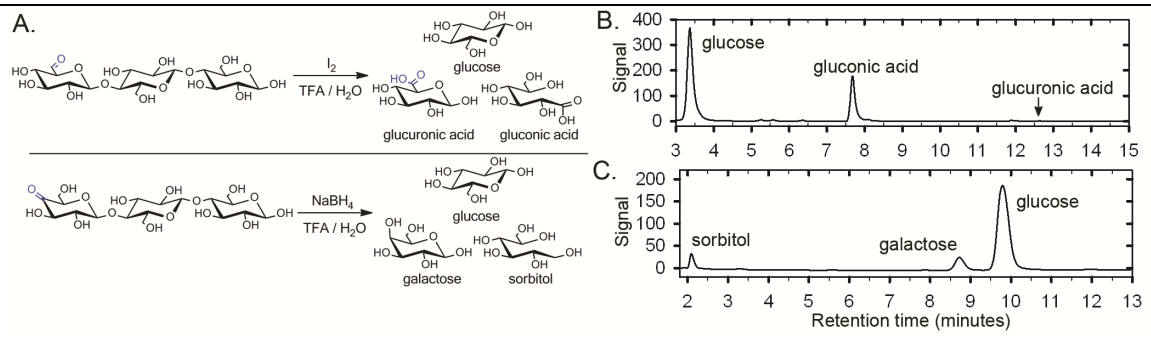

Figure 5.4. Product identification of a type 2 PMO. (A) Schematic showing the experimental design for identification of PMO products by oxidation or reduction followed by TFA hydrolysis. (B) HPLC chromatogram (Dionex PA-200) showing the products of a type-2 PMO (NCU01050) and CDH after hypoiodite oxidation and TFA hydrolysis. (C) HPLC chromatogram (Dionex PA-20) of NCU01050 products following reduction with sodium borohydride and TFA hydrolysis.

The formation of a 4-keto-aldose by NCU01050 was investigated next. Direct hydrolysis of the NCU01050 and *Mt*CDH-2 reaction products generated three peaks on a Dionex PA-200 column (Figure 5.4B). As expected, glucose and gluconic acid are formed from the internal carbohydrates and the oxidation of the reducing end by CDH. The third peak, eluting at 6.4 minutes, is absent in control reactions with NCU08760 and *Mt*CDH-2 and probably is the PMO-oxidized non-reducing end carbohydrate. If a ketone functional group was introduced in the ring, reduction with sodium borohydride would convert it back to a racemic mixture of alcohols at that position (Figure 5.4A). Galactose is the C4 epimer of glucose and can be readily separated from glucose using a Dionex PA-20 column. Initial reaction products from the NCU01050 reaction were treated with 10 mg/mL sodium borohydride in 500 mM ammonium hydroxide for 2 hours at room temperature. After reduction, residual borohydride was removed by addition of glacial acetic acid. The reduced sample was dried under a stream of nitrogen and hydrolyzed using TFA as described above. Analysis of the monosaccharide products on a Dionex HPAEC confirmed the formation of galactose (Figure 5.4C). In control experiments where NCU08760 was substituted for NCU01050, 10-fold less galactose was formed (Figure 5.5).

Together, these results provide support for the reaction pathway shown in Figure 5.6. Type 1 PMOs insert oxygen at C1, while the type 2 PMO, NCU01050, inserts oxygen at the 4 position. After oxygen insertion, the glycosidic bond is destabilized and likely broken by an elimination reaction, which may be catalyzed by the PMO or occur spontaneously. This elimination is irreversible because the carbon on the reducing or non-reducing end has been oxidized.

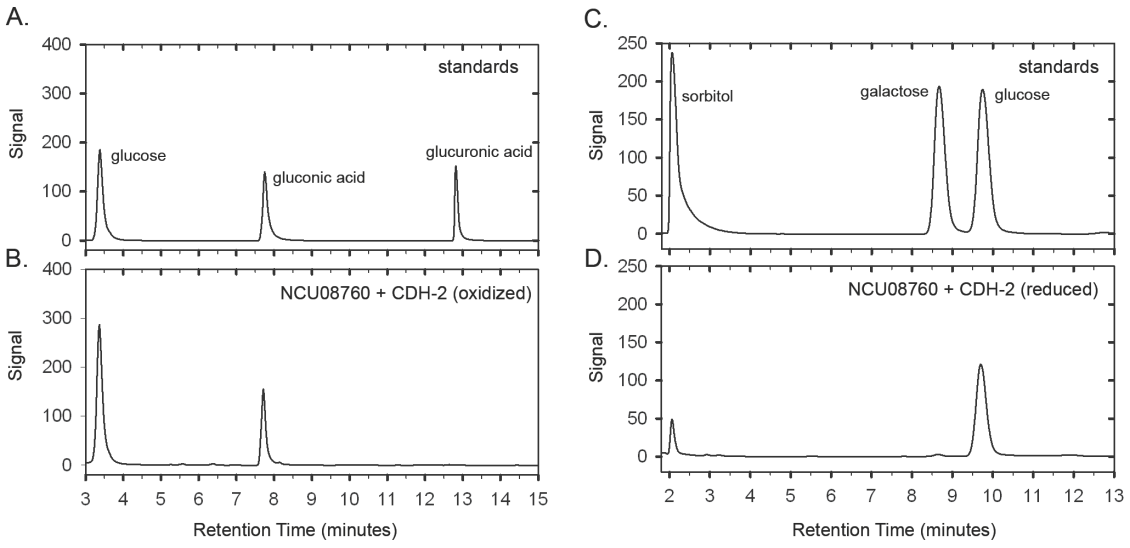

Figure 5.5. Standards and controls for PMO product identification. (A) Standards for carbohydrates predicted to be present following hypoiodite oxidation and TFA hydrolysis of oligosaccharides with a C6 aldehyde at the non-reducing end. (B) Products from the reaction of NCU08760, a type 1 PMO, and MtCDH-2 following hypoiodite oxidation and TFA hydrolysis. (C) Standards for sugars predicted to be present following sodium borohydride reduction and TFA hydrolysis of oligosaccharides with a 4-keto modification at the non-reducing end. (D) Products from the reaction of NCU08760 and CDH-2 following sodium borohydride reduction and TFA hydrolysis.

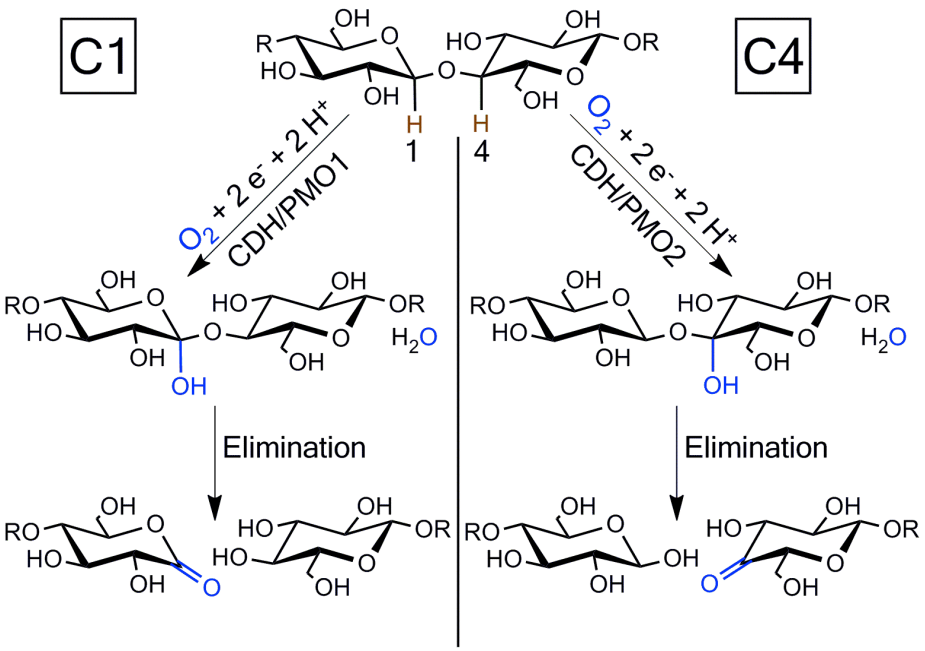

Figure 5.6. Proposed reaction pathway for oxidative cleavage of cellulose by PMOs.

Insertion of oxygen likely occurs following PMO mediated hydrogen abstraction from C1 or C4 to generate a substrate radical. This substrate radical could recombine with a copper-oxo species in the PMO active site hydroxylating the glucan chain to form the intermediate shown. The C-H bond dissociation energy for C4 is higher than C1, and likely similar to the remaining positions on the pyranose ring, suggesting that a PMO could insert oxygen at any position (*121*). The advantage of oxygen insertion at C1 or C4 is that a simple elimination reaction leads to bond cleavage. Oxygen insertion at other positions will require the involvement of additional amino acid residues on the surface of the PMO to potentiate bond cleavage and there would be nothing preventing reformation of the glycosidic bond on the cellulose surface. There is a vast amount of sequence variation in the PMO super-family and many highly cellulolytic fungi express more than ten different PMOs during growth on cellulose (*39, 40*). The residues controlling regiospecificity in PMOs are unknown. Future work identifying the reaction products of divergent members of the PMO super-family may reveal what factors control the position of oxygen insertion.

PREVIOUSLY PUBLISHED MATERIAL

Parts of this chapter are from a submitted article co-authored by William T. Beeson, Jamie H. Cate, and Michael A. Marletta.

CHAPTER 6: Homologous expression of endoglucanase GH5-1.

ABSTRACT

Filamentous fungi secrete a wide range of enzymes, including cellulases and hemicellulases, with potential applications in the production of lignocellulosic biofuels. Of the cellulolytic fungi, *Hypocrea jecorina* (anamorph *Trichoderma reesei*) is the best characterized in terms of cellulose degradation, but other cellulolytic fungi such as the model filamentous fungus *Neurospora crassa* could serve a crucial role in building our knowledge about the fungal response to biomass due to the many molecular and genetic tools developed for *Neurospora*. Here we cloned and expressed GH5-1 (NCU00762), a secreted endoglucanase in *N. crassa*. The protein was produced with the *ccg-1* promoter under conditions in which no other cellulases are present. Native GH5-1 (nGH5-1) and this recombinant GH5-1 (rGH5-1) were purified to gauge differences in glycosylation and activity; both rGH5-1 and nGH5-1 were similarly glycosylated, with an estimated molecular weight of 52 kDa. On azo-carboxymethylcellulose, rGH5-1 activity was equal to that of nGH5-1, and on cellulose (Avicel) rGH5-1 was 20% more active. The activity of a GH5-1-GFP fusion protein (rGH5-1-GFP-6xHis) was similar to rGH5-1 and nGH5-1. To determine the binding pattern of catalytically active rGH5-1-GFP-6xHis to plant cell walls, *Arabidopsis* seedlings were incubated with rGH5-1-GFP-6xHis or Pontamine Fast Scarlet 4B (S4B), a cellulose-specific dye. Confocal microscopy showed that rGH5-1-GFP-6xHis bound in linear, longitudinal patterns on seedling roots, similar to S4B. The functional expression and characterization of rGH5-1 and its GFP fusion derivative set important precedents for further investigation of biomass degradation by filamentous fungi, especially *N. crassa,* with applications for characterization and manipulation of novel enzymes.

INTRODUCTION

Filamentous fungi have proven to be industrially important for the production of secreted enzymes used in a wide variety of applications from textile manufacturing to food processing (*122*), and their ability to secrete large quantities of protein is well documented (*123*). In addition, many filamentous fungi are efficient degraders of lignocellulosic biomass and hold great potential to make the production of lignocellulosic biofuels economically viable. We recently initiated a study of *Neurospora crassa* as a model organism for biomass degradation because of the abundant molecular and genetic tools available, and reported that it efficiently degrades cellulose and hemicellulose (*44, 59*). This previous work capitalized on the *N. crassa* functional genomics project to make use of whole genome microarrays, shotgun proteomics, and a partially completed whole genome gene deletion set to understand how *N. crassa* responds to and degrades plant biomass. These advances make *N. crassa* a promising host for investigating the structure and function of secreted lignocellulolytic proteins.

Although filamentous fungi have been widely used for the recombinant production of homologous and heterologous proteins in industry, heterologous expression of functional secreted lignocellulolytic enzymes from filamentous fungi has proven problematic. Heterologous expression of cellobiohydrolase I from *H. jecorina* (*Hj*Cel7A) has been attempted in *Escherichia coli* (*124*), *Saccharomyces cerevisiae* (*125*), *Pichia pastoris* (*126*), *Ashbya gossypii* (*127*), insect cells (*128*), *Aspergillus oryzae* (*129*), and *Aspergillus niger* (*32*), but reduced activity and incorrect post-translational modifications, especially disulfide bond formation and glycosylation, have been detected. In addition, the endoglucanase II (Cel5A) of

H. jecorina has been heterologously expressed in a variety of hosts, while activity similar to the native Cel5A has been reported in *S. cerevisiae*, overglycosylation was also observed (*130*). Given these concerns with heterologous expression of secreted fungal enzymes, recombinant expression of homologous genes seems to be a viable alternative for production of proteins. For example, homologous expression of Cel61A in *H. jecorina* has been performed and a 6xHis tag has been used to facilitate rapid metal affinity purification (*101*). To better study secreted lignocellulolytic enzymes from *N. crassa*, we have developed and validated a method for recombinant expression and purification in the native host.

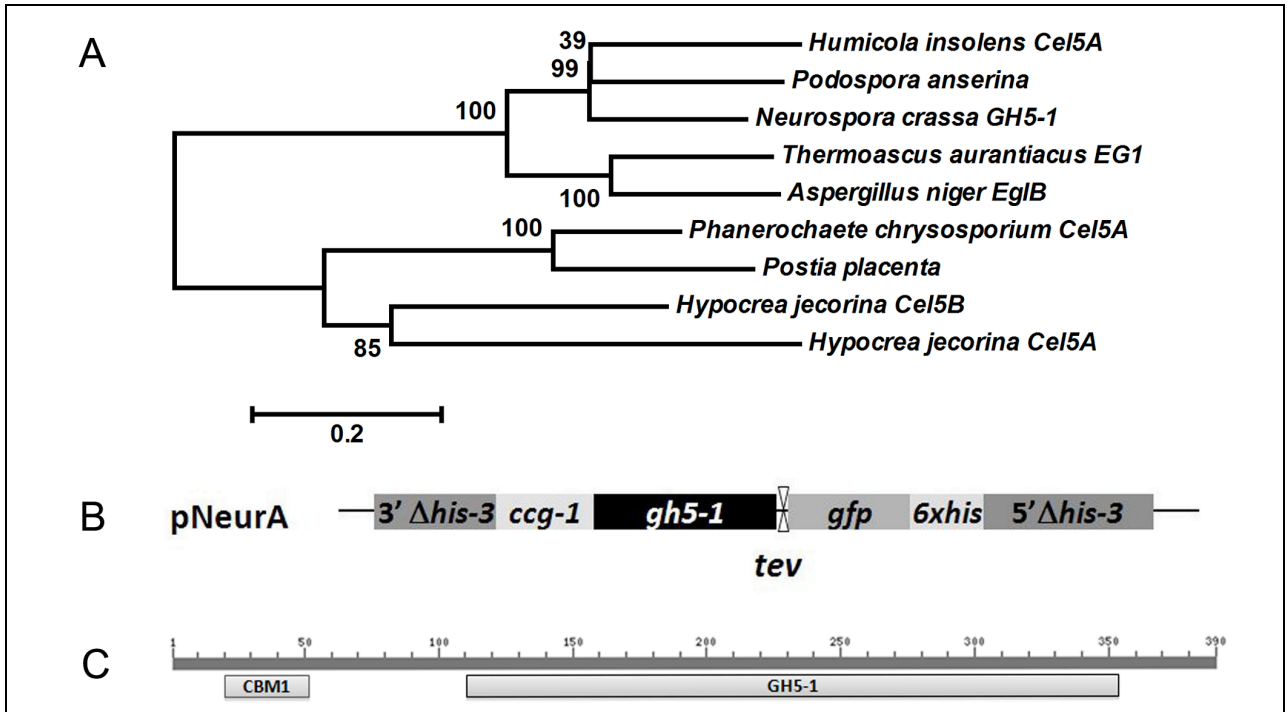

Figure 6.1 Phylogeny, schematic of expression, and domain structure of GH5-1. A. Glycoside hydrolase family 5 cellulases are highly conserved across most sequenced cellulolytic fungi and are found in both basidiomycete and ascomycete species. The neighbor joining tree above shows the phylogenetic relationship of some of the fungal GH5 enzymes in the CAZy database and their relationship to *N. crassa* GH5-1. The bootstrap values are shown and the scale bar = 0.2 substitutions per amino acid residue. **B**. To facilitate recombinant expression of GH5-1 in *N. crassa*, the pNeurA vector was designed for ectopic insertion of an *rgh5-1-gfp-6xhis* fusion gene into the *N. crassa his-3* locus. A schematic of that vector following incorporation of the *rgh5-1-gfp-6xhis* gene is shown. **C**. The domain structure of *N. crassa* GH5-1 contains an N-terminal signal peptide (SignalP 3.0), a carbohydrate binding module (CBM1) and a C-terminal glycoside hydrolase family 5 catalytic domain.

As a proof of principle, *N. crassa* GH5-1 was recombinantly expressed and purified. The GH5 enzyme family is the most widely conserved family of cellulases and has members in all three domains of evolutionary descent. GH5 enzymes are found in nearly all cellulolytic fungi, including ascomycete and basidiomycete species, especially those species that cause brown rot, white rot and soft rot (Figure 6.1A). In *N. crassa*, a strain containing a deletion of the *gh5* cellulase gene (Δ*gh5-1*) showed decreased ability to degrade azo-carboxymethylcellulose (azo-

CMC) (*59*). This effect was unique to GH5 among the endoglucanases tested. Here we expressed and characterized the GH5-1 which complements the phenotype of Δ*gh5-1* mutant from *N. crassa*. We also compare native and recombinantly expressed GH5-1 to gauge differences in glycosylation and activity. Furthermore, the recombinantly expressed GH5-1 binds to *Arabidopsis* seedling roots in linear, longitudinal patterns. Our data clearly show that *N. crassa* is capable of efficient expression and can be used as a vehicle to further investigate the structure and function of secreted lignocellulolytic proteins.

MATERIALS AND METHODS

Phylogenetic analyses

The predicted orthologs of *gh5-1* in *N. crassa* (NCU00762) were retrieved from NCBI, JGI, and CAZy databases based on amino acid similarity. GH5-1 members from *Humicola insolens* (BAA12676.1), *Podospora anserina* (XP_001912812.1), *Thermoascus aurantiacus* (AF487830_1), *Aspergillus niger* (XP_001391969.1), *Hypocrea jecorina* (120312 and 82616), *Phanerochaete chrysosporium* (AAU12275.2), and *Postia placenta* (XP_002477041.1) were chosen and the neighbor joining tree was made by MEGA4.1. Bar = 0.2 substitutions per amino acid residue.

Strains

All *N. crassa* strains were obtained from the Fungal Genetics Stock Center (FGSC) including the wild type (WT) (FGSC 2489), Δ*gh5-1* (NCU00762) deletion strain (FGSC 16746 and FGSC 16747), and Δ*gh6-2* (NCU09680) deletion strain (FGSC 15633). Gene deletion strains were constructed as part of the *N. crassa* functional genomics project (*44, 91*). *N. crassa* was grown on Vogel's salts (*131*) with 2 % (w/v) carbon source (sucrose or Avicel PH 101 (Sigma)).

Plasmid construction

Template gDNA from *N. crassa* WT strain was extracted according to the method of Lee and Taylor (http://www.fgsc.net/fgn35/lee35.pdf). pNeurA was derived from pMF272 (*132*) and contains the glucose repressible *ccg-1* promoter (*133*) and LIC (ligation independent cloning) sites (*134*) followed by a *tev-gfp-6xhis* tag. Vectors were constructed in collaboration with the Macrolab (http://macrolab.berkeley.edu/).

Plasmid pNeurA-*rgh5-1* harboring *gh5-1* was constructed as follows: a DNA fragment corresponding to the *gh5-1* open reading frame (ORF) was amplified by PCR using FGSC 2489 gDNA as the template and PCR primers *gh5-1*-AF 5'- tacttccaatccaatgcaATGAAGGCTACGATTCTTGC-3' and *gh5-1*-R 5'- ctcccactaccaatgcc AGGGGTATAGGTCTTGAGAA -3' which contained the LIC adapter (lower case). PCR fragments were checked on 1 % agarose gels and were purified by Qiagen PCR mini-prep kit. The vector was digested with Ssp1 (NEB) and treated with T4 DNA polymerase with dGTP (Invitrogen). Purified PCR fragments were treated with T4 DNA polymerase with dCTP (Invitrogen) at room temperature for 30 minutes followed by heat inactivation at 70°C for 30 minutes. 2.5 µl of the resulting vector and PCR products were mixed in 20 µl total volume and 6 µL was transformed into *E. coli* competent cells. Correct sequence and orientation of the *ccg-1-rgh5-1-gfp-6xhis* construct were confirmed by sequence analysis (UC Berkeley DNA Sequencing Facility).

Transformation of *N. crassa* strains

Plasmid DNA (1µg) was transformed into a (*his-3* Δ*gh5-1::hph a*) strain as described (*135*). The constructs were targeted to the *his-3* locus by homologous recombination and integration of the constructs at the *his-3* locus in heterokaryotic transformants was confirmed by GFP fluorescence. The brightest GFP positive transformant was selected from 10 GFP positive transformants and then was crossed with the Δ*gh5-1* strain (FGSC 16747) to recover homokaryotic strains, The hygromycin B resistant/GFP-positive progeny were selected. Quantitative RT-PCR was used to compare the *gh5-1* mRNA expression level and the progeny with highest gene expression was selected for our study. The resulting progeny was subsequently grown on Avicel and assayed for endoglucanase activity using azo-CMC (see details below) and for complementation of the Δ*gh5-1* phenotype.

Protein purification

The *N. crassa his-3::gh5-1-gfp-6xhis* strain was grown in 1 L of medium in a 2 L Erlenmeyer flask under constant light at 200 rpm and 28°C. Ten-day-old conidia were inoculated into 1x Vogel's salts with 2 % sucrose for 40 hours. Hyphae were filtered and washed over cheesecloth with sterile water and transferred into 1 x Vogel's salts with 2 % sodium acetate as the sole carbon source for 48 hours.

The culture supernatant had a pH of 8-9 and was harvested by filtration over a Whatman glass microfiber filter on a Buchner funnel followed by filtration over a 0.22 µm polyethersulfone membrane. The filtered culture supernatant was then concentrated 10-fold on a Pellicon-2 tangential flow filtration device with a 10 kDa Biomax membrane (Millipore). The concentrated supernatant was adjusted to contain 20 mM Tris pH 8.0, 300 mM NaCl, and 20 mM imidazole and was subsequently loaded onto a Ni-NTA column, washed with 3-5 column volumes of buffer (20 mM Tris pH 8, 300 mM NaCl), and eluted on a step gradient containing 20, 50, 100, and 200 mM imidazole. Fractions with rGH5-1-GFP-6xHis were visibly green and were pooled, buffer exchanged to remove > 90 % of the imidazole and either frozen at -80°C for further characterization or treated with TEV protease (UC Berkeley Macrolab) at room temperature for 3 hours and repurified through a Ni-NTA column to remove the GFP-6xHis tag. Enzyme concentrations were determined by the predicted extinction coefficient at 280 nm as determined by protparam (Expasy).

Native GH5-1 (nGH5-1) was purified from the culture supernatant of a Δ*gh6-2 N. crassa* strain (NCU09680, FGSC 15633) grown on Vogel's salts with 2 % Avicel. Cultures were maintained at 25°C, shaken at 200 rpm, and kept in constant light until complete degradation of the Avicel was visualized under a microscope, 7 days post inoculation. The Δ*gh6-2* strain was used because GH6-2 was difficult to separate from GH5-1. Culture supernatant was subjected to affinity digestion to isolate cellulose binding proteins based on their affinity for PASC as described previously (*136*). Following dialysis into 25 mM Tris pH 8.5, NaCl was added to a final concentration of 100 mM and the mixture of proteins was purified over a Hiload 16/10 Q Sepharose HP column. GH5-1 in the flow through was collected, buffer exchanged into 25 mM Tris pH 8.5 and repurified over a Mono Q 10/100 GL column using a shallow gradient from 0-100 mM NaCl over 10 minutes.

Protein gel electrophoresis

Samples were treated with 4 x SDS loading dye and boiled for 5 minutes before loading onto Criterion 4-15 % Tris-HCl polyacrylamide gels. For the PASC binding assay, 100 µL of 8 g/L PASC was added to 1 mL of *N. crassa* culture supernatant and the pH was adjusted to 5 with 1 M sodium acetate buffer. After inverting for 10 minutes samples were centrifuged and the

pellet washed 3 times with 100 mM sodium acetate pH 5. The resulting pellet was mixed with 4 x SDS loading buffer and boiled for 10 minutes. PASC was prepared according to (*137*). ProtoBlue safe colloidal Coomassie stain (National Diagnostics) was used for staining.

Enzyme activity measurements

Endoglucanase activity was measured with an azo-CMC kit (Megazyme, Cat# SCMCL, Lot# 90504) according to manufacturer's instructions. Cellulase assays were performed in 1.5 mL microcentrifuge tubes with 1 mL as a total reaction volume on an inverter at 30 revolutions per minute. Reactions containing 5 mg/mL Avicel and 50 mM sodium acetate pH 5 were pre-warmed at 40°C for 30 minutes then 15 µL of enzyme solution was added to give a final concentration of 0.5 µM enzyme/mL reaction. Time points were taken at 0, 2, 6, and 24 hours. A 100 µL aliquot was removed and centrifuged to pellet the Avicel, followed by boiling of the supernatant for 10 minutes. Samples were analyzed using coupled enzyme assays with glucose oxidase/peroxidase and cellobiose dehydrogenase as described previously (*59*). All assays were performed in triplicate.

Characterization of *N. crassa* Δ*gh5-1*

WT and Δ*gh5-1* strains were grown in biological triplicate on Avicel for 7 days as previously described (*59*) and culture supernatant was harvested by filtration over a 0.22 µm polyethersulfone membrane; protein concentration was determined by the Bio-Rad Protein Assay kit (Bio-Rad). All assays were performed as above with the following exceptions. The cellulase assays were performed in a 2 mL 96 well plate (Nunc) with 1 mL as a total reaction volume. Each well contained 0.2 mg/mL supernatant and 5 mg/mL cellulose (PASC, Avicel PH 101 (Sigma), Whatman #1 filter paper, or dewaxed cotton (*137*)). Switchgrass stems were a gift from the Energy Biosciences Institute at the University of Illinois and were ground using a Retsch SM2000 cutting mill and a Retsch SR300 rotor mill followed by passage through a 0.08 mm sieve. Switchgrass at 12 mg/mL was used for the assays and assuming 40 % cellulose by weight there was an effective concentration of 5 mg/mL cellulose. After 24 hours the supernatant was centrifuged, boiled 10 minutes, treated with 0.1 µM β-glucosidase (NCU04952) for 1 hour at 37°C to give complete conversion of cellobiose to glucose, and then assayed by the glucose oxidase/peroxidase assay. β-glucosidase was expressed and purified in *Pichia pastoris* and was a gift from Jon Galazka and Jamie Cate (Energy Biosciences Institute, UC Berkeley).

Confocal microscopy

For images showing localization to the plant cell wall, three 5-day-old *Arabidopsis* seedlings were placed in 500 µL PBS buffer containing 10 µM BSA and 0.1 µM rGH5-1-GFP-6xHis or GFP-6xHis. Samples were incubated in the dark at room temperature for 1 hour followed by three successive washes with PBS buffer. Some seedlings were incubated with 0.001 % (w/v) S4B (*138*) for 15 minutes before imaging. Seedlings were imaged on a Leica confocal microscope with a 100 x 1.4 NA oil objective and a Yokogawa spinning disc head.

RESULTS

Plasmid construction

Ligation-independent cloning (LIC) was used to generate complementary single-stranded overhangs that can anneal without the need for restriction enzymes thus facilitating high throughput cloning (*134, 139, 140*). We modified the pMF272 vector (*132, 141*) to be LIC-compatible and inserted a C-terminal *tev-gfp-6xhis* tag to maintain the integrity of the N-terminal

signal peptide. The plasmid, named pNeurA, contained the *ccg-1* promoter (*133*) which is highly induced by poor carbon sources such as sodium acetate and was designed for targeted insertion into the *his-3* locus of *N. crassa* by homologous recombination (Figure 6.1B) (*135*). In addition, *ccg-1* is upregulated in response to cellulose which allows complementation studies of gene-enzyme constructs under plant wall deconstruction conditions (*59*). The ORF corresponding to the *Neurospora gh5-1* gene (NCU00762) was inserted into pNeurA and this construct was used to express rGH5-1. In *N. crassa* this enzyme is predicted to contain an N-terminal signal peptide (SignalP 3.0), a carbohydrate binding module (CBM1) and a C-terminal catalytic domain (glycoside hydrolase family 5) (Figure 6.1C) and it was detected in supernatants of *N. crassa* grown on either *Miscanthus* or Avicel using mass spectrometry (*59*). The *tev-gfp-6xhis* tag allowed us to screen for positive transformants based on GFP fluorescence in conidia and purify recombinant protein using affinity column chromatography.

Δ*gh5-1* phenotype and complementation

Previous work (*59*) showed that in wild-type (WT) *N. crassa*, *gh5-1* expression was highly induced during growth on cellulose and that deletion of endoglucanase *gh5-1* resulted in significantly lower azo-CMC activity in the culture supernatant when grown on Avicel. To further investigate the phenotype of *gh5-1* deletion both WT and Δ*gh5-1* strains were grown for 7 days in 1 x Vogel's salts with 2 % Avicel as a sole carbon source. Culture supernatants were then assayed for activity on PASC, Avicel, filter paper, cotton, switchgrass (Figure 6.2A) and soluble azo-CMC. A comparison of the WT and Δ*gh5-1* strain revealed lower azo-CMC activity in the Δ*gh5-1* supernatant but insignificant differences in activity on all the other substrates tested (Figure 6.2B).

To determine whether recombinant and epitope-tagged GH5-1 could complement the Δ*gh5-1* phenotype on azo-CMC and to purify recombinant GH5-1 (rGH5-1), a pNeurA-*rgh5-1* plasmid (Figure 6.1B) was transformed into a *N. crassa* Δ*gh5-1* strain bearing a second mutation at the *his-3* locus (*his-3* Δ*gh5-1::hph a*) to allow targeting of constructs to the *his-3* locus by selection of *his+* prototrophy (*135*). GFP-positive transformants were back-crossed with Δ*gh5-1* (Δ*gh5-1::hph A*, FGSC 16747) to obtain homokaryotic progeny of the genotype *his-3::rgh5-1-gfp-6xhis* Δ*gh5-1*, which we refer to as *rgh5-1-gfp-6xhis*. When grown on Avicel, the *rgh5-1-gfp-6xhis* strain expressed similar levels of total secreted protein relative to the Δ*gh5-1* and WT strains, but had 225 % more azo-CMC activity relative to the Δ*gh5-1* strain. The Δ*gh5-1* strain and the *rgh5-1-gfp-6xhis* strain showed 24% and 78 % of WT activity, respectively (Figure 6.3). These results indicated that the introduced *rgh5-1* gene was functionally expressed and secreted. The reduction in azo-CMC activity in the *rgh5-1-gfp-6xhis* strain compared to WT when grown on Avicel was likely due to slightly lower expression levels of *rgh5-1-gfp-6xhis* under the regulation of the *ccg-1* promoter as compared to the native *gh5-1* promoter (data not shown).

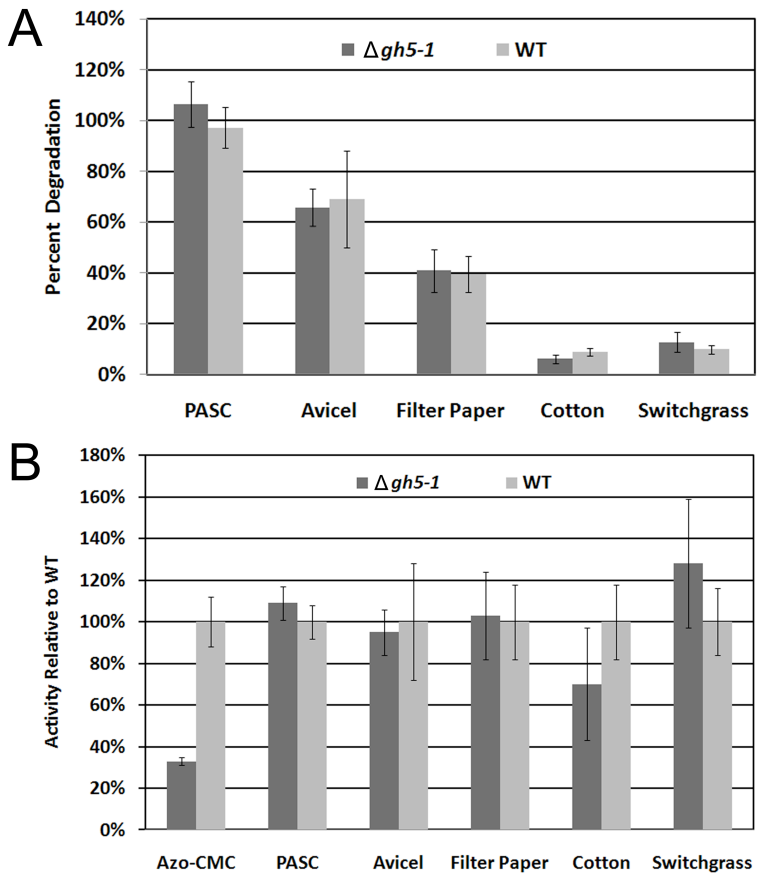

Figure 6.2 Phenotype of Δ*gh5-1*. *N. crassa* WT strain and the Δ*gh5-1* strain were grown on 1 x Vogel's salts and 2 % Avicel for 7 days. Culture supernatants were assayed on different substrates at 40°C in 50 mM sodium acetate pH 5. At 24 hours, reactions were stopped by boiling and the total glucose released was determined by treatment of assay supernatants with β-glucosidase followed by analysis with the glucose oxidase/peroxidase assay. Results are represented as percent degradation (**A**) and as activity relative to WT (**B**). Standard deviation is shown.

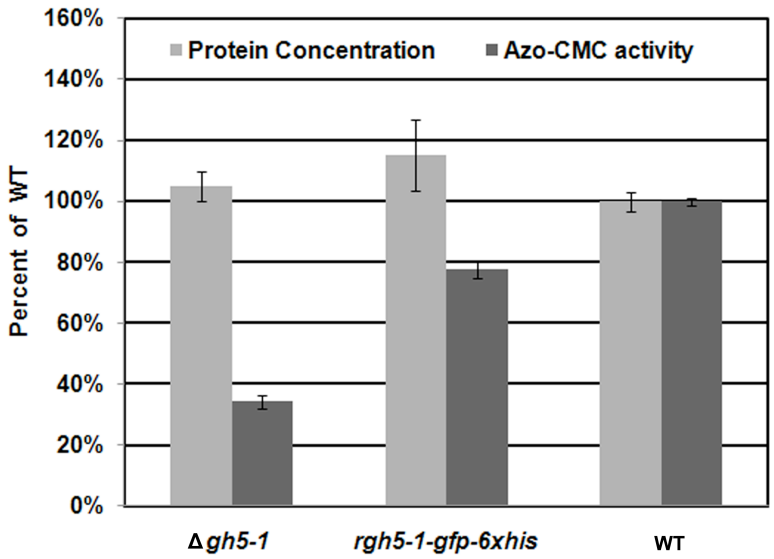

Figure 6.3 Complementation of a Δ*gh5-1* strain. Strains were grown on 1 x Vogel's salts with 2% Avicel for 7 days. Culture supernatant from the *rgh5-1-gfp-6xhis* strain had 225% more activity on azo-CMC relative to the Δ*gh5-1* strain but only 78% of WT activity. Standard deviation is shown.

Purification of GH5-1 from *N. crassa* culture supernatants

rGH5-1 was expressed with a TEV-GFP-6xHis affinity tag to facilitate purification with subsequent removal of GFP-6xHis tag via proteolytic cleavage with TEV protease. The *rgh5-1-gfp-6xhis* construct is regulated by the *ccg-1* promoter and previous work has shown that *ccg-1* gene is regulated by carbon catabolite repression with a 50-fold induction during the first 90 minutes under de-repressing conditions (*133*). Sodium acetate was used as the sole carbon source, which induces expression of *ccg-1* to high levels. Cellulase activity was not detected in culture supernatants of WT *N. crassa* grown in sodium acetate media nor were secreted cellulases detected by mass spectrometry under these conditions (data not shown). Thus, these culture conditions and our expression system allowed the purification of an expressed cellulase independently from all other plant cell wall degrading enzymes. We also found that there was less protease activity when using sodium acetate as the sole carbon sources which reduced the degradation of our expressed protein. The *rgh5-1-gfp-6xhis* strain was grown in minimal medium (*131*) with 2 % sucrose for 40 hours to increase hyphal mass. The culture was filtered and then transferred to minimal medium with 2 % sodium acetate as a sole carbon source. Endoglucanase activity of the supernatant from the *rgh5-1-gfp-6xhis* strain was monitored by measuring activity on azo-CMC. After 48 hours of growth on sodium acetate media, the endoglucanase activity peaked. The culture supernatant was filtered, concentrated and placed over a Ni-NTA column for purification of rGH5-1.

The presence of an affinity tag and the lack of other cellulases in the culture supernatant during the growth of *rgh5-1-gfp-6xhis* strain in sodium acetate media facilitated the rapid purification of rGH5-1 (see Materials and Methods). An SDS-PAGE gel of the purification is shown in Figure 6.4. Fractions eluted from the Ni-NTA column were visibly green and consisted of 2 bands corresponding to the rGH5-1-GFP-6xHis protein at 85 kDa (corresponding to the top arrow in Figure 6.4) and a proteolyzed fragment identified as GFP-6xHis at 28 kDa. The sample was then treated with TEV protease to cleave GFP-6xHis and release rGH5-1. This

step was followed by re-purification over a Ni-NTA column. Typical yields of rGH5-1 varied from 100-400 μg/L.

To assess glycosylation in rGH5-1, native GH5-1 (nGH5-1) was purified from a strain containing a deletion of *gh6-2* (FGSC 15633; Δ*gh6-2*). This strain was used to eliminate the GH6-2 protein from the supernatant during growth on pure cellulose (Avicel), as nGH5-1 is difficult to separate from GH6-2 in a wild-type strain. Both nGH5-1 and rGH5-1 had apparent molecular weights of 52 kDa (corresponding to the bottom arrow in Figure 6.4), suggesting that they were glycosylated similarly (the predicted molecular mass of GH5-1 is 39.7 kDa) (Figure 6.4). To test the cellulose binding ability of rGH5-1, we performed a phosphoric acid swollen cellulose (PASC) pulldown of culture supernatant from the *rgh5-1-gfp-6xhis* strain grown in acetate media inducing conditions. The resulting sample was analyzed on a SDS-PAGE gel and a single band at 85 kDa was identified, consistent with the mass of purified rGH5-1-GFP-6xHis protein (Figure 6.4).

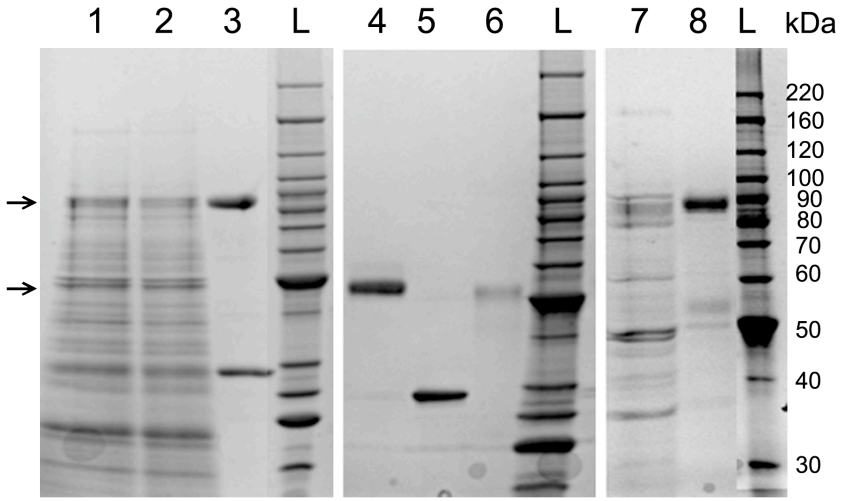

Figure 6.4 Recombinant GH5-1 purification. Concentrated supernatant (lane 1) was then placed over a Ni-NTA column (flow-through of the supernatant, lane 2) and rGH5-1-GFP-6xHis was eluted with 100 mM imidazole (lane 3). rGH5-1-GFP-6xHis was then treated with TEV protease to cleave rGH5-1 from GFP-6xHis and the two were separated over a second Ni-NTA column (lanes 4-5). Recombinant GH5-1 had the same molecular mass as native GH5-1 purified from WT (lane 6). Finally, supernatant from *N. crassa rgh5-1-gfp-6xhis* strain grown on sodium acetate (lane 7) was incubated with PASC to confirm the ability of rGH5-1-GFP-6xHis to bind cellulose (lane 8). L represents the BenchMark™ protein ladder. An arrow corresponding to a molecular weight at 85 kDa indicated protein rGH5-1-GFP-6xHis and the arrow between 50-60 kDa indicates the rGH5 without any tag linked.

Determination of GH5-1 activity

Complementation of the Δ*gh5-1* phenotype showed that rGH5-1 and rGH5-1-GFP-6xHis were active on azo-CMC, and the PASC pulldown showed that rGH5-1 and rGH5-1-GFP-6xHis bound to cellulose. A more rigorous comparison of the specific activity of purified nGH5-1, rGH5-1 and rGH5-1-GFP-6xHis to identify any difference in the enzymatic activity of the purified proteins was then carried out. Activity on azo-CMC was determined to be the same for

all three proteins within error (Figure 6.5A, C). The activity of these enzymes was also measured on Avicel, and the cellobiose and glucose produced were measured using the cellobiose dehydrogenase and glucose oxidase/peroxidase assays (*59*). These values were used to calculate the percent conversion of Avicel and results show that after 24 hours rGH5-1 and rGH5-1-GFP-6xHis had resulted in 1.1 % ± 0.1 % and 1.3 % ± 0.1 % percent degradation respectively while nGH5-1 had only degraded 0.9 % ± 0.1 % (Figure 6.5B, C). These data show that the recombinantly expressed and tagged versions of GH5-1 are fully active and correctly glycosylated. It may be that the higher activity of the recombinant enzymes is the result of a much less intensive purification procedure. Native GH5-1 was separated from the culture supernatant following degradation of Avicel and the enzyme was affinity purified using phosphoric acid swollen cellulose (PASC) and two ion exchange columns. In contrast, the recombinant GH5-1 enzymes were isolated and purified in the absence of cellulose and underwent only one chromatography step in the case of rGH5-1-GFP-6xHis or two steps in the case of rGH5-1.

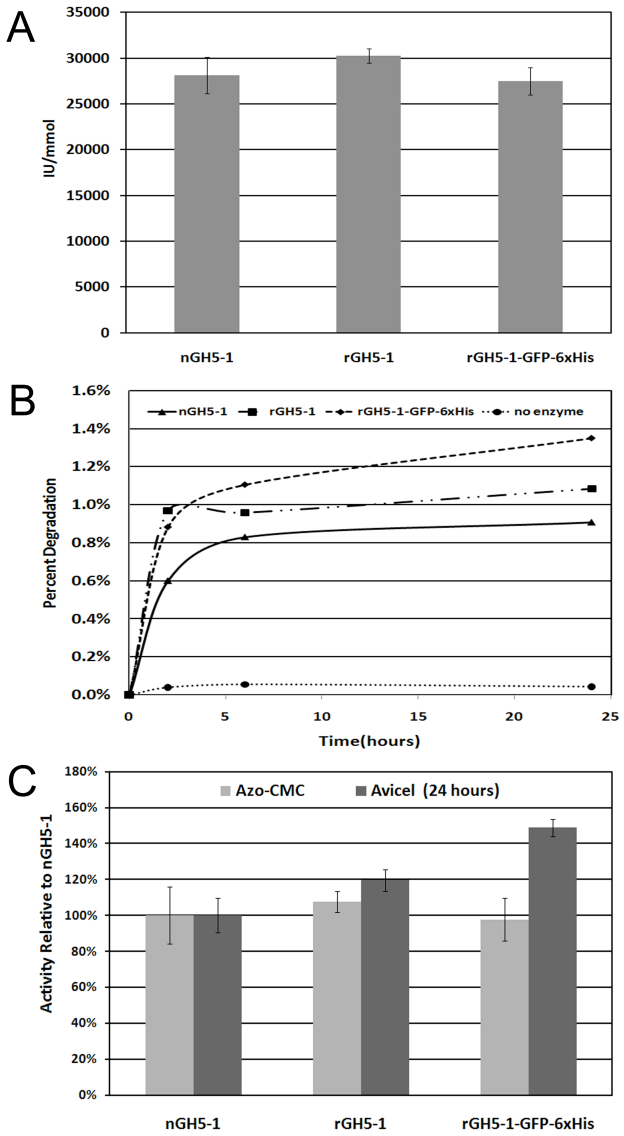

Figure 6.5 Activity of purified GH5-1 enzymes. The endoglucanase activities of the native and recombinantly purified GH5-1 proteins were measured on azo-CMC (Megazyme) according to the manufacturer's instructions (A). Enzyme activity is calculated by reference to the standard curve in the instruction manual to convert absorbance to units of activity per assay. For each assay, 0.15 µmol GH5-1 was used. Avicelase activity (B) was measured over a 24 hour time course with 0.5 uM enzyme and 5 mg/ml Avicel in 50 mM sodium acetate pH 5 at 40°C. Cellobiose and glucose were measured using the cellobiose dehydrogenase assay and glucose oxidase/peroxidase assay and these numbers were used to calculate the percent degradation. A summary of rGH5-1 and rGH5-1-GFP-6xHis activity on azo-CMC and Avicel relative to the native GH5-1 purified from *N. crassa* WT strain is shown in (**C**) and reveals that both recombinant proteins have equal or greater activity relative to the native enzyme.

Cell wall localization

Degradation of insoluble substrates from plant biomass requires the absorption of hemicellulases and cellulases onto the plant cell wall, which is mediated by CBMs (*142*). The function of CBMs, such as that present in GH5-1 (Figure 6.1C), is to localize the catalytic module to the cellulose substrate. Our studies revealed that the rGH5-1-GFP-6xHis enzyme is comparable in catalytic activity to both native and recombinant GH5-1. Therefore, we evaluated the ability of rGH5-1-GFP-6xHis to bind to plant cell walls by evaluating binding to root cell walls in live *Arabidopsis* seedlings. Roots of 5-day-old *Arabidopsis* seedlings were incubated with 0.1 μM rGH5-1-GFP-6xHis with a molar excess of BSA, washed, and imaged using confocal microscopy. Figure 6.6 shows representative images of *Arabidopsis* seedlings incubated with rGH5-1-GFP-6xHis, as compared to Pontamine Fast Scarlet 4B (S4B), a cellulose-specific fluorescent dye (*138, 143*). GFP-6xHis was used as a negative control and did not show specific binding (Figure 6.6C). Images were taken in the differentiation zone of the seedling root (Figure 6.6A) where the rGH5-1-GFP-6xHis binding was strongest and a linear pattern of fluorescence was evident in the images of both S4B and rGH5-1-GFP-6xHis. This observation is in agreement with studies of *Arabidopsis* cell wall architecture performed with S4B showing that cellulose in the differentiation zone of *Arabidopsis* roots is organized in a longitudinal fashion with hemicellulose (*138*). Xyloarabinan, xyloglucan, and/or pectin likely occupy areas of the root where rGH5-1-GFP-6xHis and S4B did not bind with high affinity (*143*). To our knowledge, this is the first time a catalytically active GFP-tagged cellulase has been imaged in the context of living plant cell walls.

DISCUSSION

Characterization of secreted proteins from filamentous fungi requires an expression system that produces properly folded proteins containing all the necessary post-translational modifications. *N. crassa* has been used for expression of intracellular proteins (*132, 141*), and heterologous expression of bovine protein and human antibodies (*144-146*). Most recently, a secreted bovine RNase A and its homolog in Neurospora (RNase N_1) were also expressed (*147*), however its use for expression of secreted lignocellulolytic enzymes has not been investigated. In this study, a native and recombinant form of GH5-1 were expressed and characterized. The recombinant GH5-1 was used to complement the phenotype of a Δ*gh5-1* deletion strain. Our expression system takes advantage of LIC technology and the availability of the whole genome deletion set in *N. crassa* (*44, 91*) and can be easily expanded to express and purify other secreted enzymes.

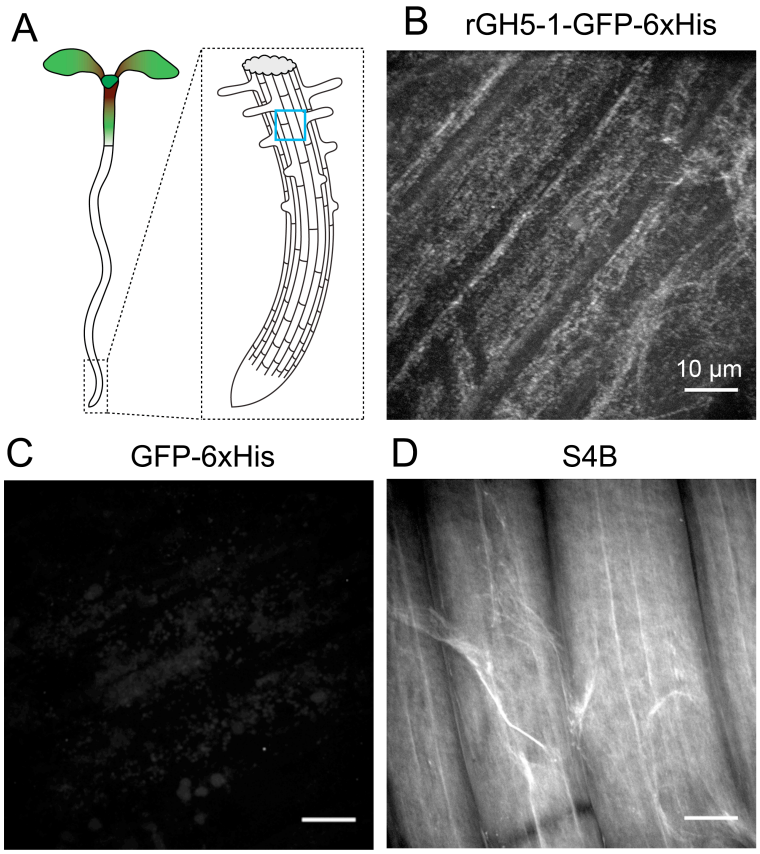

Figure 6.6 GFP tagged GH5-1 binding to *Arabidopsis* root. A. Cartoon of *Arabidopsis* seedling showing enlarged root tip (dashed box); blue box in differentiation zone of root, where root hairs begin to appear, represents location of images in panels B-D. Root differentiation zones of 5-day-old *Arabidopsis* seedlings incubated for 1 hour in 1 x PBS with 10 µM BSA and 0.1 µM rGH5-GFP-6xHis (B), 10 µM BSA and 0.1 µM GFP-6xHis (C), or 0.001% S4B (a cellulose-specific dye) (D). Seedlings were washed 3 times with PBS and imaged on a Leica confocal microscope with a 100 x 1.4 NA oil objective and a Yokogawa spinning disc head. Images are maximum projections of z-series. Scale bars = 10 µm.

A comparison of *N. crassa* GH5-1 with other glycoside hydrolase family 5 endoglucanases reveals similar characteristics. *N. crassa* GH5-1 was active on CMC but showed significantly reduced activity beyond 1 % degradation of Avicel. Similar behavior was observed for Cel5A from *H. jecorina* (*125, 148*) and *Thermoascus aurantiacus* (*149*) on CMC and Avicel. Consistent with these observations, the culture supernatant from the Δ*gh5-1* deletion strain showed a 3-fold lower activity than WT on azo-CMC but no other significant decrease in activity when assayed on insoluble forms of cellulose. These data suggest that GH5-1 is either much more abundant than the other *Neurospora* endoglucanases or has a much higher specific activity towards CMC substrates. Transcriptional profiling data showed that *gh5-1* is the second most highly expressed endoglucanase gene in *N. crassa*. The relative abundance of endoglucanases GH5-1, GH6-3 (NCU07190), and GH7-1 (NCU05057) appear to be similar by SDS-PAGE (*59*). This evidence supports the idea that GH5-1 is not necessarily the most abundant endoglucanase present, but rather, it has substantial activity towards azo-CMC. It is possible that these other

endoglucanases could diminish the effect of a *gh5-1* deletion in *N. crassa* during action on Avicel despite their inability to compensate for azo-CMC activity.

In addition to looking at the activity of native and recombinant GH5-1, a rGH5-1-GFP-6xHis fusion protein was found to be fully active on both CMC and Avicel and bound to both PASC and *Arabidopsis* seedlings (Figure 6.4 and 6.6). While confocal microscopy does not have the resolution required to image individual glucan chains or cellulose microfibrils, it did show a longitudinal pattern of binding on Arabidopsis seedlings and could be used to look at binding to different plant tissues or species. Similar experiments have been performed using immunostaining of CBM modules (*150, 151*) and a GFP (*152, 153*) or fluorescein labeled CBM (*154*). However, these studies did not investigate the influence of catalytic domain on substrate binding.

In addition to investigating the role of GH5-1 in cellulose degradation by *N. crassa,* we also validated the use of *N. crassa* as a host for homologous expression of secreted enzymes. By optimizing expression conditions in *N. crassa*, we successfully reduced the degree of protease cleavage and eliminated background cellulase activity. The functional expression and purification of rGH5-1 makes possible the expression of other uncharacterized low abundance proteins identified as candidates for accessory roles in cellulose hydrolysis. Further characterization and optimization of lignocellulolytic enzymes and investigation of *N. crassa* as a host for heterologous expression of secreted enzymes from other species are also underway.

PREVIOUSLY PUBLISHED MATERIAL

This chapter was adapted from a previously published article co-authored by Jianping Sun, Charlie T. Anderson, William T. Beeson, Michael A. Marletta, and N. Louise Glass. Thanks to the co-authors and publishers at the Journal of Protein Expression and Purification for allowing use of this material.

CHAPTER 7: Conclusions and Outlook

The use of the cellulolytic filamentous fungus *Neurospora crassa* as a model organism has been a powerful tool for advancing our understanding of biomass depolymerization and utilization in fungi. Capitalizing on genomic, transcriptomic, and proteomic analyses of *N. crassa*, we have developed a systematic understanding of how fungi respond to plant biomass and began to characterize the multiple genes and proteins involved. Similar to studies performed in other filamentous fungi, *N. crassa* uses a number of hydrolytic enzymes for depolymerization of cellulose and hemicellulose in the plant cell wall. However, it has also been shown that oxidative enzymes such as cellobiose dehydrogenase (CDH) and the polysaccharide monooxygenases (PMOs) play a significant role in depolymerization of cellulose by *N. crassa*.

In many cellulolytic Ascomycetes, CDH contains a C-terminal cellulose-binding module that targets the enzyme to the cellulose surface, probably to facilitate electron transfer and reductively activate phylogenetically diverse PMOs. Basidiomycete CDHs do not contain CBMs; however, some CDHs have been shown to bind cellulose (*155*), and many Basidiomycetes secrete high levels of a protein with a CDH heme domain fused to a CBM (*156*). These "free" heme domains would require electrons from another, unidentified reductase, to potentiate the action of PMOs. A glucose/sorbosone dehydrogenase with a CDH-like heme domain has also been identified suggesting that other oxidoreductases may function in the reductive activation of PMOs. Oxidoreductases functionally similar to CDH presumably exist in bacteria, but to our knowledge none have been identified.

Polysaccharide monooxygenases are a large family of copper-dependent metalloenzymes that function in the oxidative depolymerization of cellulose and other polysaccharides. Bacterial proteins with structural homology to the fungal PMOs discussed in this dissertation have recently been biochemically characterized and shown to oxidize cellulose (*157*) and chitin (*100*). These bacterial proteins have the same conserved metal ligands as fungal PMOs and are likely copper metalloenzymes employing a similar mechanism. Further work is needed to confirm that the activity of these proteins is dependent on bound copper. These PMOs are conserved in every cellulolytic fungus sequenced to date and many aerobic cellulolytic bacteria. These enzymes are also expressed at very high levels during growth on cellulose and a fungal PMO was the most highly upregulated protein in the brown rot fungus *Serpula lacrymans* and the white rot fungus *Phanerochaete chrysosporium* during growth on plant biomass (*36, 38*).

N. crassa has a potent genome defense mechanism, RIP, which prevents nearly all gene duplications (*45*). Surprisingly, in the *N. crassa* genome, there are 14 genes encoding predicted PMOs. Previous expression profiling studies showed that expression of at least 10 of the PMOs was induced during growth on cellulose. The average pairwise sequence identity between PMOs in *N. crassa* is only 33%, suggesting that these proteins may have diverse functions. The biochemical characterization of three members of the PMO superfamily reported here showed that different PMOs catalyze reactions with different regiospecificity. In addition to the Type 1 (NCU08760) and Type 2 PMOs (NCU01050) discussed above (Figure 6.6), it is also emerging that there may be Type 3 PMOs that may produce a combination of aldonic acids and 4-ketoaldose products. This was clearly seen with GH61A from *Thermoascus aurantiacus* (*104*) and a similar result is emerging for NCU07898. Recombinant expression must be used to test such a theory where contamination by another PMO is a non-issue. At this point, phylogenetic inference in uncharacterized clades does not allow for regioselective prediction. Further work

exploring the activity of the PMOs encoded by NCU00836, NCU03328, and NCU07760 may reveal new reactions or phylogenetic trends that allow for functional prediction.

The development of *N. crassa* as a host for recombinant expression of enzymes would be an excellent step enabling these studies. While some progress has been made, significant optimization must improve yields for expression in *N. crassa*. Since development of the pNeurA vector for homologous expression of *gh5-1*, some alternatives have been tried. The development of the pNEV vector by Terry Shock (post-doc, Glass lab) and myself included a new terminator from the *N. crassa gh5-1* gene and a C-terminal his tag that was located immediately after the *gh5-1* gene without use of a linker. Such a strategy facilitated purification of *N. crassa* GH5-1 and CBH-1 at ~1mg/L quantities following purification on a Ni-NTA column. The same vector was initially unsuccessful for trials attempting to express PMO enzymes from diverse fungi. Recently, Will Beeson has developed a strategy that uses a constitutive promotor and the pCRS vector for selection with cyclosporine A. Such an approach has been used for expression of NCU08760 with promising applications in expression of other PMOs.

The recombinant expression of phylogenetically diverse PMOs will help increase our understanding of the need for multiple PMOs in fungi. An expression system will also enable mutagenesis to further investigate the core mechanism used by PMOs in substrate oxidation. There are only 5 residues that are absolutely conserved throughout all PMOs and each is likely to be necessary for the core function of these enzymes. In addition to the two histidine residues that coordinate the copper in the metal-binding site, there is a tyrosine ligand located nearly 3 Angstroms from the copper and above the plane of nitrogen ligands. This residue is an absolutely conserved phenylalanine in the bacterial CBP21 suggesting an important difference between bacterial chitin oxidizing enzymes and the fungal PMOs that work on cellulose. A fourth conserved residue is a histidine located roughly 0.5 nm from the copper metal. This histidine may be acting as a general acid to protonate the glycosidic bond following hydroxylation and would faciliate elimination of the adjacent carbohydrate moiety. In the bacterial CBP21 this residue is an asparatic acid that could also act as a general acid. The fifth conserved residue is a glutamine located on the substrate-binding surface that may be important for hydrogen bonding to cellulose. Site-directed mutagenesis at each of these residues could help uncover their roles in catalysis by PMOs.

The discovery that CDH and PMO enzymes participate in a novel, and previously unknown, mechanism for cellulose degradation suggests that other novel enzymes with applications in biotechnology may exist in fungal secretomes. Our quantitative proteomic analysis of *N. crassa* on cellulase identified 2 additional proteins whose function remains elusive. NCU05137 is present in the secretome of *N. crassa* during growth on cellulose and many other carbon sources. Its deletion resulted in an increase in cellulase secretion but the reason for this remains unknown.

The second protein identified was NCU09764, a CBM1 containing protein that contains a domain of unknown function. This gene is upregulated in response to cellulose along with NCU00449, a homologous domain of unknown function that lacks a CBM1. Both of these genes are likely involved in cellulose degradation, utilization, or signaling because their expression profiles are very specific to the presence of cellulose, but not other polysaccharides. NCU09764 was purified in ~200 microgram quantities from *N. crassa*, its CBM1 was removed, and the domain of unknown function was characterized for polysaccharide binding in collaboration with Alex Fagerstrom (post-doc, William Willats lab). The domain only had a strong positive interaction with pectins, negatively charged polysaccharides in the plant cell wall consisting of

mostly uronic acids. Interestingly neither NCU09764 nor NCU00449 are upregulated by pectin. Niether was identified in the secretome of *N. crassa* during growth on pectin (*158*). It is possible that these proteins are involved in oxidative degradation of cellulose or utilization of the oxidized products. This hypothesis is tempting because NCU09764 had an affinity for oxidized sugars (ie. uronic acids in pectin). Further work could be done to investigate this hypothesis. In particular it is unclear how 4-ketoaldoses could be metabolized by fungi. NCU09764 or NCU00449 may be candidates for this role.

The outlook for future investigations of *N. crassa* as a model organism for studying biomass degradation in fungi remains strong. Multiple projects have began to identify and characterize the major players involved in regulation (both transcriptional and translational), signaling, secretion, and glycosylation during growth on plant biomass. In this dissertation, the secreted enzymes of *N. crassa* were identified and characterized with a specific emphasis on oxidative proteins that contribute to cellulose degradation. As discussed, the discovery of these enzymes opens up substantial opportunities in expanding our knowledge of polysaccharide degradation in fungi and bacteria. These enzymes can also lead to generation of more economic biofuels or chemicals, and further studies on their diversity and mechanism will only enhance their utility.

REFERENCES

1. United Nations: Millenium Development Goals (2011) http://www.un.org/millenniumgoals/.
2. Perry W, e. a. (2010) Grand Challenges for Engineering, National Academy of Engineering. http://www.engineeringchallenges.org/.
3. Obama administration (2009) A strategy for american innovation: driving towards sustainable growth and quality jobs. http://www.whitehouse.gov/innovation/strategy, http://www.whitehouse.gov/innovation/strategy.
4. United States Energy Information Administration (2011) http://www.eia.gov/petroleum/.
5. Solomon S, Q. D., Manning M, Chen Z, Marquis M, Averyt KB, Tignor M, Miller HL, et al. (2007) Climate Change 2007: The Physical Science Basis. Contribution of Working Group 1 to the Fourth Assessment Report of th International Panel on Clmate Change., IPCC.
6. Rosillo-Calle, F., and Cortez, L. A. B. (1998) Towards ProAlcool II - A review of the Brazilian bioethanol programme, *Biomass Bioenerg 14*, 115-124.
7. Romanelli, R. A., Houston, C. W., and Barnett, S. M. (1975) Studies on thermophilic cellulolytic fungi, *Appl Microbiol 30*, 276-281.
8. Perlack RD, W., LL, Turhollow AF, Graham RL, Stokes BJ, Erbach DC. (2005) Biomass as feedstock for a Bioenergy and Bioproducts Industry: The Technical Feasibility of a Billion-Ton Annual Supply, Department of Energy, Oak Ridge National Lab, DOE/GO-102005-2135, Oak Ridge, TN.
9. Perlack RD, S. B. (2011) U.S. Billion-Ton Update: Biomass Supply for a Bioenergy and Bioproducts Industry, Department of Energy, Oak Ridge National Lab ORNL/TM-2011/224, Oak Ridge, TN.
10. Singh, S., Madlala, A. M., and Prior, B. A. (2003) Thermomyces lanuginosus: properties of strains and their hemicellulases, *FEMS Microbiol Rev 27*, 3-16.
11. West T, D.-G. K., Sun A, Malczynski L, Reichmuth D, Larson R, Ellison J, Taylor R, Tidwell V, Klebanoff L, Hough P, Lutz A, Shaddix C, Brinkman N, Wheeler C, O'Toole D. (2009) Feasibility, economics, and environmental impact of producing 90 billion gallons of ethanol per year by 2030., Sandia National Laboratories, SAND 2009-3076J, Livermore, CA.
12. Humbird, D., Davis, R., Tao, L., Kinchin, C., Hsu, D., Aden, A., Schoen, P., Lukas, J., Olthof, B., Worley, M., Sexton, D., and Dudgeon, D. (2011) Process Design and Economics for Biochemical Conversion of Lignocellulosic Biomass to Ethanol, NREL TP-5100-47764, Golden, CO.
13. McMillan, J. D., Jennings, E. W., Mohagheghi, A., and Zuccarello, M. (2011) Comparative performance of precommercial cellulases hydrolyzing pretreated corn stover, *Biotechnol Biofuels 4*, 29.
14. Kuhls, K., Lieckfeldt, E., Samuels, G. J., Kovacs, W., Meyer, W., Petrini, O., Gams, W., Borner, T., and Kubicek, C. P. (1996) Molecular evidence that the asexual industrial fungus Trichoderma reesei is a clonal derivative of the ascomycete Hypocrea jecorina, *Proc Natl Acad Sci U S A 93*, 7755-7760.
15. Martinez, D., Berka, R. M., Henrissat, B., Saloheimo, M., Arvas, M., Baker, S. E., Chapman, J., Chertkov, O., Coutinho, P. M., Cullen, D., Danchin, E. G., Grigoriev, I. V., Harris, P., Jackson, M., Kubicek, C. P., Han, C. S., Ho, I., Larrondo, L. F., de Leon, A.

L., Magnuson, J. K., Merino, S., Misra, M., Nelson, B., Putnam, N., Robbertse, B., Salamov, A. A., Schmoll, M., Terry, A., Thayer, N., Westerholm-Parvinen, A., Schoch, C. L., Yao, J., Barabote, R., Nelson, M. A., Detter, C., Bruce, D., Kuske, C. R., Xie, G., Richardson, P., Rokhsar, D. S., Lucas, S. M., Rubin, E. M., Dunn-Coleman, N., Ward, M., and Brettin, T. S. (2008) Genome sequencing and analysis of the biomass-degrading fungus Trichoderma reesei (syn. Hypocrea jecorina), *Nat Biotechnol 26 (5)*, 553-560.

16. Powell AJ, P. K., Bustamante JM, Ricken B, Hutchinson MI, Natvig DO. (2011) Thermophilic Fungi in an aridland ecosystem, *Submitted*.
17. Khandke, K. M., Vithayathil, P. J., and Murthy, S. K. (1989) Purification of xylanase, beta-glucosidase, endocellulase, and exocellulase from a thermophilic fungus, Thermoascus aurantiacus, *Arch Biochem Biophys 274*, 491-500.
18. Folan, M. A., and Coughlan, M. P. (1978) The cellulase complex in the culture filtrate of the thermophyllic fungus, Talaromyces emersonii, *Int J Biochem 9*, 717-722.
19. Meyer, V., Wu, B., and Ram, A. F. (2011) Aspergillus as a multi-purpose cell factory: current status and perspectives, *Biotechnol Lett 33*, 469-476.
20. Barr, B. K., Hsieh, Y. L., Ganem, B., and Wilson, D. B. (1996) Identification of two functionally different classes of exocellulases, *Biochemistry 35 (2)*, 586-592.
21. Gusakov, A. V., and Sinitsyn, A. P. (1992) A theoretical analysis of cellulase product inhibition: effect of cellulase binding constant, enzyme/substrate ratio, and beta-glucosidase activity on the inhibition pattern, *Biotechnol Bioeng 40 (6)*, 663-671.
22. Rye, C. S., and Withers, S. G. (2000) Glycosidase mechanisms, *Curr Opin Chem Biol 4*, 573-580.
23. Kraulis, J., Clore, G. M., Nilges, M., Jones, T. A., Pettersson, G., Knowles, J., and Gronenborn, A. M. (1989) Determination of the three-dimensional solution structure of the C-terminal domain of cellobiohydrolase I from Trichoderma reesei. A study using nuclear magnetic resonance and hybrid distance geometry-dynamical simulated annealing, *Biochemistry 28*, 7241-7257.
24. Linder, M., Mattinen, M. L., Kontteli, M., Lindeberg, G., Stahlberg, J., Drakenberg, T., Reinikainen, T., Pettersson, G., and Annila, A. (1995) Identification of functionally important amino acids in the cellulose-binding domain of Trichoderma reesei cellobiohydrolase I, *Protein Sci 4*, 1056-1064.
25. Beckham, G. T., Matthews, J. F., Bomble, Y. J., Bu, L., Adney, W. S., Himmel, M. E., Nimlos, M. R., and Crowley, M. F. (2010) Identification of amino acids responsible for processivity in a Family 1 carbohydrate-binding module from a fungal cellulase, *J Phys Chem B 114*, 1447-1453.
26. Henrissat, B., Driguez, H., Viet, C., and Schulein, M. (1985) Synergism of Cellulases from Trichoderma-Reesei in the Degradation of Cellulose, *Bio-Technol 3*, 722-726.
27. Medve, J., Karlsson, J., Lee, D., and Tjerneld, F. (1998) Hydrolysis of microcrystalline cellulose by cellobiohydrolase I and endoglucanase II from Trichoderma reesei: adsorption, sugar production pattern, and synergism of the enzymes, *Biotechnology and bioengineering 59*, 621-634.
28. Lynd, L. R., Weimer, P. J., van Zyl, W. H., and Pretorius, I. S. (2002) Microbial cellulose utilization: fundamentals and biotechnology, *Microbiol Mol Biol Rev 66* 506-577.
29. Boisset, C., Petrequin, C., Chanzy, H., Henrissat, B., and Schulein, M. (2001) Optimized mixtures of recombinant Humicola insolens cellulases for the biodegradation of crystalline cellulose, *Biotechnology and bioengineering 72*, 339-345.

30. Banerjee, G., Car, S., Scott-Craig, J. S., Borrusch, M. S., and Walton, J. D. (2010) Rapid optimization of enzyme mixtures for deconstruction of diverse pretreatment/biomass feedstock combinations, *Biotechnol Biofuels 3*, 22.
31. Banerjee, G., Car, S., Scott-Craig, J. S., Borrusch, M. S., Aslam, N., and Walton, J. D. (2010) Synthetic enzyme mixtures for biomass deconstruction: production and optimization of a core set, *Biotechnol Bioeng 106 (5)*, 707-720.
32. Jeoh, T., Michener, W., Himmel, M. E., Decker, S. R., and Adney, W. S. (2008) Implications of cellobiohydrolase glycosylation for use in biomass conversion, *Biotechnol Biofuels 1*, 10.
33. Eriksson, K. E., Pettersson, B., and Westermark, U. (1974) Oxidation: an important enzyme reaction in fungal degradation of cellulose, *FEBS Lett 49*, 282-285.
34. Zamocky, M., Ludwig, R., Peterbauer, C., Hallberg, B. M., Divne, C., Nicholls, P., and Haltrich, D. (2006) Cellobiose dehydrogenase--a flavocytochrome from wood-degrading, phytopathogenic and saprotropic fungi, *Curr Protein Pept Sci 7*, 255-280.
35. Mason, M. G., Nicholls, P., and Wilson, M. T. (2003) Rotting by radicals--the role of cellobiose oxidoreductase?, *Biochem Soc Trans 31*, 1335-1336.
36. Eastwood, D. C., Floudas, D., Binder, M., Majcherczyk, A., Schneider, P., Aerts, A., Asiegbu, F. O., Baker, S. E., Barry, K., Bendiksby, M., Blumentritt, M., Coutinho, P. M., Cullen, D., de Vries, R. P., Gathman, A., Goodell, B., Henrissat, B., Ihrmark, K., Kauserud, H., Kohler, A., LaButti, K., Lapidus, A., Lavin, J. L., Lee, Y. H., Lindquist, E., Lilly, W., Lucas, S., Morin, E., Murat, C., Oguiza, J. A., Park, J., Pisabarro, A. G., Riley, R., Rosling, A., Salamov, A., Schmidt, O., Schmutz, J., Skrede, I., Stenlid, J., Wiebenga, A., Xie, X., Kues, U., Hibbett, D. S., Hoffmeister, D., Hogberg, N., Martin, F., Grigoriev, I. V., and Watkinson, S. C. (2011) The plant cell wall-decomposing machinery underlies the functional diversity of forest fungi, *Science 333*, 762-765.
37. Martinez, D., Challacombe, J., Morgenstern, I., Hibbett, D., Schmoll, M., Kubicek, C. P., Ferreira, P., Ruiz-Duenas, F. J., Martinez, A. T., Kersten, P., Hammel, K. E., Vanden Wymelenberg, A., Gaskell, J., Lindquist, E., Sabat, G., Bondurant, S. S., Larrondo, L. F., Canessa, P., Vicuna, R., Yadav, J., Doddapaneni, H., Subramanian, V., Pisabarro, A. G., Lavin, J. L., Oguiza, J. A., Master, E., Henrissat, B., Coutinho, P. M., Harris, P., Magnuson, J. K., Baker, S. E., Bruno, K., Kenealy, W., Hoegger, P. J., Kues, U., Ramaiya, P., Lucas, S., Salamov, A., Shapiro, H., Tu, H., Chee, C. L., Misra, M., Xie, G., Teter, S., Yaver, D., James, T., Mokrejs, M., Pospisek, M., Grigoriev, I. V., Brettin, T., Rokhsar, D., Berka, R., and Cullen, D. (2009) Genome, transcriptome, and secretome analysis of wood decay fungus *Postia placenta* supports unique mechanisms of lignocellulose conversion, *Proc Natl Acad Sci U S A 106 (6)*, 1954-1959.
38. Vanden Wymelenberg, A., Gaskell, J., Mozuch, M., Sabat, G., Ralph, J., Skyba, O., Mansfield, S. D., Blanchette, R. A., Martinez, D., Grigoriev, I., Kersten, P. J., and Cullen, D. (2010) Comparative transcriptome and secretome analysis of wood decay fungi Postia placenta and Phanerochaete chrysosporium, *Appl Environ Microbiol 76*, 3599-3610.
39. Tian, C., Beeson, W. T., Iavarone, A. T., Sun, J., Marletta, M. A., Cate, J. H., and Glass, N. L. (2009) Systems analysis of plant cell wall degradation by the model filamentous fungus *Neurospora crassa*, *Proc Natl Acad Sci U S A 106*, 22157-22162.
40. Berka, R. M., Grigoriev, I. V., Otillar, R., Salamov, A., Grimwood, J., Reid, I., Ishmael, N., John, T., Darmond, C., Moisan, M. C., Henrissat, B., Coutinho, P. M., Lombard, V., Natvig, D. O., Lindquist, E., Schmutz, J., Lucas, S., Harris, P., Powlowski, J., Bellemare,

A., Taylor, D., Butler, G., de Vries, R. P., Allijn, I. E., van den Brink, J., Ushinsky, S., Storms, R., Powell, A. J., Paulsen, I. T., Elbourne, L. D., Baker, S. E., Magnuson, J., Laboissiere, S., Clutterbuck, A. J., Martinez, D., Wogulis, M., de Leon, A. L., Rey, M. W., and Tsang, A. (2011) Comparative genomic analysis of the thermophilic biomass-degrading fungi Myceliophthora thermophila and Thielavia terrestris, *Nat Biotechnol 29*, 922-927.

41. Nidetzky, B., and Claeyssens, M. (1994) Specific quantification of *Trichoderma reesei* cellulases in reconstituted mixtures and its application to cellulase-cellulose binding studies, *Biotechnol Bioeng 44 (8)*, 961-966.
42. Foreman, P. K., Brown, D., Dankmeyer, L., Dean, R., Diener, S., Dunn-Coleman, N. S., Goedegebuur, F., Houfek, T. D., England, G. J., Kelley, A. S., Meerman, H. J., Mitchell, T., Mitchinson, C., Olivares, H. A., Teunissen, P. J., Yao, J., and Ward, M. (2003) Transcriptional regulation of biomass-degrading enzymes in the filamentous fungus Trichoderma reesei, *J Biol Chem 278*, 31988-31997.
43. Visser, H., Joosten, V., Gusakov, A. V., Olson, P. T., Joosten, R., Bartels, J., Visser, J., Sinitsyn, A. P., Emalfar, M. A., Verdoes, J. C., and Wery, J. (2011) Development of a mature fungal technology and production platform for industrial enzymes on a Myceliophthora thermophila isolate, previously known as Chrysosporium lucknowense C1., *Appl Environ Microbiol 7*, 214-223.
44. Dunlap, J. C., Borkovich, K. A., Henn, M. R., Turner, G. E., Sachs, M. S., Glass, N. L., McCluskey, K., Plamann, M., Galagan, J. E., Birren, B. W., Weiss, R. L., Townsend, J. P., Loros, J. J., Nelson, M. A., Lambreghts, R., Colot, H. V., Park, G., Collopy, P., Ringelberg, C., Crew, C., Litvinkova, L., DeCaprio, D., Hood, H. M., Curilla, S., Shi, M., Crawford, M., Koerhsen, M., Montgomery, P., Larson, L., Pearson, M., Kasuga, T., Tian, C., Basturkmen, M., Altamirano, L., and Xu, J. (2007) Enabling a community to dissect an organism: overview of the Neurospora functional genomics project, *Adv Genet 57*, 49-96.
45. Galagan, J. E., Calvo, S. E., Borkovich, K. A., Selker, E. U., Read, N. D., Jaffe, D., FitzHugh, W., Ma, L. J., Smirnov, S., Purcell, S., Rehman, B., Elkins, T., Engels, R., Wang, S., Nielsen, C. B., Butler, J., Endrizzi, M., Qui, D., Ianakiev, P., Bell-Pedersen, D., Nelson, M. A., Werner-Washburne, M., Selitrennikoff, C. P., Kinsey, J. A., Braun, E. L., Zelter, A., Schulte, U., Kothe, G. O., Jedd, G., Mewes, W., Staben, C., Marcotte, E., Greenberg, D., Roy, A., Foley, K., Naylor, J., Stange-Thomann, N., Barrett, R., Gnerre, S., Kamal, M., Kamvysselis, M., Mauceli, E., Bielke, C., Rudd, S., Frishman, D., Krystofova, S., Rasmussen, C., Metzenberg, R. L., Perkins, D. D., Kroken, S., Cogoni, C., Macino, G., Catcheside, D., Li, W., Pratt, R. J., Osmani, S. A., DeSouza, C. P., Glass, L., Orbach, M. J., Berglund, J. A., Voelker, R., Yarden, O., Plamann, M., Seiler, S., Dunlap, J., Radford, A., Aramayo, R., Natvig, D. O., Alex, L. A., Mannhaupt, G., Ebbole, D. J., Freitag, M., Paulsen, I., Sachs, M. S., Lander, E. S., Nusbaum, C., and Birren, B. (2003) The genome sequence of the filamentous fungus Neurospora crassa, *Nature 422*, 859-868.
46. Tian, C., Beeson, W. T., Iavarone, A. T., Sun, J., Marletta, M. A., Cate, J. H., and Glass, N. L. (2009) Systems analysis of plant cell wall degradation by the model filamentous fungus Neurospora crassa, *Proc Natl Acad Sci U S A 106*, 22157-22162.

47. Baker, J. O., Ehrman, C. I., Adney, W. S., Thomas, S. R., and Himmel, M. E. (1998) Hydrolysis of cellulose using ternary mixtures of purified cellulases, *Appl Biochem Biotechnol 70-72*, 395-403.
48. Boisset, C., Fraschini, C., Schulein, M., Henrissat, B., and Chanzy, H. (2000) Imaging the enzymatic digestion of bacterial cellulose ribbons reveals the endo character of the cellobiohydrolase Cel6A from *Humicola insolens* and its mode of synergy with cellobiohydrolase Cel7A, *Appl Environ Microbiol 66 (4)*, 1444-1452.
49. Gold, N. D., and Martin, V. J. (2007) Global view of the *Clostridium thermocellum* cellulosome revealed by quantitative proteomic analysis, *J Bacteriol 189 (19)*, 6787-6795.
50. Adav, S. S., Li, A. A., Manavalan, A., Punt, P., and Sze, S. K. (2010) Quantitative iTRAQ secretome analysis of *Aspergillus niger* reveals novel hydrolytic enzymes, *J Proteome Res 9 (8)*, 3932-3940.
51. Adav, S. S., Ng, C. S., Arulmani, M., and Sze, S. K. (2009) Quantitative iTRAQ secretome analysis of cellulolytic *Thermobifida fusca*, *J Proteome Res 9 (6)*, 3016-3024.
52. Raman, B., Pan, C., Hurst, G. B., Rodriguez, M., Jr., McKeown, C. K., Lankford, P. K., Samatova, N. F., and Mielenz, J. R. (2009) Impact of pretreated Switchgrass and biomass carbohydrates on Clostridium thermocellum ATCC 27405 cellulosome composition: a quantitative proteomic analysis, *PLoS One 4*, e5271.
53. Lochner, A., Giannone, R. J., Rodriguez, M., Jr., Shah, M. B., Mielenz, J. R., Keller, M., Antranikian, G., Graham, D. E., and Hettich, R. L. Use of Label-Free Quantitative Proteomics To Distinguish the Secreted Cellulolytic Systems of Caldicellulosiruptor bescii and Caldicellulosiruptor obsidiansis, *Appl Environ Microbiol 77*, 4042-4054.
54. Gerber, S. A., Rush, J., Stemman, O., Kirschner, M. W., and Gygi, S. P. (2003) Absolute quantification of proteins and phosphoproteins from cell lysates by tandem MS, *Proc Natl Acad Sci U S A 100 (12)*, 6940-6945.
55. Hanke, S., Besir, H., Oesterhelt, D., and Mann, M. (2008) Absolute SILAC for accurate quantitation of proteins in complex mixtures down to the attomole level, *J Proteome Res 7 (3)*, 1118-1130.
56. Morgenstern, E. M., Bayer, E. A., and Lamed, R. (1992) Affinity digestion for the near-total recovery of purified cellulosome from *Clostridium thermocellum*, *Enzyme and Microbial Technology 14 (4)*, 289-292.
57. Sun, J., Phillips, C. M., Anderson, C. T., Beeson, W. T., Marletta, M. A., and Glass, N. L. (2011) Expression and characterization of the *Neurospora crassa* endoglucanase GH5-1, *Protein Expr Purif 75 (2)*, 147-154.
58. Oldenburg, K. R., Vo, K. T., Michaelis, S., and Paddon, C. (1997) Recombination-mediated PCR-directed plasmid construction in vivo in yeast, *Nucleic Acids Res 25 (2)*, 451-452.
59. Tian, C., Beeson, W. T., Iavarone, A. T., Sun, J., Marletta, M. A., Cate, J. H., and Glass, N. L. (2009) Systems analysis of plant cell wall degradation by the model filamentous fungus *Neurospora crassa*, *Proc Natl Acad Sci U S A 106*, 22157-22162.
60. Marshall, A. G., and Hendrickson, C. L. (2008) High-resolution mass spectrometers, *Annu Rev Anal Chem (Palo Alto Calif) 1*, 579-599.
61. Zhou, S., and Hamburger, M. (1996) Formation of sodium cluster ions in electrospray mass spectrometry, *Rapid Communications in Mass Spectrometry 10 (7)*, 797-800.

62. Herpoel-Gimbert, I., Margeot, A., Dolla, A., Jan, G., Molle, D., Lignon, S., Mathis, H., Sigoillot, J. C., Monot, F., and Asther, M. (2008) Comparative secretome analyses of two *Trichoderma reesei* RUT-C30 and CL847 hypersecretory strains, *Biotechnol Biofuels 1 (1)*, 18.
63. Beeson, W. T. t., Iavarone, A. T., Hausmann, C. D., Cate, J. H., and Marletta, M. A. (2010) Extracellular aldonolactonase from *Myceliophthora thermophila*, *Appl Environ Microbiol 77 (2)*, 650-656.
64. Brun, V., Dupuis, A., Adrait, A., Marcellin, M., Thomas, D., Court, M., Vandenesch, F., and Garin, J. (2007) Isotope-labeled protein standards: toward absolute quantitative proteomics, *Mol Cell Proteomics 6 (12)*, 2139-2149.
65. Holtzapple, M., Cognata, M., Shu, Y., and Hendrickson, C. (1990) Inhibition of *Trichoderma reesei* cellulase by sugars and solvents, *Biotechnol Bioeng 36 (3)*, 275-287.
66. Sharma, M., Soni, R., Nazir, A., Oberoi, H. S., and Chadha, B. S. Evaluation of glycosyl hydrolases in the secretome of Aspergillus fumigatus and saccharification of alkali-treated rice straw, *Appl Biochem Biotechnol 163*, 577-591.
67. Fernandez-Acero, F. J., Colby, T., Harzen, A., Carbu, M., Wieneke, U., Cantoral, J. M., and Schmidt, J. 2-DE proteomic approach to the Botrytis cinerea secretome induced with different carbon sources and plant-based elicitors, *Proteomics 10*, 2270-2280.
68. Shah, P., Atwood, J. A., Orlando, R., El Mubarek, H., Podila, G. K., and Davis, M. R. (2009) Comparative proteomic analysis of Botrytis cinerea secretome, *J Proteome Res 8*, 1123-1130.
69. Phalip, V., Delalande, F., Carapito, C., Goubet, F., Hatsch, D., Leize-Wagner, E., Dupree, P., Dorsselaer, A. V., and Jeltsch, J. M. (2005) Diversity of the exoproteome of Fusarium graminearum grown on plant cell wall, *Curr Genet 48*, 366-379.
70. Vanden Wymelenberg, A., Gaskell, J., Mozuch, M., Sabat, G., Ralph, J., Skyba, O., Mansfield, S. D., Blanchette, R. A., Martinez, D., Grigoriev, I., Kersten, P. J., and Cullen, D. (2010) Comparative transcriptome and secretome analysis of wood decay fungi *Postia placenta* and *Phanerochaete chrysosporium*, *Appl Environ Microbiol 76 (11)*, 3599-3610.
71. Harris, P. V., Welner, D., McFarland, K. C., Re, E., Navarro Poulsen, J. C., Brown, K., Salbo, R., Ding, H., Vlasenko, E., Merino, S., Xu, F., Cherry, J., Larsen, S., and Lo Leggio, L. (2010) Stimulation of lignocellulosic biomass hydrolysis by proteins of glycoside hydrolase family 61: structure and function of a large, enigmatic family, *Biochemistry 49 (15)*, 3305-3316.
72. Henriksson, G., Johansson, G., and Pettersson, G. (2000) A critical review of cellobiose dehydrogenases, *J Biotechnol 78*, 93-113.
73. Jovanovic, I., Magnuson, J. K., Collart, F., Robbertse, B., Adney, W. S., Himmel, M. E., and Baker, S. E. (2009) Fungal glycoside hydrolases for saccharification of lignocellulose: outlook for new discoveries fueled by genomics and functional studies, *Cellulose 16 (4)*, 687-697.
74. Zhang, R., Fan, Z., and Kasuga, T. (2011) Expression of cellobiose dehydrogenase from *Neurospora crassa* in *Pichia pastoris* and its purification and characterization, *Protein Expr Purif 75*, 63-69.
75. Harreither, W., Sygmund, C., Augustin, M., Narciso, M., Rabinovich, M. L., Gorton, L., Haltrich, D., and Ludwig, R. (2011) Cellobiose dehydrogenases from ascomycetes: Catalytic properties and classification, *Appl Environ Microbiol*.

76. Fang, J., Qu, Y. B., and Gao, P. J. (1997) Wide distribution of cellobiose-oxidizing enzymes in wood-rot fungus indicates a physiological importance in lignocellulosics degradation, *Biotechnol Tech 11*, 195-197.
77. Westermark, U., and Eriksson, K. E. (1974) Cellobiose-quinone oxidoreductase, a new wood-degrading enzyme from white-rot fungi, *Acta Chem Scand B B 28*, 209-214.
78. Hallberg, B. M., Bergfors, T., Backbro, K., Pettersson, G., Henriksson, G., and Divne, C. (2000) A new scaffold for binding haem in the cytochrome domain of the extracellular flavocytochrome cellobiose dehydrogenase, *Structure 8*, 79-88.
79. Hallberg, B. M., Henriksson, G., Pettersson, G., and Divne, C. (2002) Crystal structure of the flavoprotein domain of the extracellular flavocytochrome cellobiose dehydrogenase, *J Mol Biol 315*, 421-434.
80. Zamocky, M., Ludwig, R., Peterbauer, C., Hallberg, B. M., Divne, C., Nicholls, P., and Haltrich, D. (2006) Cellobiose dehydrogenase -- A flavocytochrome from wood-degrading, phytopathogenic and saprotropic fungi, *Curr. Protein Pept. Sci. 7*, 255-280.
81. Cavener, D. R. (1992) GMC oxidoreductases. A newly defined family of homologous proteins with diverse catalytic activities, *J Mol Biol 223*, 811-814.
82. Zamocky, M., Hallberg, M., Ludwig, R., Divne, C., and Haltrich, D. (2004) Ancestral gene fusion in cellobiose dehydrogenases reflects a specific evolution of GMC oxidoreductases in fungi, *Gene 338*, 1-14.
83. Canevascini, G., Borer, P., and Dreyer, J. L. (1991) Cellobiose dehydrogenases of *Sporotrichum (Chrysosporium) thermophile*, *Eur J Biochem 198*, 43-52.
84. Baldrian, P., and Valaskova, V. (2008) Degradation of cellulose by basidiomycetous fungi, *Fems Microbiol Rev 32*, 501-521.
85. Kremer, S. M., and Wood, P. M. (1992) Production of Fenton reagent by cellobiose oxidase from cellulolytic cultures of *Phanerochaete Chrysosporium*, *Eur. J. Biochem. 208*, 807-814.
86. Mason, M. G., Nicholls, P., and Wilson, M. T. (2003) Rotting by radicals--the role of cellobiose oxidoreductase?, *Biochem Soc Trans 31*, 1335-1336.
87. Ayers, A. R., Ayers, S. B., and Eriksson, K. E. (1978) Cellobiose oxidase, purification and partial characterization of a hemoprotein from *Sporotrichum Pulverulentum*, *Eur. J. Biochem. 90*, 171-181.
88. Roy, B. P., Paice, M. G., Archibald, F. S., Misra, S. K., and Misiak, L. E. (1994) Creation of metal-complexing agents, reduction of manganese-dioxide, and promotion of manganese peroxidase-mediated Mn(III) production by cellobiose-quinone oxidoreductase from *Trametes Versicolor*, *J. Biol. Chem. 269*, 19745-19750.
89. Vogel, H. (1956) A convenient growth medium for *Neurospora*, *Microbiology Genetics Bulletin 13*, 42-43.
90. Beeson, W. T., Iavarone, A. T., Hausmann, C. D., Cate, J. H., and Marletta, M. A. (2011) Extracellular Aldonolactonase from *Myceliophthora thermophila*, *Appl Environ Microbiol 77*, 650-656.
91. Colot, H. V., Park, G., Turner, G. E., Ringelberg, C., Crew, C. M., Litvinkova, L., Weiss, R. L., Borkovich, K. A., and Dunlap, J. C. (2006) A high-throughput gene knockout procedure for *Neurospora* reveals functions for multiple transcription factors, *Proc Natl Acad Sci U S A 103*, 10352-10357.

92. Ninomiya, Y., Suzuki, K., Ishii, C., and Inoue, H. (2004) Highly efficient gene replacements in *Neurospora* strains deficient for nonhomologous end-joining, *Proc Natl Acad Sci U S A 101*, 12248-12253.
93. OSullivan, A. C. (1997) Cellulose: the structure slowly unravels, *Cellulose 4*, 173-207.
94. Bao, W., Usha, S. N., and Renganathan, V. (1993) Purification and characterization of cellobiose dehydrogenase, a novel extracellular hemoflavoenzyme from the white-rot fungus *Phanerochaete chrysosporium*, *Arch Biochem Biophys 300*, 705-713.
95. Yoshida, M., Igarashi, K., Wada, M., Kaneko, S., Suzuki, N., Matsumura, H., Nakamura, N., Ohno, H., and Samejima, M. (2005) Characterization of carbohydrate-binding cytochrome b(562) from the white-rot fungus *Phanerochaete chrysosporium*, *Appl. Environ. Microbiol. 71*, 4548-4555.
96. Tullius, T. D. (1988) DNA footprinting with hydroxyl radical, *Nature 332*, 663-664.
97. Harris, P. V., Welner, D., McFarland, K. C., Re, E., Poulsen, J. C. N., Brown, K., Salbo, R., Ding, H. S., Vlasenko, E., Merino, S., Xu, F., Cherry, J., Larsen, S., and Lo Leggio, L. (2010) Stimulation of lignocellulosic biomass hydrolysis by proteins of glycoside hydrolase family 61: Structure and function of a large, enigmatic family, *Biochemistry 49*, 3305-3316.
98. Vaaje-Kolstad, G., Horn, S. J., van Aalten, D. M. F., Synstad, B., and Eijsink, V. G. H. (2005) The non-catalytic chitin-binding protein CBP21 from *Serratia marcescens* is essential for chitin degradation, *J. Biol. Chem. 280*, 28492-28497.
99. Vaaje-Kolstad, G., Houston, D. R., Riemen, A. H. K., Eijsink, V. G. H., and van Aalten, D. M. F. (2005) Crystal structure and binding properties of the *Serratia marcescens* chitin-binding protein CBP21, *J. Biol. Chem. 280*, 11313-11319.
100. Vaaje-Kolstad, G., Westereng, B., Horn, S. J., Liu, Z., Zhai, H., Sorlie, M., and Eijsink, V. G. (2010) An oxidative enzyme boosting the enzymatic conversion of recalcitrant polysaccharides, *Science 330*, 219-222.
101. Karlsson, J., Saloheimo, M., Siika-Aho, M., Tenkanen, M., Penttila, M., and Tjerneld, F. (2001) Homologous expression and characterization of Cel61A (EG IV) of Trichoderma reesei, *Eur J Biochem 268*, 6498-6507.
102. Karkehabadi, S., Hansson, H., Kim, S., Piens, K., Mitchinson, C., and Sandgren, M. (2008) The first structure of a glycoside hydrolase family 61 member, Cel61B from Hypocrea jecorina, at 1.6 A resolution, *J Mol Biol 383*, 144-154.
103. Harris, P. V., Welner, D., McFarland, K. C., Re, E., Navarro Poulsen, J. C., Brown, K., Salbo, R., Ding, H., Vlasenko, E., Merino, S., Xu, F., Cherry, J., Larsen, S., and Lo Leggio, L. (2010) Stimulation of lignocellulosic biomass hydrolysis by proteins of glycoside hydrolase family 61: structure and function of a large, enigmatic family, *Biochemistry 49*, 3305-3316.
104. Quinlan, R. J., Sweeney, M. D., Lo Leggio, L., Otten, H., Poulsen, J. C., Johansen, K. S., Krogh, K. B., Jorgensen, C. I., Tovborg, M., Anthonsen, A., Tryfona, T., Walter, C. P., Dupree, P., Xu, F., Davies, G. J., and Walton, P. H. (2011) Insights into the oxidative degradation of cellulose by a copper metalloenzyme that exploits biomass components, *Proc Natl Acad Sci U S A*, In press.
105. Phillips, C. M., Iavarone, A. T., and Marletta, M. A. (2011) Quantitative Proteomic Approach for Cellulose Degradation by Neurospora crassa, *J Proteome Res*, In press.
106. Notredame, C., Higgins, D. G., and Heringa, J. (2000) T-Coffee: A novel method for fast and accurate multiple sequence alignment, *Journal of Molecular Biology 302*, 205-217.

107. Dereeper, A., Guignon, V., Blanc, G., Audic, S., Buffet, S., Chevenet, F., Dufayard, J. F., Guindon, S., Lefort, V., Lescot, M., Claverie, J. M., and Gascuel, O. (2008) Phylogeny.fr: robust phylogenetic analysis for the non-specialist, *Nucleic Acids Res 36*, 465-469.
108. Zhang, L., Koay, M., Maher, M. J., Xiao, Z., and Wedd, A. G. (2006) Intermolecular transfer of copper ions from the CopC protein of Pseudomonas syringae. Crystal structures of fully loaded Cu(I)Cu(II) forms, *J Am Chem Soc 128*, 5834-5850.
109. Himes, R. A., and Karlin, K. D. (2009) Copper-dioxygen complex mediated C-H bond oxygenation: relevance for particulate methane monooxygenase (pMMO), *Curr Opin Chem Biol 13*, 119-131.
110. Freimund, S., and Kopper, S. (2004) The composition of 2-keto aldoses in organic solvents as determined by NMR spectroscopy, *Carbohydr Res 339*, 217-220.
111. Klinman, J. P. (2006) The copper-enzyme family of dopamine beta-monooxygenase and peptidylglycine alpha-hydroxylating monooxygenase: resolving the chemical pathway for substrate hydroxylation, *J Biol Chem 281*, 3013-3016.
112. Solomon, E. I., Ginsbach, J. W., Heppner, D. E., Kieber-Emmons, M. T., Kjaergaard, C. H., Smeets, P. J., Tian, L., and Woertink, J. S. (2011) Copper dioxygen (bio)inorganic chemistry, *Faraday Discuss 148*, 11-39.
113. Langston, J. A., Shaghasi, T., Abbate, E., Xu, F., Vlasenko, E., and Sweeney, M. D. (2011) Oxidoreductive cellulose depolymerization by the enzymes cellobiose dehydrogenase and glycoside hydrolase 61, *Appl Environ Microbiol*, In press.
114. Wilson, D. B. (2009) Cellulases and biofuels, *Curr Opin Biotechnol 20*, 295-299.
115. MacDonald, J., Doering, M., Canam, T., Gong, Y., Guttman, D. S., Campbell, M. M., and Master, E. R. (2011) Transcriptomic responses of the softwood-degrading white-rot fungus Phanerochaete carnosa during growth on coniferous and deciduous wood, *Appl Environ Microbiol 77*, 3211-3218.
116. Phillips, C. M., Beeson, W. T., Cate, J. H., and Marletta, M. A. (2011) Cellobiose Dehydrogenase and a Copper-Dependent Polysaccharide Monooxygenase Potentiate Cellulose Degradation by Neurospora crassa, *ACS Chem Biol*.
117. Campbell, R. E., and Tanner, M. E. (1997) Uridine diphospho-alpha-D-gluco-hexodialdose: Synthesis and kinetic competence in the reaction catalyzed by UDP-glucose dehydrogenase, *Angew Chem Int Edit 36*, 1520-1522.
118. Naundorf, A., and Klaffke, W. (1996) Substrate specificity of native dTDP-D-glucose-4,6-dehydratase: chemo-enzymatic syntheses of artificial and naturally occurring deoxy sugars, *Carbohydrate research 285*, 141-150.
119. Kelleher, F. M., and Bhavanandan, V. P. (1986) Re-examination of the products of the action of galactose oxidase. Evidence for the conversion of raffinose to 6"-carboxyraffinose, *The Journal of biological chemistry 261*, 11045-11048.
120. Kelleher, F. M., and Bhavanandan, V. P. (1986) Preparation and characterization of beta-D-fructofuranosyl O-(alpha-D-galactopyranosyl uronic acid)-(1----6)-O-alpha-D-glucopyranoside and O-(alpha-D-galactopyranosyl uronic acid)-(1----6)-D-glucose, *Carbohydrate research 155*, 89-97.
121. Blanksby, S. J., and Ellison, G. B. (2003) Bond dissociation energies of organic molecules, *Accounts Chem Res 36*, 255-263.
122. Arora, D. K. (2004) *Handbook of Fungal Biotechnology*, Second Edition,Revised and Expanded (Mycology) ed., Marcel Dekker Inc., New York.

123. Kubicek, C. P., Messner, R., Gruber, F., Mach, R. L., and Kubicek-Pranz, E. M. (1993) The Trichoderma cellulase regulatory puzzle: from the interior life of a secretory fungus, *Enzyme Microb Technol 15*, 90-99.
124. Laymon, R. A., Adney, W. S., Mohagheghi, A., Himmel, M. E., and Thomas, S. R. (1996) Cloning and expression of full-length Trichoderma reesi cellobiohydrolase I cDNAs in Escherichia coli., *Applied Biochemistry and Biotechnology 57*, 389-397.
125. Saloheimo, M., Lehtovaara, P., Penttila, M., Teeri, T. T., Stahlberg, J., Johansson, G., Pettersson, G., Claeyssens, M., Tomme, P., and Knowles, J. K. (1988) EGIII, a new endoglucanase from Trichoderma reesei: the characterization of both gene and enzyme, *Gene 63*, 11-22.
126. Godbole, S., Decker, S. R., Nieves, R. A., Adney, W. S., Vinzant, T. B., Baker, J. O., Thomas, S. R., and Himmel, M. E. (1999) Cloning and expression of Trichoderma reesei cellobiohydrolase I in Pichia pastoris, *Biotechnol Prog 15*, 828-833.
127. Ribeiro, O., Wiebe, M., Ilmen, M., Domingues, L., and Penttila, M. (2010) Expression of Trichoderma reesei cellulases CBHI and EGI in Ashbya gossypii, *Appl Microbiol Biotechnol 87*, 1437-1446.
128. Von Ossowski, I., Teeri, T. T., Kalkkinen, N., and Oker-Blom, C. (1997) Expression of a Fungal Cellobiohydrolase in Insect Cells, *Biochem Biophys Res Com- mun 233*, 25-29.
129. Takashima, S., Iikura, H., Nakamura, A., Hidaka, M., Masaki, H., and Uozumi, T. (1998) Overproduction of recombinant T*richoderma reesei* cellulases by *Aspergillus oryzae* and their enzymatic properties., *J Biotechnol 65*, 163-171.
130. Qin, Y., Wei, X., Liu, X., Wang, T., and Qu, Y. (2008) Purification and characterization of recombinant endoglucanase of Trichoderma reesei expressed in Saccharomyces cerevisiae with higher glycosylation and stability, *Protein Expr Purif 58*, 162-167.
131. Vogel, H. J. (1956) A convenient growth medium for Neurospora., *Microbiol. Genet. Bull. 13*, 42-46.
132. Folco, H. D., Freitag, M., Ramon, A., Temporini, E. D., Alvarez, M. E., Garcia, I., Scazzocchio, C., Selker, E. U., and Rosa, A. L. (2003) Histone H1 Is required for proper regulation of pyruvate decarboxylase gene expression in Neurospora crassa, *Eukaryot Cell 2*, 341-350.
133. McNally, M. T., and Free, S. J. (1988) Isolation and characterization of a Neurospora glucose-repressible gene, *Curr Genet 14*, 545-551.
134. Aslanidis, C., and de Jong, P. J. (1990) Ligation-independent cloning of PCR products (LIC-PCR), *Nucleic Acids Res 18*, 6069-6074.
135. Margolin, B. S., M. Freitag, and E.U. Selker. (1997) Improved plasmids for gene targeting at the his-3 locus of Neurospora crassa by electroporation, *Fungal Genet. Newslett 44*, 34-36.
136. Morag, E., Bayer, E. A., and Lamed, R. (1992) Affinity digestion for the near-total recovery of purified cellulosome from Clostridium thermocellum, *Enzyme Microb. Technol. 14*, 289–292.
137. Wood, T. M. (1988) Preparation of Crystalline, Amorphous, and Dyed Cellulase Substrates, *Methods in Enzymology 160*, 19-25.
138. Hoch, H. C., Galvani, C. D., Szarowski, D. H., and Turner, J. N. (2005) Two new fluorescent dyes applicable for visualization of fungal cell walls, *Mycologia 97*, 580-588.
139. Haun, R. S., Serventi, I. M., and Moss, J. (1992) Rapid, reliable ligation-independent cloning of PCR products using modified plasmid vectors, *Biotechniques 13*, 515-518.

140. Doyle, S. A. (2005) High-throughput cloning for proteomics research, *Methods Mol Biol 310*, 107-113.
141. Freitag, M., Hickey, P. C., Raju, N. B., Selker, E. U., and Read, N. D. (2004) GFP as a tool to analyze the organization, dynamics and function of nuclei and microtubules in Neurospora crassa, *Fungal Genet Biol 41*, 897-910.
142. Shoseyov, O., Shani, Z., and Levy, I. (2006) Carbohydrate binding modules: biochemical properties and novel applications, *Microbiol Mol Biol Rev 70*, 283-295.
143. Anderson, C. T., Carroll, A., Akhmetova, L., and Somerville, C. (2010) Real-time imaging of cellulose reorientation during cell wall expansion in Arabidopsis roots, *Plant Physiol 152*, 787-796.
144. Nakano, E. T., Fox, R. D., Clements, D. E., Koo, K., Stuart, W. D., and Ivy, J. M. (1993) Expression vectors for Neurospora crassa and expression of a bovine preprochymosin cDNA, *Fungal Genetics Newsletter 40*, 54-56
145. Stuart, D. W., Ivy, J. M., and Koo, K. (1997) *Neurospora* expression system, (States, U., Ed.), United States.
146. Hori, N., Davis, C. G., Zsebo, K. M., and Jakobovits, A. (1999) Production of a multimeric protein by cell fusion method, (States, U., Ed.), United States.
147. Allgaier, S., Weiland, N., Hamad, I., and Kempken, F. (2010) Expression of ribonuclease A and ribonuclease N1 in the filamentous fungus Neurospora crassa, *Appl Microbiol Biotechnol 85*, 1041-1049.
148. Medve, J., Karlsson, J., Lee, D., and Tjerneld, F. (1998) Hydrolysis of microcrystalline cellulose by cellobiohydrolase I and endoglucanase II from Trichoderma reesei: adsorption, sugar production pattern, and synergism of the enzymes, *Biotechnol Bioeng 59*, 621-634.
149. Parry, N. J., Beever, D. E., Owen, E., Nerinckx, W., Claeyssens, M., Van Beeumen, J., and Bhat, M. K. (2002) Biochemical characterization and mode of action of a thermostable endoglucanase purified from Thermoascus aurantiacus, *Arch Biochem Biophys 404*, 243-253.
150. Blake, A. W., McCartney, L., Flint, J. E., Bolam, D. N., Boraston, A. B., Gilbert, H. J., and Knox, J. P. (2006) Understanding the biological rationale for the diversity of cellulose-directed carbohydrate-binding modules in prokaryotic enzymes, *J Biol Chem 281*, 29321-29329.
151. McCartney, L., Blake, A. W., Flint, J., Bolam, D. N., Boraston, A. B., Gilbert, H. J., and Knox, J. P. (2006) Differential recognition of plant cell walls by microbial xylan-specific carbohydrate-binding modules, *Proc Natl Acad Sci U S A 103*, 4765-4770.
152. Ding, S. Y., Xu, Q., Ali, M. K., Baker, J. O., Bayer, E. A., Barak, Y., Lamed, R., Sugiyama, J., Rumbles, G., and Himmel, M. E. (2006) Versatile derivatives of carbohydrate-binding modules for imaging of complex carbohydrates approaching the molecular level of resolution, *Biotechniques 41*, 435-436, 438, 440 passim.
153. Hong, J., Ye, X., and Zhang, Y. H. (2007) Quantitative determination of cellulose accessibility to cellulase based on adsorption of a nonhydrolytic fusion protein containing CBM and GFP with its applications, *Langmuir 23*, 12535-12540.
154. Hilden, L., Daniel, G., and Johansson, G. (2003) Use of a fluorescence labelled, carbohydrate-binding module from Phanerochaete chrysosporium Cel7D for studying wood cell wall ultrastructure, *Biotechnol Lett 25*, 553-558.

155. Henriksson, G., Salumets, A., Divne, C., and Pettersson, G. (1997) Studies of cellulose binding by cellobiose dehydrogenase and a comparison with cellobiohydrolase 1, *Biochem J 324 (Pt 3)*, 833-838.
156. Yoshida, M., Igarashi, K., Wada, M., Kaneko, S., Suzuki, N., Matsumura, H., Nakamura, N., Ohno, H., and Samejima, M. (2005) Characterization of carbohydrate-binding cytochrome b562 from the white-rot fungus Phanerochaete chrysosporium, *Appl Environ Microbiol 71*, 4548-4555.
157. Forsberg, Z., Vaaje-Kolstad, G., Westereng, B., Bunaes, A. C., Stenstrom, Y., Mackenzie, A., Sorlie, M., Horn, S. J., and Eijsink, V. G. (2011) Cleavage of cellulose by a CBM33 protein, *Protein Sci 20*, 1479-1483.
158. Benz, P. (2011) Personal communication.